MECHANICAL PROPERTIES OF NATURAL FIBER-REINFORCED EARTH-BASED COMPOSITES

DISSERTATION

Submitted to the Graduate Faculty

In Partial Fulfillment of the Requirement for the

Degree of **Doctor of Philosophy** In the

Department of Materials Science and Engineering

African University of Science and Technology, Abuja-Nigeria

By:

KABIRU MUSTAPHA (ID No: 70054)

November, 2015.

PhD Dissertation Committee:

Professor Winston Oluwole Soboyejo (Princeton University, NJ, USA)

Professor Leo Daniel (Kwara State University, Nigeria & University of New Orleans, USA)

Associate Professor M. G. Zebaze Kana (Kwara State University, Malete, Nigeria)

MECHANICAL PROPERTIES OF NATURAL FIBER-REINFORCED EARTH-BASED COMPOSITES

By:

Kabiru Mustapha

A THESIS APPROVED BY THE MATERIALS SCIENCE AND ENGINEERING DEPARTMENT

RECOMMENDED**: …….**
Supervisor, Professor Winston Oluwole Soboyejo

…….
Co-supervisor, Professor Leo Daniel

…….
Co-supervisor, Associate Professor M. G. Zebaze Kana

…….
Head, Dept. of Materials Science and Engineering

Approved: …….
Vice President, Academics

Date: ……..

DEDICATION

This thesis is dedicated my entire family for their numerous effort in my academic carrier. May Allah (SWT) continue to strengthen us (Amin).

ABSTRACT

This study presents the results of a combined experimental and theoretical study of the strength, fracture toughness and interfacial properties of natural fiber-reinforced earth-based composite materials. The composites, which consist of mixtures of laterite, clay and straw, are stabilized with controlled levels of Portland cement. The compositional dependence of compressive, flexural/bend strength and fracture toughness are explored for different proportions of the constituent materials using composites and crack-tip shielding models. The underlying crack-microstructure interactions associated with Resistance-curve behavior is studied using in situ/ex situ optical microscopy. This reveals evidence of crack bridging by the straw fibers. The measured resistance-curve behavior is also shown to be consistent with predictions from small- and large-scale bridging models. The study also presents an experimental investigation on pullout tests of natural fiber (straw) from earth-based matrices. A specially designed single fiber pullout apparatus is used to provide a quantitative determination of interfacial properties that are relevant to toughening brittle materials through fiber reinforcement. The parameters investigated includes a specially designed high strength earth-based matrix comprising of 60% laterite, 20% clay and 20% cement. The mediums from which the fibers are pulled includes a control mortar mix without fibers and a mortar mix with 5, 10 and 20 percent fibers by volume. The toughening behavior of whisker-reinforced earth-based matrix is analyzed in terms of a whisker bridging zone immediately behind the crack tip and interface strength. This approach is consistent with microscopy observations which reveal that intact bridging whiskers exist behind the crack tip as a result of debonding of the whisker-matrix interface. The implications of the results are then discussed for potential applications in the design of robust earth-based building materials for sustainable eco-friendly homes.

TABLE OF CONTENTS

PREFACE

This dissertation is an original intellectual property of Kabiru Mustapha containing work done from the period of January 2012 to November 2015 for the fulfillment of doctorate of philosophy degree in the Department of Materials Science and Engineering at the African University of Science and Technology, Abuja-Nigeria.

I was the lead investigator in this work, responsible for all major activities: experiments, data collection and analysis including manuscript composition while Prof. Winston Oluwole Soboyejo was the supervisory author who was involved in the early stages of the concept formation and manuscript composition.

The mechanical properties of natural fiber reinforced earth-based composites are presented in this work. Locally earth-based materials were sourced to design fiber-reinforced composites for affordable and sustainable building. Strengths and fracture toughness of the composites are presented as well as the toughening mechanisms involved to provide scientific and engineering bases for the design.

As at the time this thesis was submitted, two of its chapters (3 and 4) have been published in a peer reviewed journal; Journal of Composite Materials. Other chapters (5 and 6) have been accepted for publication in the same journal.

ACKNOWLEDGEMENTS

I would like to thank The World Bank, The African Development Bank, the Nelson Mandela Institution and the African University of Science and Technology, Abuja, for financial support. I also thank the management and staff of Mateng Nigeria Limited, Abeokuta, Sheda Science and Technology Complex, Abuja, and the Materials Science and Engineering Laboratory, Kwara State University, Malete, for their assistance with the laboratory work.

I want to extend my sincere appreciation to my PhD Dissertation Committee: Prof. Winston Oluwole Soboyejo, Prof. Leo Daniel and Dr. M. G. Zebaze Kana for their numerous support and guidance. Specifically, I want to appreciate the efforts of Prof. Soboyejo for bringing me this far. His contributions to my academic carrier are immeasurable. Thank you for everything.

My gratitude also goes to the Multifunctional Materials Research Group at the African University of Science and Technology, Abuja-Nigeria and the African Materials Research Society (AMRS) for their encouragement and useful suggestions throughout the duration of the program.

PEER REVIEW PUBLICATIONS

1. **K. Mustapha**, E. Annan, S. T. Azeko, M. G. Zebaze Kana, L. Daniel and W. O. Soboyejo. "Pull-out Behavior of Natural Fiber From Earth-based Matrix". Publisher (SAGE); *Journal of Composite Materials* (Accepted for publication on November 20, 2015).
2. **K. Mustapha**, E. Annan, S. T. Azeko, M. G. Zebaze Kana and W. O. Soboyejo. Strength and fracture toughness of earth-based natural fiber-reinforced composites. *Journal of Composite Materials*, 2015, 0021998315589769.
3. S. T. Azeko, **K. Mustapha**, E. Annan, O. S. Odusanya and A. B. Soboyejo and W. O. Soboyejo, W. O. (2015). Statistical Distributions of the Strength and Fracture Toughness of Recycled Polyethylene-Reinforced Laterite Composites. *Journal of Materials in Civil Engineering*, 2015, 04015146.
4. S. T. Azeko, **K. Mustapha**, E. Annan, O. S. Odusanya and W. O. Soboyejo. Recycling of polyethylene into strong and tough earth-based composite building materials. *Journal of Materials in Civil Engineering*, 2015, 04015104.
5. E. Annan, **K. Mustapha**, O. S. Odusanya, K. Malatesta and W. O. Soboyejo. Statistics of Flow and the Scaling of Ceramic Water Filters. *Journal of Environmental Engineering*, 2014 *140*(11), 04014039.
6. B. Agyei-Tuffour, E. Annan, E. R. Rwenyagila, E. Ampaw, E. Arthur, **K. Mustapha**, S. Kolawole, W. O. Soboyejo, M. I. Marinov and D. D. Radev (2013). Untraditional synthesis of Ni-based alloys for medical application. ARPN Journal of Engineering and Applied Sciences. Vol. 8, No. 4: 270-276.
7. B. Agyei-Tuffour, E. Annan, E. R. Rwenyagila, E. Ampaw, E. Arthur, **K. Mustapha**, S. Kolawole, W. O. Soboyejo and D. D. Radev (2013). Untraditional synthesis of boron-

containing super hard and refractory materials – A review. Global journal of Enginnering, Design & Technology. Vol. 2(1) 21-26.

LIST OF CONFERENCE PRESENTATIONS

1. **K. Mustapha**, L. Daniel and W. O. Soboyejo. Mechanical Properties of Earth-based Natural Fiber-reinforced Composites. AUST PhD Colloquium 2015. Book of Proceedings. 22nd January 2015.
2. **K. Mustapha**, E. Annan, S. T. Azeko, M. G. Zebaze Kana and W. O. Soboyejo. Pull-out Behavior of Natural Fiber From Earth-based Matrices. Nigerian Materials Congress (NIMACON) Conference at Yaba College of Technology, Lagos. (November, 2014).
3. **K. Mustapha**, E. Annan, S. T. Azeko, M. G. Zebaze Kana and W. O. Soboyejo. Strength and Fracture Toughness of Earth-based Natural Fiber-reinforced Composites. The 7th International African Materials Research Society, Addis-Ethiopia, (December, 2013).
4. **K. Mustapha**, E. Annan, S. T. Azeko, M. G. Zebaze Kana and W. O. Soboyejo. Resistance curve Behavior of Earth-based and Natural Fiber Reinforced Composites. Nigerian Materials Congress (NIMACON) Conference at African University of Science and Technology, Abuja. (November, 2013).
5. **K. Mustapha**, E. Annan, S. T. Azeko, M. G. Zebaze Kana and W. O. Soboyejo. Toughnening Behavior of Earth-based and Natural Fiber Reinforced Composites. UNESCO workshop on sustainable Materials at Kwara State University, Malete (June, 2013).
6. **K. Mustapha**, E. Annan, S. T. Azeko, M. G. Zebaze Kana and W. O. Soboyejo. Strength and Fracture Toughness of Earth-based Natural Fiber-reinforced Composites. Nigerian Materials Congress (NIMACON) Conference at Obafemi Awolowo University, Ile Ife. (November, 2012).

LIST OF FIGURES

LIST OF TABLES

CHAPTER ONE: INTRODUCTION

1.1 Background

The choice of materials for building is greatly influenced by the cost, properties (mechanical and chemical) and availability [1]. Industrialized societies have developed various materials which are applied in all works of construction (including buildings). Unfortunately, developing countries, such as Nigeria, where alternative materials exist have failed to explore such opportunities even, when there is the possibility of producing such materials locally. There is therefore, a need to explore new ways of producing robust building materials from locally available materials.

Such needs have stimulated recent efforts to develop affordable building materials that are strengthened and toughened by locally available natural fibers [2] and matrix materials that are available in developing countries. However, in most cases, the matrix materials utilize cement, which is a relatively expensive synthetic material and associated with ~5% of the global carbon dioxide emissions [3] that are thought to contribute to global warming. This has made it relatively difficult for poor people to afford durable homes in most developing countries. However, in most of these countries, there are large deposits of industrial, agricultural and human wastes that can be recycled into robust building materials that could make homes more affordable for a significant fraction of the world's rural and urban poor [4].

In contrast, earth-based materials are readily available materials that could be used as matrix materials in building composites. They can also be stabilized by the use of binders, such as dung or cement, to produce materials that are strong and tough enough for applications in buildings [1]. They can also be reinforced with natural fibers (such as sisal and straw) [5-11] while the matrices

can be optimized by the use of industrial wastes, such as blast furnace slag and crushed charcoal from the burning of wood [12].

1.2 Problem Statement

There has been great progress in both the production and application of reinforced materials (except little for earth-based materials). In most cases where high strength and toughness of earth-based materials are required, the materials are stabilized with cement or dung [3]. Some local people have also used straw, and other natural fibers, to strengthen earth-based materials that are used in local construction of earthen homes. However, the scientific and engineering bases for such applications are very limited. There is, therefore, a need to develop the scientific understanding that can provide the necessary basis for the design of novel earth-based materials that can be used in rural and urban construction.

1.3 Scope of Work

This study examines the effect of processing, composition and natural fiber reinforcement on the mechanical properties of natural fiber-reinforced earth-based composites. The study includes:

The processing of local (earth-based) materials with different compositions;

The material characterization of local materials and processed materials with:

i. Scanning electron microscopy (SEM);
ii. Energy Dispersive X-ray Spectroscopy (EDS).

The mechanical characterization of natural fiber-reinforced earth-based composites. These include:

i. Compressive and Flexural strength.

ii. Fracture toughness and resistance-curve behavior

iii. The determination of compositional dependence of constituents' materials (laterite, clay, cement and straw) on the mechanical properties of the composites.

iv. The study of resistance-curve behavior of natural fiber-reinforced earth-based composite to determine the contribution of fiber-reinforcement to composite toughness.

v. Comparison of experimental results with those obtained from mechanistic models (rule-of-mixture, short fiber theory, crack bridging, fiber pull-out, etc.).

vi. Pullout behavior of natural fiber (Straw) from earth based matrices and its contribution to toughening of earth-based composites.

Following the background and introduction in chapter one, chapter two presents a review of current literature on composites and cement and earth materials. The effects of composition and composite structure on the strengths (compressive and flexural) and fracture toughness of natural fiber-reinforced earth-based composites are examined in chapter three.

In chapter four, we explored the resistance curve behavior of natural fiber-reinforced earth-based composites. The pullout behavior of straw fiber from earth based matrices is presented in chapter five. In chapter six, we elucidated the overall toughening behavior of natural fiber-reinforced earth-based composites resulting from the multiple toughening mechanisms in fiber-reinforced composites.

Lastly, chapter seven presents the conclusions arising from the current study along with some suggestions for future research.

References

[1] Appropriate building materials for low cost housing, vol. 2. International Council for Building Research Studies and Documentation, International Union of Testing and Research Laboratories for Material and Structures, 1985.

[2] Savastano Jr. H, Warden PG, Coutts RSP. Potential of alternative fiber cements as building materials for developing areas. Cement & Concrete Composites 2003; 27(5):585-92.

[3] Ernst W, Lynn P, Nathan M, Chris H and Leticia OM. Carbon dioxide emissions from the global cement industry, Annual Review of Energy and the Environment, Environment and Resources, 2001. vol. 26: 303-329.

[4] John VM, Zordan SE. Research and development methodology for recycling residues as building materials –a proposal. Waste Mgmt 2001; 21:213-9

[5] Toledo Filho RD, Scrivener K, England GL, Ghavami K. Durability of alkali sensitive sisal and coconut fibers in cement mortar composites. Cem Corncr Compos 2000; 2 (22):127-43

[6] Coutts RSP. Wood fiber reinforced cement composites. In: Swamy RN, editor. Natural Fiber Reinforced Cement and Concrete. Glasgow: Blackie; 1988. p. 1-62.

[7] Savastano Jr H, Warden PG, Coutts RSP. Brazilian waste fibers as reinforcement for cement based composites. Cement Concr Compos 2000; 22: 379–84.

[8] Coutts RSP. Waste paper fibers in cement products. Int J Cement Comp Lightweight Conc 1989; 11: 143–7.

[9] Coutts RSP. Flax fibers as reinforcement in cement mortars. Int J Cement Comp Lightweight Conc 1983;5(4):257–62.

[10] Coutts RSP, Warden PG. Air cured, Abaca reinforced cement composites. Int J Cement Comp Lightweight Conc 1987; 9(2):69–73.

[11] Coutts RSP. Banana fibers as reinforcement for building products. J Mater Sci Lett 1990; 9:1235–6.

[12] Savastano Jr H, Warden PG, Coutts RSP. Blast furnace Slag cement reinforced with cellulose fibers. In: Proc. 8th National Meeting on Technology of the Built Environment: Modernity and Sustainability, Salvador, Brazil, April 25-28, 2000. VII. p 948-55.

CHAPTER TWO: LITERATURE SURVEY

2.1 Earth-based Materials

Earth-based materials are naturally occurring materials found on the earth. They are vital resources (raw materials) that provide the basic component of life, agriculture and industry. These materials include minerals, rocks, soil and water. These studies focus on soils (locally available and affordable), which can be used as alternative building materials. The earth-based materials to be studied include laterite, clay and straw.

2.1.1 Laterites

Laterites (figure 2.1) are soil type rich in iron and aluminum [1]. They are formed in hot and wet tropical areas [2]. Nearly all laterites are rusty-red because of the iron oxide contained in them. They develop by intensive long-lasting tropical weathering of the underlying parent rocks. Tropical weathering (laterization) is a prolonged process of mechanical and chemical weathering which produce a wide variety in the thickness, grade, chemistry and mineralogy of the resulting soils [3]. Laterites cover about one-third of the earth's continental land area, with the majority of that in the land areas between the Tropics of Cancer and Capricorn [4].

Figure 2.1: Photograph of laterite

Francis Buchanan Hamilton first described and named laterite formation in southern India in 1807. He named it laterite from the Latin word "Later", which means a brick. Thick rock can be easily cut into brick-shaped blocks for building [5]. Historically, laterite was cut into brick-like shapes and used in monument buildings. When moist, laterites can be easily cut into regular-sized blocks. Upon exposure to air, it gradually hardens as the moisture between the particles evaporates and the larger iron salts lock into a rigid lattice structure and become resistant to atmospheric conditions [6]. The act of quarrying laterite material into masonry is suspected to have been introduced in the Indian sub-continent.

After 1000 CE, construction at Angkor Wat and other south-east Asian sites changed to rectangular temple enclosures made of laterite bricks and stones. Since the mid-1970s, trial sections of bituminous-surfaced low volume roads have used laterite in place of stones as base course [7]. Thick laterite layers are porous and slightly permeable, so layers can function as aquifers in rural areas. Locally available laterites are used in an acid solution, followed by precipitation to remove phosphorous and heavy metal at sewage treatment facilities [8].

2.1.2 Clay

In simple terms, clay is seen as a naturally occurring earth material composed primarily of fine-grained particles (minerals) [9]. It differs from other soils by difference in size and mineral content. Clay (Figure 2.2) is typically formed over long period of time, by the gradual weathering (chemical or physical) of rocks [10]. In addition to the weathering process, some clays are formed by hydrothermal activities [11]. Clay deposits may be formed in places as residual deposits in soils,

but thick deposits usually are found as a result of secondary sedimentary deposition process after they must have been eroded and transported from their original location of formation [12]. With respect to location, clay soils can be classified as either primary or secondary. Primary clay (Kaolin) is located at the site of formation, while secondary clay deposits have been moved by erosion from their primary location [13].

Figure 2.2: Photograph of clay

Elemental compositions of clay minerals are same as that of hydro aluminum phyllosilicate with variable amount of iron, magnesium, alkali metals, alkali earth and other cations. Structurally, they are composed of two dimensional sheets of corner sharing SiO_4 and AlO_4 tetrahedra. The resulting tetrahedral sheets give a chemical composition of $(Al, Si)_3O_4$. The tetrahedral sheets are always bonded to octahedral sheets formed from small cations, such as aluminum or magnesium, coordinated by six oxygen atoms [14].

Clay soils exhibit plasticity, when mixed with water in certain proportions. When dried, clay becomes firm and when fired in a Kiln, permanent physical and chemical reactions occur which cause it to be converted into ceramic materials. Clays also serve as binders, when used in matrices.

As a result of these properties, clay is used for making pottery items, both for utilization and decoration. Bricks, cooking pots, art objects, dishware, etc can all be shaped from clay, before being fired. Recent studies have investigated clay's absorption capacities in various applications, such as the removal of heavy metals from waste water and air. Also, clay finds application in medicine and agriculture [15].

2.1.3 Straw (Andropogon spp.)

Straw (Figure 2.3) is the dry stalk of cereal plants. It is an agricultural by-product obtained after the grain and chaff have been removed. Straw makes up about half of the yield of cereal crops such as barley, oats, rice, and wheat. It has many uses, including fuel, livestock bedding and fodder, thatching and basket-making. Straw can also be used to bind clay and concrete in the production of building materials. Mechanically, straw filament breaks, when subjected to a force of about 0.25 kg/mm^2 by which it extended 4% of its original length [16].

Figure 2.3: Photograph of straw (Andropogon spp.)

2.2 Cement and Cement Reactions

Cement is a substance that sets and hardens independently via hydration, and can bind other materials together [17]. It is made by heating a mixture of limestone and clay or other materials of similar bulk composition and sufficient reactivity, ultimately to a temperature of about 1450°C [18]. Partial fusion occurs, and nodules of clinker are produced. The clinker is mixed with a few per cent of gypsum and finely ground to make the cement. The gypsum controls the rate of set and may be partly replaced by other forms of calcium sulphate [19]. Some specifications allow the addition of other materials at the grinding stage. The clinker typically has a composition in the region of 67% CaO, 22% SO_2, 5% AI,O, 3% Fe,O, and 3% of other components. It normally contains four major phases. These are called alite, belite, aluminate phase and ferrite phase [20]. Several other phases, such as alkali sulphates and calcium oxide are normally present in minor amounts.

In cement chemistry, the term 'hydration' refers to the totality of the changes that occur when anhydrous cement, or one of its constituent phases, is mixed with water [21]. The chemical reactions that occur are generally more complex than simple conversions of anhydrous compounds into the corresponding hydrates. A mixture of cement and water in such proportions that setting and hardening occurs is called a paste, the meaning of this term being extended to include the hardened material. The water-cement (w/c) or water/solid (w/s) ratio refers to proportions by weight; for a paste, it is typically 0.3-0.6 [22]. Setting is stiffening without significant development of compressive strength, and typically occurs within a few hours. Hardening is significant development of compressive strength, and is normally a slower process.

2.2.1 Properties of the major cement minerals

About 90-95% of a Portland cement is comprised of the four main cement minerals, which are C_3S, C_2S, C_3A, and C_4AF, with the remainder consisting of calcium sulphate, alkali sulphates, unreacted (free) CaO, MgO, and other minor constituents left over from the clinkering and grinding steps [23]. The four cement minerals play very different roles in the hydration process that converts the dry cement into hardened cement paste. The C_3S and the C_2S contribute virtually all of the beneficial properties by generating the main hydration product, C-S-H gel. However, the C_3S hydrates much more quickly than the C_2S, and are thus responsible for the early strength development [24]. The C_3A and C_4AF minerals also hydrate, but the products that are formed contribute little to the properties of the cement paste. Although the crystal structures of cement minerals are quite complex, some important features are presented below.

2.2.1.1 Tricalcium Silicate (C_3S)

C_3S is the most abundant mineral in Portland cement, occupying 40–70 wt% of the cement, and it is also the most important [25]. The hydration of C_3S gives cement pastes most of its strength, particularly at early times. Pure C_3S can form with three different crystal structures. At temperatures below 980˚C, the equilibrium structure is triclinic. At temperatures between 980˚C – 1070˚C, the structure is monoclinic while above 1070˚C, it is rhombohedral [26]. In addition, the triclinic and monoclinic structures, each have three polymorphs, so there is a total of seven possible structures. However, all of these structures are rather similar and there are no significant differences in the reactivity. The most important feature of the structure is an awkward and asymmetric packing of the calcium and oxygen ions that leaves large “holes” in the crystal

lattice. Essentially, the ions do not fit together very well, causing the crystal structure to have high internal energies. As a result, C_3S is highly reactive [27].

2.2.1.2 Dicalcium Silicate (C_2S)

As with C_3S, C_2S can form with a variety of different structures. There is a high temperature α structure with three polymorphs, a β structure that is in equilibrium at intermediate temperatures, and a low temperature γ structure [28]. An important aspect of C_2S is that γ-C_2S has a very stable crystal structure that is completely unreactive in water. Fortunately, the β- structure is easily stabilized by the other oxide components of the clinker and thus the γ form is never present in Portland cement [29]. The C_2S in cement contains slightly higher levels of impurities than C_3S. According to Taylor [30], the overall substitution of oxides is 4-6%, with significant amounts of Al_2O_3, Fe_2O_3 and K_2O.

2.2.1.3 Tricalcium Aluminate (C_3A)

C_3A comprises between zero and 14% by volume of a Portland cement [25]. Like C_3S, it is highly reactive, releasing a significant amount of exothermic heat during the early hydration period [31]. Unfortunately, however, the hydration products that are formed from C_3A contribute little to the strength or other engineering properties of cement paste. In certain environmental conditions (i.e., the presence of sulphate ions), C_3A and its products can actually harm the concrete by participating in expansive reactions that lead to stress and cracking [32].

Pure C_3A forms only with a cubic crystal structure [33]. The structure is characterized by Ca^{2+} atoms and rings of six AlO_4 tetrahedra. As with C_3S, the bonds are distorted from their equilibrium positions, leading to a high internal energy and thus a high reactivity. Significant amounts of CaO and the Al_2O_3 in the C_3A structure can be replaced by other oxides, and at high levels of substitution, this can lead to other crystal structures. The C_3A in Portland cement clinker, which typically contains about 13% oxide substitution, is primarily cubic, with smaller amounts of orthorhombic C_3A. The C_3A and C_4AF minerals form by simultaneous precipitation as the liquid phase formed during the clinkering process cools, and thus, they are closely intermixed. This makes it difficult to ascertain the exact compositions of the two phases. The cubic form generally contains ~4% substitution of SiO_2, ~5% substitution of Fe_2O_3, and about 1% each of Na_2O, K_2O, and MgO. The orthorhombic form has similar levels, but with a greater (~5%) substitution of K_2O [34].

2.2.1.4 Tetracalcium Aluminoferrite (C_4AF)

A stable compound with any composition between C_2A and C_2F can be formed, and the cement mineral termed C_4AF is an approximation that simply represents the midpoint of this compositional series [35]. The crystal structure is complex, and is believed to be related to that of the mineral perovskite [36]. The actual composition of C_4AF in cement clinker is generally higher in aluminum than in iron, and there is considerable substitution of SiO_2 and MgO. Taylor [30] reports a typical composition (in normal chemical notation) to be $Ca_2AlFe0.6Mg0.2Si0.15Ti0.5O_5$. However, the composition will vary somewhat, depending on the overall composition of the cement clinker.

2.2.2 Types of Portland cement

The ASTM has designated five types of Portland cement, designated Types I-V [37]. Physically and chemically, these cement types differ primarily in their content of C_3A and in their fineness. In terms of performance, they differ primarily in the rate of early hydration and in their ability to resist sulphate attack. Table 2.1 presents the general features of the main types of Portland cement.

Table 2.1: General features of the main types of Portland cement.

	Classification	Characteristics	Applications
Type I	General purpose	Fairly high C_3S content for good early strength development	General construction (most buildings, bridges, pavements, precast units, etc)
Type II	Moderate sulphate resistance	Low C_3A content (< 8%)	Structures exposed to soil or water containing sulphate ions
Type III	High early strength	Ground more finely, may have slightly more C_3S	Rapid construction, cold weather concreting
Type IV	Low heat of hydration (slow reacting)	Low content of C_3S (< 50%) and C_3A	Massive structures such as dams. Now rare.
Type V	High sulphate resistance	Very low C_3A content (< 5%)	Structures exposed to high levels of sulphate ions
White	White color	No C4AF, low MgO	Decorative (otherwise has properties similar to Type I)

The differences between these cement types are rather subtle. All five types contain about 75 wt% calcium silicate minerals, and the properties of mature concretes made with all five are quite similar. Thus, these five types are often described by the term "Ordinary Portland Cement", or OPC.

2.2.3 The Hydration reactions

The hydration of cement can be thought of as a two-step process [38]. In the first step, called dissolution, the cement dissolves and releases ions into the mix water. The mix water is thus no longer pure, but an aqueous solution containing a variety of ionic species, called the pore solution. The gypsum and the cement minerals C_3S and C_3A are all highly soluble, meaning that they dissolve quickly. Therefore, the concentrations of ionic species in the pore solution increase rapidly, as soon as the cement and water are combined. Eventually the concentrations increase to the point that the pore solution is supersaturated, meaning that it is energetically favorable for some of the ions to combine into new solid phases, rather than remain dissolved. The second step of the hydration process is called precipitation. A key point, of course, is that these new precipitated solid phases, called hydration products, are different from the starting cement minerals. Precipitation relieves the super saturation of the pore solution and allows dissolution of the cement minerals to continue [39]. Thus, cement hydration is a continuous process by which the cement minerals are replaced by new hydration products, with the pore solution acting as a necessary transition zone between the two solid states [40]. The reactions between Portland cement and water have been studied for more than a hundred years, and the fact that hydration proceeds by a dissolution-precipitation process was first elaborated by the famous chemist Le Chatelier [41].

Each of the four main cement minerals reacts at a different rate and tends to form different solid phases when it hydrates. The behavior of each of these minerals has been studied and presented in several papers [42] by synthesizing it in its pure form and hydrating it under controlled conditions. During the actual cement hydration process, all the minerals dissolve into the same pore solution, and thus the solid hydration products are associated with the pore solution as a whole, rather than a particular cement mineral. However, the individual reactions provide a good approximation of the overall hydration behavior of cement [43].

2.2.3.1 Hydration of calcium silicate mineral (C_3S and C_2S)

Tricalcium silicate (C_3S) is the most abundant and important cement mineral in Portland cements, contributing most of the early strength development. The hydration of C_3S can be written as [44]:

$$C_3S + (1.3 + x)H \rightarrow C_{1.7}SH_x + 1.3CH \qquad (2.1)$$

where 1.7C-S-H_x is the calcium silicate hydrate (C-S-H) gel phase and CH is calcium hydroxide, which has the mineral name Portlandite. The variable x in equation 2.1 represents the amount of water associated with the C-S-H gel, which varies from about 1.4 to 4, depending on the relative humidity inside the paste and on how much of the water associated with the C-S-H is considered to be part of its actual composition. The kinetics of hydration of C_3S is substantially similar to those of Portland cement as a whole. Much of the reaction occurs during the first few days, leading to substantial strength gains and reduction in capillary porosity. The dicalcium silicate phase (C_2S) reacts according to [45]:

$$C_2S + (0.3 + x)H \rightarrow C_{1.7}SH_x + 0.3CH \qquad (2.2)$$

The hydration products are the same as those of C_3S, but the relative amount of CH formed is less. C_2S is much less soluble than C_3S, so the rate of hydration is much slower. C_2S hydration contributes little to the early strength of cement, but makes substantial contributions to the strength of mature cement paste and concrete.

2.2.3.2 Hydration of calcium aluminate/ferrite mineral (C_3A and C_4AF)

The hydration of the aluminate and ferrite minerals is somewhat more complex than that of the calcium silicate minerals, and the reactions that occur depend on whether sulphate ions are present in the pore solution [46]. C_3A is highly soluble, even more so than C_3S. If C_3A is hydrated in pure water, calcium aluminate hydrates form. The reaction sequence is [47]:

$$2C_3A + 21H \rightarrow C_4AH_{19} + C_2AH_8 \rightarrow 2C_3AH_6 + 9H \qquad (2.3)$$

where the first reaction is very rapid and the second reaction occurs more slowly. The final reaction product, C_3AH_6, is called hydrogarnet. The initial reaction is so rapid that if it is allowed to occur in a Portland cement paste it would release large amounts of heat and could cause the paste to set within a few minutes after mixing, an undesirable condition known as flash set. The purpose of adding gypsum (CSH_2) to Portland cement is to prevent this from happening. The gypsum is also highly soluble, rapidly releasing calcium and sulphate ions into the pore solution [48]. The presence of the sulphate ions causes the C_3A to undergo a different hydration reaction. The reaction of C_3A and gypsum together is [49]:

$$C_3A + 3CSH_2 + 26H \rightarrow C_6AS_3H_{32} \qquad (2.4)$$

where $C_6AS_3H_{32}$ is the mineral ettringite. Since all Portland cements contain gypsum, equation 2.4 is the main hydration reaction for C_3A. Small amounts of hydrogarnet formed by equation 2.3

can sometimes be found in cement pastes. However, if the gypsum in the cement reacts completely before the C_3A, then the concentration of sulphate ions in the pore solution decreases drastically and the ettringite becomes unstable and converts to a different solid phase with less sulphate [50]:

$$2C_3A + C_6AS_3H_{32} + 4H \rightarrow 3C_4ASH_{12} \quad (2.5)$$

where the new reaction product, C_4ASH_{12}, is called monosulfoaluminate. Most cement does not contain enough gypsum to react with all of the C_3A, and as a result, most or all of the ettringite is converted to monosulfoaluminate within the first day or two of hydration via the reaction of equation 2.5.

Reactions 2.4 and 2.5 are both exothermic and contribute to the heat of hydration of cement. The early hydration of C_3A to form ettringite via equation 2.4 is quite rapid. The ferrite phase (C_4AF) reacts in a similar fashion to the C_3A (equations 2.1-2.5), but more slowly. One important difference is that some of the aluminum in the reaction products is substituted for iron. The amount of substitution depends on many factors, including the composition of the C_4AF and the local conditions in the paste. A convenient way to represent these reactions is [41]:

$$C_4AF + 3CSH_2 + 21H \rightarrow C_6(A,F)S_3H_{32} + (F,A)H_3 \quad (2.6)$$

$$C_4AF + C_6(A,F)S_3H_{32} + 7H \rightarrow 3C_4(A,F)SH_{12} + (F,A)H_3 \quad (2.7)$$

where (A,F) indicates aluminum with variable substitution of iron, and (F,A) indicates iron with variable substitution of aluminum. The $(F,A)H_3$ is an amorphous phase that forms in small amounts to maintain the correct reaction stoichiometry. Due to the substituted iron, the main reaction products are not pure ettringite and monosulfoaluminate, although they have the same crystal structure [51]. Instead, cement chemists have given them the names AFt and AFm,

respectively, where the m indicates monosulphate (one sulphate ion) and the t indicates trisulphate [52]. In a Portland cement paste where the C_3A and C_4AF are intimately mixed together, it can be safely assumed that the aluminum-bearing reaction products are never completely free of iron, and so the terms AFm and AFt are more correct [53]. However, as with the terms alite (impure C_3S) and belite (impure C_2S), this is a bit more confusion than many people are willing to deal with, and thus the terms ettringite and monosulfoaluminate are commonly used to refer to these phases in cement pastes [51].

2.2.3.3 Reaction with additional sulphate ions

As noted above, most Portland cements do not contain enough added gypsum to fully hydrate the C_3A and C_4AF via reactions 2.4 and 2.6 to form ettringite. Once the gypsum is consumed, the ettringite reacts with the remaining C_3A and C_4AF to form a new lower-sulphate phase called monosulphate (reactions 2.5 and 2.7). Thus in a mature Portland cement paste it is normal to find monosulphate and little or no ettringite. However, if a new source of sulphate ions becomes available in the pore solution, then it becomes thermodynamically favorable to form ettringite again, just as it was initially. This will occur at the expense of the existing monosulphate [53]:

$$C_4ASH_{12} + 2CSH_2 + 16H \rightarrow C_6AS_3H_{32} \qquad (2.8)$$

where it is understood that the A sites will contain some F. The gypsum on the left side of equation 2.8 represents the equivalent amount of dissolved ion, as no solid gypsum need form in the paste. Reaction 2.8 is more than just a theoretical point: in fact, it is all too common for sulphate ions present in ground water, sea water, and soil to diffuse into concrete, allowing the reformation of ettringite to proceed [51]. This occurs primarily, but not exclusively, in concrete below ground

level, such as building foundations. The problem with this phenomenon is that reaction 5.8 is expansive, meaning that the ettringite occupies a larger volume than the monosulphate it replaces. Thus, expansive stresses are created that can cause cracking and other deterioration. Unfortunately, this is actually only the first step in the sulphate attack process, as once all of the monosulphate is consumed other chemical reactions can occur that further weaken the cement paste (assuming a continued ingress of sulphate ions) [54].

2.3 Composite concepts

A composite material is made by combining two or more materials to give unique combination of properties. This definition is found to be more general and can include metal alloys, plastic co-polymers, minerals and wood. One of the most unique composites is fiber-reinforced. They differ from the earlier mentioned materials in that their constituent materials are different at molecular level and are mechanically separable. The constituent materials together provide the desired properties but remain in their original forms. The final properties of the composite materials are often better than the matrix materials properties [55]. This study focus on fiber-reinforced composites.

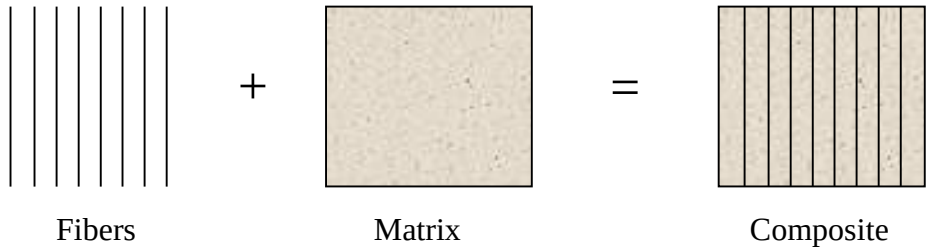

Fig. 2.4: Formation of a composite material

The main concept of a composite is that it is made up of matrix materials. Most composites are formed by reinforcing fibers in a certain matrix resin, as illustrated in Figure 2.4. The reinforcements can be fibers, particulates or whiskers and the matrix material can be metals, plastics or ceramics. Figure 2.4 shows a schematic diagram illustrating the formation of a composite.

In a composite, the fibers can be continuous, long or short. All these or only one form can be used in a composite. Most importantly is to note that the fiber carries the load and its strength is greatest along the axis of the fiber. Figure 2.5 shows the fiber forms in a composite.

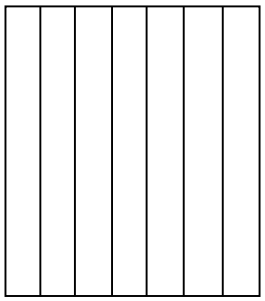

Continuous fiber composite

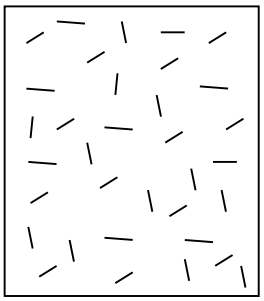

Shorter fiber composite

Figure 2.5: Fiber forms in a composite

Long continuous fibers in the direction of the load results in a composite with properties far better than the plain matrix. The same is obtainable with the shorter fibers except that it provides improved properties less than that offered by the continuous fiber composites. The fiber form is selected, depending on the application and manufacturing method.

2.4 Natural Fiber-reinforced Composites (NFRC)

The main purpose of reinforcement in composites is to increase their mechanical properties (strengths and fracture toughness), which literarily means to improve on the material's resistance to cracking by control of crack initiation and propagation. The reinforcement increases the composite material mechanical properties, if fiber reinforcement is sufficiently effective. For instance, the tensile strength of a given matrix may be low; much higher composite tensile strength can be obtained via various systems of reinforcement, including systems reinforced with natural fibers.

The classification of fibers was proposed by Gram *et al.* [56] as shown in Figure 2.6. This research is focused on only natural vegetal fibers. These are considered in more detail because of their importance and applications as reinforcements in brittle matrices. Natural fibers are prioritized because of their low cost and availability for local applications. They are also efficient as reinforcements.

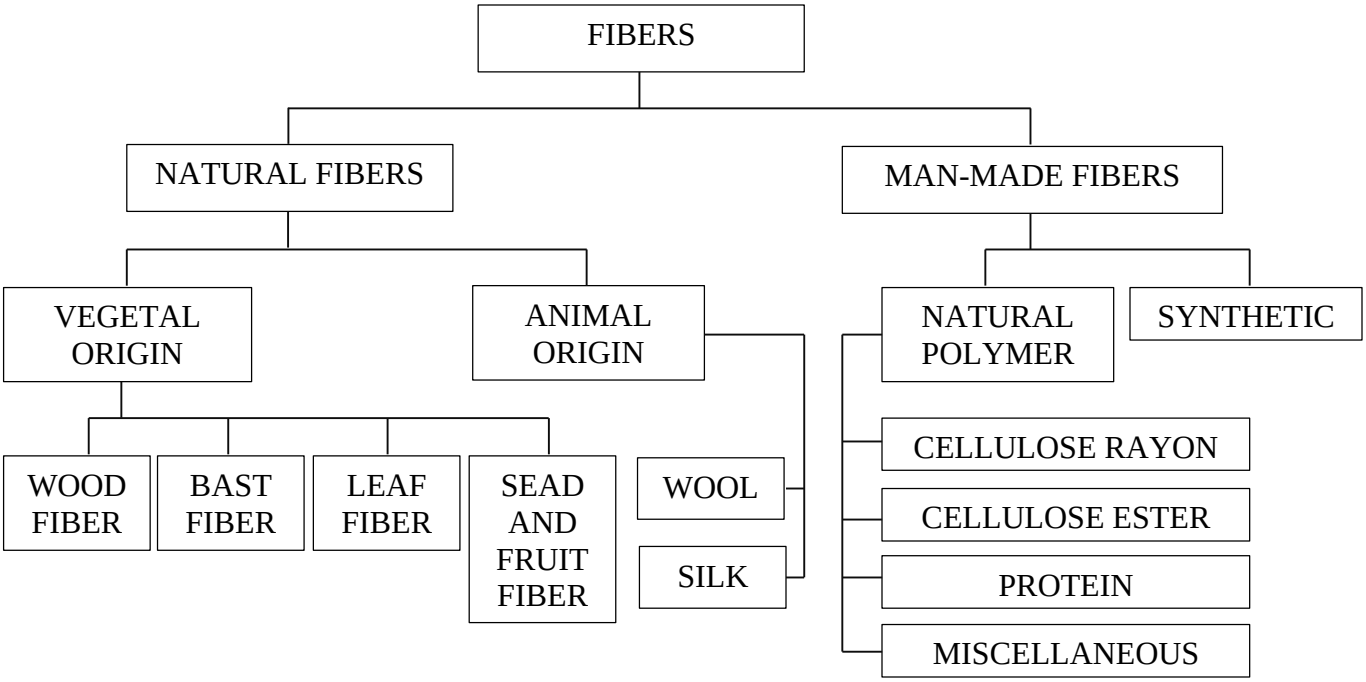

Figure 2.6: Classification of organic fibers, adapted from Gram et al. [56]

Composites produced with fiber reinforcement are expected to show increased strength and post-cracking resistance, sufficient fatigue strength and energy absorption at fracture. The influence of volume fraction on composite strength and fracture toughness will also be considered in this research. Various structural elements for low cost houses and non-structural elements can be achieved with earth-based materials reinforced with natural fibers. A short review of the application of vegetal fibers in cementitious composites is given by Brandt [57].

Several problems may arise in connection to fiber reinforcement of earth-based composites. One of such is durability. The durability of the fibers and of composite materials is endangered by biological attack (e.g. bacteria, fungus). The fiber's instability appears in high humidity and flow of moisture. All these factors are particularly significant in tropical climates. Hence, the effect of degradation on the composite mechanical properties will also be considered in this study. Another problem is the fiber-matrix bond, which is based mostly on mechanical interlocking. This study

will also elucidate the effect of fiber pull-out on the mechanical properties of natural fiber reinforced earth-based composites.

The amount of fibers in a cement matrix may vary from 0.1% to 0.9% of mass of cement [58, 59]. The dispersion of fiber properties is usually rather large because of natural variations in the plant population and simple production techniques. This also increases the variability of composite material properties. Vegetable fibers are also used to replace asbestos fibers, which are expensive and dangerous to health [57]. Coconut fibers were tested for that purpose and their strength and deformability, as well as thermal and acoustic properties, and were proved comparable with those of asbestos fibers [60]. Similar tests on specimens reinforced with flax fibers from New Zealand and Australia also showed their ability to replace asbestos in thin cement sheets [61]. Vegetable fibers are used mostly in developing subtropical and tropical countries in Africa and South-East Asia. They are used as reinforcement for concrete elements for housing. The application of cheap and locally available fibers may help considerably in the building of low-cost houses [62].

Wood fibers are produced in the form of chips, which is usually a waste material in the wood industry [63]. Wood chips mixed with cement paste have been used since the 1920s for the production of sheets applied for thermal insulation in housing. The chips are subjected to chemical pre-treatment to avoid any disturbance of cement hydration by organic acids. The application of wood-origin fibers as a reinforcement for minor structural elements has been developing at a local level [64]. Bast fibers (also known as phloem or skin fibers) are obtained from a few kinds of plants, for example, bamboo, hemp, flax, jute and ramie. The fibers are longer, stronger and stiffer than other vegetal fibers; jute fibers, for example, may be 3.0 m in length [65]. For reinforcement of brittle matrices the jute fibers are chopped for sections of 12–50 mm. Bamboo fibers have low Young’s moduli and tend to be used in the form of woven meshes [66].

Leaf fibers are mainly obtained from agave plants and are called sisal. Sisal is planted on an industrial scale in a few countries – the most important producers are Indonesia, Tanzania and Haiti [67]. Sisal fibers are chopped or used as continuous fibers up to 1.5 m in length for making non-woven mats. Their maximum strain to failure is 2–4% [68]. Sisal fibers are also used as twine and spun with short chopped fibers and a small amount of steel fibers. Such a hybrid reinforcement has proved to be cheap and efficient [69].

Seed and fruit fibers are limited mostly to coconut coir applications as reinforcements [70]. The fibers are usually considered as waste in the production of copra from the coconuts. The fibers are extracted from the space between the external shell and the seed inside [71]. The maximum length of the fibers is about 300 mm, with a maximum strain to failure of around 30%. The fibers are also used to produce ropes and mats. Other plants with fibers applicable for reinforcement are: sugarcane bagasse, akwara, elephant grass, water reed, plantain and musamba [72].

2.5 Mechanical Properties of Natural Fiber-reinforced Composites

The literatures on natural fibers that are used in cement composites have increased recently [73-75]. The results suggest some advantages of natural fibers when used in cement-based composites. Among them is increased flexural strength, post-crack load bearing capacity and impact toughness [76, 77]. Natural fibers generally improve the mechanical properties of composites, when compared to the matrix materials [78-85]. When compared with synthetic fibers, natural fibers also offer significant cost reductions [86, 87]. They are therefore, being considered as replacements to synthetic fibers [88].

2.5.1 Strength and fracture toughness of NFRC

During last two decades, a number of papers have appeared in which wood fibers are the sole source of fiber reinforcement. These studies have included chemical and mechanical pulps of softwoods and hardwoods in air-cured and autoclaved matrices [89-91]. In most developed countries, Wood fiber reinforced cement (WFRC) products are well known and are commercially used with a high acceptance for building purposes because the reinforcement provides improved strengths and toughness [92]. In a related study, Agopyan and John [93] showed that natural fiber-reinforced cement-based materials (NFRC) prepared with low alkali cements; provide an alternative for low cost buildings.

Brazilian agricultural wastes such as sisal and banana fibers, have been studied as possible reinforcement materials in cementitious matrix materials [94]. They compared the results with similar materials reinforced with chopped strands of vegetable fibers. Although vegetable pulp-reinforced cements present superior mechanical performance, the incorporation of 12% by weight of Brazilian waste fiber pulps in cement produced composites with modulus of rupture values of about 20 MPa and toughnesses in the range of 1.0-1.5 kJm^{-2}.

A report by Al-Oraimi and Seibi [95] revealed that the use of low percentage of natural fibers improved the mechanical properties and the impact resistance of concrete. The composites also had similar performance, when compared to synthetic fiber-reinforced concretes. In another paper [96], it was reported that concrete reinforced with natural fiber increases impact resistance 3–18 times than when no fibers were used. The use of small volumes (0.6–0.8%) of Arenga pinata fibers show capacity to increase the toughness in cement based composites [97]. Hemp fiber-reinforced

concrete leads to an increase of flexural toughness by 144%, and an increase in flexural toughness index by 214% [98].

Reis [99] showed that the mechanical properties of fiber polymer concrete can be influenced by the type of fiber. Their studies revealed that coconut and sugar cane bagasse fibers increases polymer concrete fracture toughness but banana pseudo stem fiber does not. Li et al. [100] reported that flexural toughness and flexural toughness index of cementitious composites with coir fiber increased by more than 10 times. In a study by Silva et al. [101], the addition of sisal fibers to concrete showed that compressive strength was lower than concrete samples without the fibers. The explanation given for such mechanical behavior was related to low concrete workability.

Savastano et al. [102] compared the mechanical performance of cement composites reinforced with sisal, banana and eucalyptus fibers. They found that blast furnace slag and ordinary Portland cement-based pastes reinforced with non-conventional Kraft pulps exhibited initiation fracture toughness levels between ~ 0.6 and 1.9 MPa$\sqrt{m}$, respectively. When compared to a report by Nelson et al. [103], this fracture toughness was considered significantly greater than that of the plain cement paste (0.2–0.3 MPa$\sqrt{m}$). The possibility of replacing steel reinforcement with bamboo was explored by Khare [104]. He reported that the ultimate load capacity of bamboo was about 35% of the equivalent reinforced steel concrete beams.

2.5.2 Resistance-curve measurement

The need for robust, sustainable and affordable housing has stimulated considerable research on natural fiber-reinforced composites consisting of cementitious matrices with natural fibers such as sisal [102, 105, 106], bamboo fibers [107, 108], eucalyptus fibers [94, 102, 109] and coconut fibers [110, 111]. Similarly, there have been several studies that have explored the use of steel fibers

[112-114] in the design of steel fiber-reinforced concrete. These studies have shown that both natural fiber-reinforced composites and steel fiber-reinforced cementitious composites results in resistance-curve behavior due to crack bridging.

Eissa and Batson [115] have studied the resistance-curve behavior of steel fiber-reinforced concrete with hooked-end and crimped fibers with fiber volume percentages between 1.0 and 1.5%. Their studies showed that the crimped fibers result in higher toughening than equivalent volume percentages of hooked-end fibers. Similar studies of resistance-curve behavior have been carried out by Savastano and co-workers [102] on cementitious composites with natural fibers [116]. These studies, which were carried out on composites with matrices produced from recycled blast furnace slag and ordinary Portland cement, have been used to explore the role of small- and large-scale bridging on the toughening of natural fiber-reinforced composites reinforced with pulped fibers of sisal, banana fibers and bleached eucalyptus pulp.

2.6 Rule-of-Mixture and Short Fiber Theory

2.6.1 Rule-of-mixture (ROM)

For a two phase whisker/fiber-reinforced composite, the strength may be estimated from rule of mixture. The constant strain rule of mixture assumes that the applied load is parallel to the fiber direction. This gives [117]:

$$\sigma_c = V_m\sigma_m + V_f\sigma_f\eta_f\eta_o \tag{2.9}$$

where V_m and V_f are volume fractions of the matrix and fiber, respectively while σ_m and σ_f are matrix and fiber strengths, respectively. The parameters η_f corresponds to a fiber length efficiency,

while η_o corresponds to the fiber orientation efficiency that will be discussed in the next sub-section.

2.6.2 Short fiber theory (SFT)

In the case of short fibers/whiskers, the average fiber stresses are less than those associated with long fibers. Under such condition, the average fiber stress is given by [117]:

$$\bar{\sigma}_f = \left(\frac{1}{2}\right)\sigma_f\left(\frac{l}{l_c}\right) \tag{2.10}$$

This expression for the average fiber strength can be substituted into the simple rule of mixture theory for very short fiber lengths. Hence, the average fiber strength for very short fibers is given by:

$$\bar{\sigma}_f = \left(\frac{l}{2l_c}\right)\sigma_f = \eta_f\sigma_f \tag{2.11}$$

where the term $\frac{l}{2l_c}$ is known as the fiber efficiency factor (η_f) for short fibers, and l_c is the critical fiber length. For fibers of intermediate lengths, the fiber efficiency is given by [118]:

$$\eta_f = \left[1 - \left(\frac{l_c}{2l}\right)\right] \tag{2.12}$$

where l is the fiber length, and l_c is the critical fiber length. In this case, the average fiber strength is now given by:

$$\bar{\sigma}_f = \left[1 - \frac{l_c}{2l}\right]\sigma_f = \eta_f\sigma_f \tag{2.13}$$

Finally, the orientation efficiency factor (η_o) accounts for the decrease in composite strength due to random orientations of the fibers. When this is taken into consideration, the average fiber strength is now given by [119]:

$$\bar{\sigma}_f = \eta_o \eta_f \sigma_f \tag{2.14}$$

where η_o have values of 0.375 and 0.2 for random two-dimensional and three-dimensional orientation respectively [220]. The composite strengths are given by equation 2.9.

2.7 Toughening Mechanisms

In order to improve the low intrinsic toughness of materials, extrinsic toughening techniques that provide crack-tip shielding mechanisms are often developed [221]. Such mechanisms, which include crack bridging via ductile or brittle reinforcements, primarily act behind the crack tip and locally shield the crack from the applied driving force. During toughening of materials, it is apparent to note that the source of the toughness in the material is associated principally with the crack-tip shielding that result from the bridging in the wake of the crack [222]. Quantitatively, the contribution to the toughness as a result of the crack bridging can be obtained by calculating the reduction in the near-tip intensity K_b, caused by the appropriate crack surface traction stress distribution. Another mechanism which contributes to toughness of brittle matrix is fiber pullout. This is achieved via frictional bond stress between the fiber and matrix.

2.7.1 Crack Bridging

The toughening due to crack bridging by the straw fibers can be modeled and added to the initiation fracture toughness to predict the resistance-curve behavior [221]. This need to be done for small-scale bridging (SSB) [223] and large-scale bridging (LSB) [224]. A small scale bridging model was proposed by Budiansky et al. [223] for modeling the initial stages of stable crack growth (bridge length < 0.5 mm) [225].

Under SSB conditions, the shielding due to crack bridging ΔK_{SSB} is given by [221]:

$$\Delta K_{SSB} = \alpha V_f \sqrt{\frac{2}{\pi}} \int_0^L \frac{\sigma_y}{\sqrt{x}} dx \tag{2.15}$$

where α is the constraint/triaxiality factor (theoretically between 1 and 3 and taken as ~ 3 in this study) [225], V_f is the volume fraction of the reinforcement phase, L is the bridging length (the distance from the crack-tip to the last unfractured reinforcement), σ_y is the uniaxial yield stress, and x is the distance from the crack face behind the crack-tip as described by Savastano et al. [226].

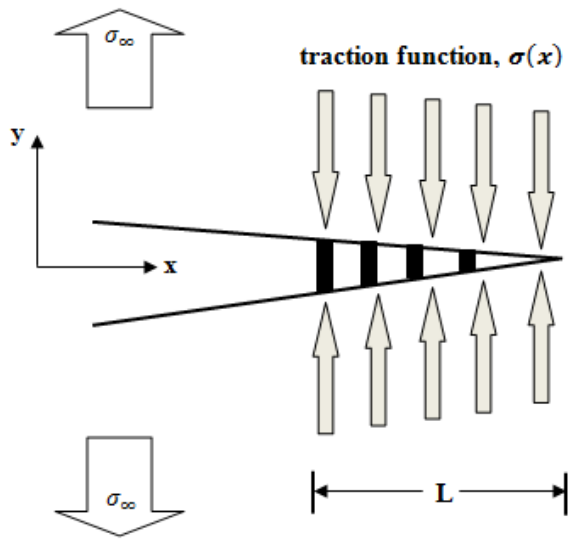

Figure 2.6: Schematic representation of a large scale bridging model [24]

For large-scale crack bridging (LSB) conditions, the contribution to composite toughness due to crack bridging [224, 227] can be modeled. The model uses a weighting function by Fett and Munz [228] to estimate the weighted distributions of bridging traction across the reinforcements as shown schematically in Figure 2.6. The shielding from large scale bridging, ΔK_{lsb}, is given by [224]:

$$\Delta K_{lsb} = V_f \int_L \alpha \sigma_y h(a,x) dx \qquad (2.16)$$

where α is the constraint/triaxiality factor (theoretically between 1 and 3 and taken as ~3 in this study) [225], V_f is the volume fraction of the reinforcement phase, L is the bridging length, σ_y is the uniaxial yield stress and x is the distance from the last unfractured fiber to the crack-tip. Also, $h(a,x)$ is the weighting function given by Fett and Munz [228] to be:

$$h(a,x) = \sqrt{\frac{2}{\pi a}} \frac{1}{\sqrt{1-\frac{x}{a}}} \left[1 + \sum_{(\nu,\mu)} \frac{A_{\nu,\mu}\left(\frac{a}{W}\right)}{\left(1-\frac{a}{W}\right)} \left(1-\frac{x}{a}\right)^{\nu+1}\right] \quad (2.17)$$

where a is the crack length and w is the specimen width. The coefficients $(A_{\nu,\mu})$ are given in Table 2.2 for the SENB specimen.

Table 2.2: Summary of Fett and Munz [228] parameters for SENB specimen

ν	μ				
	0	1	2	3	4
0	0.4980	2.4463	0.0700	1.3187	-3.067
1	0.5416	-5.0806	24.3447	-32.7208	18.1214
2	-0.19277	2.55863	-12.6415	19.7630	-10.986

Hence, the expression for the estimation of the composite fracture toughness:

$$K_R = K_i + \Delta K_B \quad (2.18)$$

where K_R is the composite fracture toughness characterized by the resistance-curve and ΔK_B is the shielding due to crack bridging. Note that $\Delta K_B = \Delta K_{SSB}$ for small-scale bridging and $\Delta K_B = \Delta K_{LSB}$ for large scale bridging.

2.7.1 Fiber Pullout

The interfacial property (bonding) between matrix and fibers is key to composite behaviors and properties in fiber-reinforced composite [229]. Best toughening conditions for ceramic matrix composites may require debonding at the interfaces and frictional sliding between the fibers and the matrix [230]. These essential conditions have motivated the studies of interfacial properties of composite materials. The mechanics of debonding have been studied by an appreciable number of authors [231].

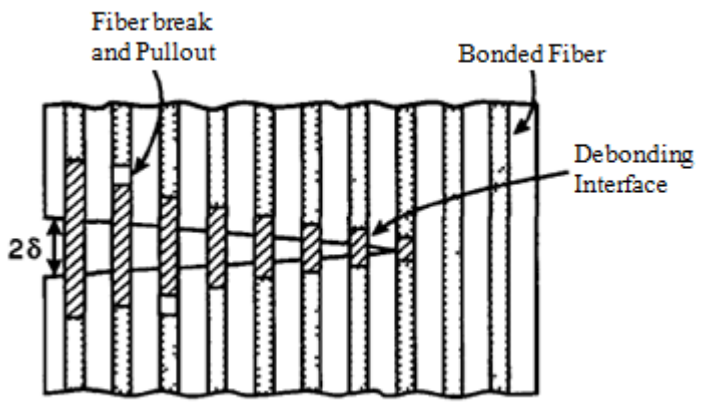

Figure 2.7: Schematic of fiber debonding and pullout

The study of interfacial properties of fiber-reinforced composites using fiber pull-out test has provided significant results [232]. During fiber pull-out test, the initial debonding requires an applied stress greater than the bonding between matrix and fiber. Subsequent stress will then be required to overcome the interfacial frictional stress along the fiber embedded length [233].

In brittle-matrix composites, interface properties are significant in determining their mechanical behavior. This has motivated several researchers to study the fiber/matrix interface properties in

such composites. An investigation by Marshall et al. and other authors was focused at determination of the force required to slip a fiber through a matrix [234, 235]. Other efforts centered on measuring interfacial strength via fiber pull-out tests [236, 237]. For cement matrix composites, there have been considerations of load-deflection behavior in fiber pull-out process [238-239]. When the fiber and matrix surfaces are loaded by a constant frictional stress τ and slides but not lose contact, the variation of K_2 is approximated as [240]:

$$K_2/\left(\tau {r_f}^{1/2}\right) = (1-\rho)^{-1/2}\left(l/r_f\right) \tag{2.19}$$

References

[1] Davy R and El-Ansary M. Geochemical patterns in the laterite profile at the Boddington gold deposit, Western Australia. Journal of Geochemical Exploration 1986. Volume 26, Issue 2, Pages 119–144.

[2] Elias, M. "Nickel laterite deposits: Geological overview, resources and exploitation." Giant ore deposits: characteristics, genesis and exploration. Center for Ore Deposits Research, University of Tasmania, Special Publication 4 (2002): 205-220.

[3] Herbilion, A. J., and D. Nahon. "Laterites and laterization processes." *Iron in Soils and Clay Minerals*. Springer Netherlands, 1988. 779-796.

[4] Thorne RL., Roberts S., and Herrington R. "Climate change and the formation of nickel laterite deposits." *Geology* 40.4 (2012): 331-334.

[5] Thurston, Edgar (1913): The Mandras Presidency, with Mysore, Coorg and the associated states, Provincial Geographic of India. Cambridge University press.

[6] Tardy, Yues (1997): Petrology of laterites and tropical soils. ISBN 90-5410-678-6.

[7] Grace, Hanry (1991). “Investigation in Kenya and Malawi using as-dug laterite as bases for bituminous surfaced roads”. Journal Geotechnical and Geological Engineering. Springer Netherland.

[8] Wood, R.B. and Macatamney, C.F. (1996). “Constructed waste lands for waste water treatments: The use of laterite in the bed medium in phosphorous and heavy metal removal”. Hydro biological, Springer Netherland.

[9] Reeves GM., Sims I, and Cripps JC, eds. "Clay materials used in construction." Geological Society of London, 2006.

[10] Righi, D., and Meunier A. "Origin of clays by rock weathering and soil formation." *Origin and mineralogy of clays*. Springer Berlin Heidelberg, 1995. 43-161.

[11] Ehlmann BL., Mustard JF, Murchie SL, Bibring JP. "Subsurface water and clay mineral formation during the early history of Mars." *Nature* 479.7371 (2011): 53-60.

[12] Blight B E. "Origin and formation of residual soils." *Mechanics of Residual Soil* (1997): 1-15.

[13] Guggenheim, Stephen and Martin, R.T. (1995). “Definition of clay and clay mineral: Journal report of the AIPEA nomenclature and CMS nomenclature committees”, clay and clay minerals 43:255-256.

[14] Moore, D. and R.C. Reynolds, Jr., 1997, X-Ray Diffraction and the Identification and Analysis of Clay Minerals, 2nd ed.: Oxford University Press, New York.

[15] Hillier, S. (2003), “Clay Mineralogy. In: Encyclopedia of sediments and sedimentary rocks”. Kluwer Academic Publishers, Dordrecht. pp 139-142.

[16] Schiesser A. et al., (1989): “Fine structure and Mechanical properties of Straw Filaments”. Biological Wastes 27, 87-100.

[17] Oss, H G., and Amy C P. "Cement Manufacture and the Environment: Part I: Chemistry and Technology." *Journal of Industrial Ecology* 6.1 (2002): 89-105.

[18] Avşar, Hakan. Control, optimization and monitoring of Portland cement (PC 42.5) quality at the ball mill. Diss. İzmir Institute of Technology, 2006.

[19] Tzouvalas, G., G. Rantis, and S. Tsimas. "Alternative calcium-sulphate-bearing materials as cement retarders: Part II. FGD gypsum." Cement and concrete research 34.11 (2004): 2119-2125.

[20] Stephan D, Mallmann R, Knöfel D and Härdtl, R. (1999). High intakes of Cr, Ni, and Zn in clinker: Part I. Influence on burning process and formation of phases. Cement and concrete research, 29(12), 1949-1957.

[21] Potgieter, J H, and Hanno K. "Hydration of Cement." South African Journal of Chemistry 52.4 (1999).

[22] Felekoğlu, B, Türkel, S and Baradan, B. Effect of water/cement ratio on the fresh and hardened properties of self-compacting concrete. *Building and Environment 2007*, *42*(4), 1795-1802.

[23] Taylor, J. C., Hinczak, I., and Matulis, C. E. (2000). Rietveld full-profile quantification of Portland cement clinker: The importance of including a full crystallography of the major phase polymorphs. *Powder diffraction*, *15*(01), 7-18.

[24] Lee, S. J., & Kriven, W. M. (2005). Synthesis and hydration study of Portland cement components prepared by the organic steric entrapment method. *Materials and structures*, *38*(1), 87-92.

[25] Midgley, H. G. (1968). The composition of alite (tricalcium silicate) in a Portland cement clinker. *Magazine of Concrete Research*, *20*(62), 41-44.

[26] Bigare, M., Guinier, A., Mazieres, C., Regourd, M., Yannaquis, N., Eysbl, W., ... & Woermann, E. (1967). Polymorphism of tricalcium silicate and its solid solutions. *Journal of the American Ceramic Society*, *50*(11), 609-619.

[27] Tadros, M. E., Skalny, J. A. N., and Kalyoncu, R. S. (1976). Early hydration of tricalcium silicate. *Journal of the American Ceramic Society*, *59*(7-8), 344-347.

[28] Barnes, P., Fentiman, C. H., and Jeffery, J. W. (1980). Structurally related dicalcium silicate phases. *Acta Crystallographica Section A: Crystal Physics, Diffraction, Theoretical and General Crystallography*, *36*(3), 353-356.

[29] de lA Torre, A. G., ArAndA, M. A. G., de AzA, A. H., PenA, P., & de AzA, S. (2005). Clínqueres Pórtland Belíticos. Síntesis y Análisis Mineralógico. *Boletín de la Sociedad Española de Cerámica y Vidrio*, *44*(3), 185-191.

[30] Taylor H.F.W., Cement Chemistry, Thomas Telford, London, 2nd Ed., 1997.

[31] Schindler A. K. and Folliard, K. J. (2005). Heat of hydration models for cementitious materials. *ACI Materials Journal*, *102*(1).

[32] Clifton, J. R. and Ponnersheim, J. M. (1994). Sulphate attack of cementitious materials: volumetric relations and expansions. *NIST IR*, *5390*.

[33] Mondal P. and Jeffery, J. W. (1975). The crystal structure of tricalcium aluminate, Ca3Al2O6. *Acta Crystallographica Section B: Structural Crystallography and Crystal Chemistry*, *31*(3), 689-697.

[34] Jawed I. and Skalny, J. (1977). Alkalies in cement: A review I. Forms of Alkalies and their effect on clinker formation. *Cement and Concrete Research*, *7*(6), 719-729.

[35] Fletcher, K. E. (1969). The composition of the tricalcium aluminate and ferrite phases in Portland cement determined by the use of an electron-probe microanalyser*. *Magazine of Concrete Research*, *21*(66), 3-14.

[36] Desmoulins, H., Malo, S., Boudin, S., Caignaert, V., and Hervieu, M. (2009). Polymorphism of the iron doped strontium aluminate. *Journal of Solid State Chemistry*, *182*(7), 1806-1820.

[37] Monshi, A. and Asgarani, M. K. (1999). Producing Portland cement from iron and steel slags and limestone. *Cement and Concrete Research*, *29*(9), 1373-1377.

[38] Bensted, J. (2003). Hydration of Portland cement. *Advances in Cement Technology: Chemistry, Manufacture and Testing (2nd edition)(Editor: SN Gosh)*, 31-86.

[39] Potgieter, J. H. and Kaspar, H. (1999). Hydration of Cement. *South African Journal of Chemistry*, *52*(4).

[40] Bullard, J. W., Jennings, H. M., Livingston, R. A., Nonat, A., Scherer, G. W., Schweitzer, J. S. and Thomas, J. J. (2011). Mechanisms of cement hydration. *Cement and Concrete Research*, *41*(12), 1208-1223.

[41] Kosmatka S.H., Kerkhoff B. and Panarese W.C., Design and Control of Concrete Mixtures, Portland Cement Association, Skokie, IL. 14th Ed., 2002.

[42] S. Barnett and D. Brew, "DCC@aberdeen: Database of cementitious material synthesis," http://www.abdn.ac.uk/chemistry/research/cement/dcc/index.htm.

[43] T.D. Dyer, J.E. Halliday, and R.K. Dhir, "An investigation of the hydration chemistry of ternary blends containing cement kiln dust," *J. Mater. Sci.* **34**, pp. 4975-4983 (1999).

[44] Nonat, A., & Lecoq, X. (1998). The structure, stoichiometry and properties of CSH prepared by C3S hydration under controlled condition. In *Nuclear magnetic resonance spectroscopy of cement-based materials* (pp. 197-207). Springer Berlin Heidelberg.

[45] Trettin, R., Oliew, G., Stadelmann, C. and Wieker, W. (1991). Very early hydration of dicalcium silicate-polymorphs. *Cement and concrete research*, *21*(5), 757-764.

[46] Tennis, P. D. and Jennings, H. M. (2000). A model for two types of calcium silicate hydrate in the microstructure of Portland cement pastes. *Cement and Concrete Research*, *30*(6), 855-863.

[47] Sorrentino, D., Sorrentino, F. and George, M. (1995). Mechanisms of hydration of calcium aluminate cements. *Mater. Sci. Concrete IV, Ed. J. Skalny, S. Mindess, Am. Ceram. Soc., Weterville, Ohio*, 41-90.

[48] Diamond, S. (1983, June). Alkali reactions in concrete-pore solution effects. In *Proceedings of the 6th International Conference on AAR, Copenhagen* (pp. 155-167).

[49] Minard, H., Garrault, S., Regnaud, L., & Nonat, A. (2007). Mechanisms and parameters controlling the tricalcium aluminate reactivity in the presence of gypsum. *Cement and Concrete Research*, *37*(10), 1418-1426.

[50] Lerch, W. (1946). *The influence of gypsum on the hydration and properties of Portland cement pastes*. Portland Cement Association.

[51] Renaudin, G., Segni, R., Mentel, D., Nedelec, J. M., Leroux, F. and Taviot-Gueho, C. (2007). A Raman study of the sulphated cement hydrates: ettringite and monosulfoaluminate. *Journal of Advanced Concrete Technology*, *5*(3), 299-312.

[52] Casanova, I., Aguado, A. and Agullo, L. (1997). Aggregate expansivity due to sulfide oxidation—II. Physico-chemical modeling of sulphate attack. *Cement and concrete research*, *27*(11), 1627-1632.

[53] Ingram, K., Poslusny, M., Daugherty, K. and Rowe, W. (1990). Carboaluminate reactions as influenced by limestone additions. *Carbonate additions to cement*, 14-23.

[54] K.J. Wang, M.S. Konsta-Gdoutos, and S.R. Shah, “Hydration, rheology, and strength of ordinary Portland cement (OPC)-cement kiln dust (CKD)-slag binders,” ACI Mater. J. 99, pp. 173-179 (2002).

[55] Sanjay, K. Mazumdar (2002),”Composites manufacturing; Materials, Products and Process Engineering”, CRC press LLC.

[56] Gram, H. E., Persson, H., Skarendahl, Å. (1984) *Natural Fibre Concrete*, Stockholm: Swedish Agency for Research Cooperation with Developing Countries.

[57] Brandt, A. M., Kucharska, L. (1999) 'Developments in cement-based materials,' in: *Proc. Int. Sem. Extending Performance of Concrete Structures*, R. K. Dhir and P. A. J. Tittle eds, Dundee; Thomas Telford: pp. 17–32.

[58] Rafiqul Islam, M. D., Khorshed Alam, A. K. M. (1987) 'Study of fiber reinforced concrete with natural fibers', in: Proc. of Int. Symp. Fibre Reinforced Concrete, Madras, 16–19 December, pp. 3.41–3.53.

[59] Singh, R. N. (1987) 'Flexure behaviour of notched coir reinforced concrete beams under cycle loading', in: Proc. of Int. Symp. Fiber Reinforced Concrete, Madras, 16–19 December, pp. 3.55–3.66.

[60] Paramasivam, P., Nathan, G. K., Das Gupta, N. C. (1984) 'Coconut fiber reinforced corrugated slabs', International Journal of Cement Composites and Lightweight Concrete, 6(1): 151–8.

[61] Coutts, R. S. P. (1983) 'Flax fibers as reinforcement in cement mortars', International Journal of Cement Composites and Lightweight Concrete, 5(4): 257–62.

[62] Nilsson, L. (1975) 'Reinforcement of concrete with sisal and other vegetal fibers', Swedish Council for Building Research, Doc. D14.

[63] Pehanich J, Blankenhorn P, Silsbee M. Wood fiber surface treatment level effects on selected mechanical properties of wood fiber-cement composites. Cem Concr Res 2004;34:59–65.

[64] Coutts, R.S.P. (1979a) Wood fiber reinforced cement composites. CSIRO Division of Chemical Technology. Research Review 1979.

[65] Atchison J.E. (1983) Data on non-wood plant fibers. Pulp and Paper Manufacture Vol.1 Properties of fibrous raw materials and their preparation for pulping. (Ed. Kocurek, M.J. and Stevens, C.F.B.), TAPPI, U.S.A. 1983.

[66] Pakotiprapha, B., Pama, R.P. and Lee, S.L. (1983) Behaviour of a bamboo fiber-cement paste composite. J. Ferrocement 13, 235-248.

[67] Coutts, R.S.P. and Warden, P.G. (1992a) Sisal pulp reinforced cement mortar. Cement & Cone. Composites. 14,17-21

[68] Swift, D.G. and Smitii, R.B.L. (1979) The flexural strength of cement-based composites using low modulus (sisal) fibres. Composites 10,145-148.

[69] Mwamila, B. L. M. (1985) 'Natural twines as main reinforcement in concrete beams', International Journal of Cement Composites and Lightweight Concrete, 7(1):11–19.

[70] Asasutjarit C, Hirunlabh J, Khedari J, Charoenvai S, Zeghmati B and Cheul Shin U. development of coconut coir-based lightweight cement board. Construction and Building Materials 2007, 21:277-288.

[71] Paramasivam P, Nathant GK, Das Gupta NC. Coconut fiber reinforced corrugated slabs. Int J Cement Compos Lightweight Concrete 1984;6(1):19–27

[72] Swamy, R.N. 1990. "Vegetable fiber reinforced cement composites - a false dream or a potential reality?" In Sobral, H.S. (ed). "Proceedings, 2nd International Symposium on Vegetable Plants and their fibers as Building Materials". Rilem Proceedings 7. Chapman and Hall, London, 3-8.

[73] Aziz, M.A., Paramasivam, P. and Lee, S.L. (1981) 'Prospects for natural fiber reinforced concrete in construction', International Journal of Cement Composites and Lightweight Concrete, 3(2): pp. 123–132

[74] Pakatiprapha B, Pama RP, Lee SL. Analysis of a bamboo fiber–cement paste composite. J Ferro cement 1983;13(2):141–59.

[75] Morrissey FE, Morrissey FE, Coutts RSP. Bond between cellulose fibers and cement. Int J Cement Compos Lightweight Concrete 1985;7(2):73–80.

[76] Do LH, Lien NT. Natural fiber concrete products. J Ferrocement 1995;25(25):17–24.

[77] Semple K, Evans D. Adverse effects of heartwood on the mechanical properties of wood wool cement boards manufactured from radiata pinewood. Wood Fiber Sci 1999;32:37–43.

[78] Brandt AM. Cement-based composite: materials, mechanical properties and performance. London: E & FN SPON; 1995. p. 90–1.

[79] Castro J, Naaman AE. Cement mortar reinforced with natural fibers. ACI J 1981;78-6:69–78.

[80] Swamy RW. Natural fibre reinforced cement and concrete. Glasgow, Great Britain: Bell & Bain; 1988. p. 285.

[81] Sera EE, Robles-Austriaco L, Pama RP. Natural fibers as reinforcement. J Ferrocement 1990; 20(2):109–24.

[82] Balaguru PN, Shah SP. Fibre-reinforced cement composites. Singapore: McGraw-Hill; 1992. p. 110–14.

[83] Aggarwal LK. Bagasse-reinforced cement composites. Cement Concrete Compos 1995;17:107–12.

[84] Toledo Filho RD, Ghavami K, England GL, Scrivener K. Development of vegetable fiber mortar composites of improved durability. Cement Concrete 2003;25:185–96.

[85] Bilba K, Arsene M-A, Ouensanga A. Sugar cane bagasse fiber reinforced cement composites. Part I. Influence of the botanical components of bagasse on the setting of bagasse/cement composite. Cement Concrete Compos 2003;25:91–6.

[86] Swift DG. Sisal-cement composites as low-cost construction material. Appropriate Technol 1979;6(3):6–8.

[87] Aziz MA, Paramasivam P, Lee SL. Natural fiber reinforced concrete in low-coat housing construction. J Ferrocement 1987; 17(3):231–40.

[88] Thielemans W, Wool RP. Butyrated kraft lignin as compatibilizing agent for natural fiber reinforced thermoset composites. Compos Part A: Appl Sci Manuf 2004;35:327–38.

[89] Coutts, R.S.P. and Warden, P.G. (1985) Air-cured wood pulp fibre cement composites. Mater. Sci. Lett. A, 117-119.

[90] Coutts, R.S.P. (1986) High yield wood pulps as reinforcement for cement products. Appita 39(1), 31-35.

[91] Coutts, R.S.P. (1987a) Eucalyptus wood fiber reinforced cement. /. Mater. Sci. Lett. 6, 955-951.

[92] Coutts RSP. Sticks and stones...!!. Forest Products Newsletter, CSIRO Div Chem Wood Technol 1986;2(1):1-4.

[93] Agopyan V, John VM. Durability evaluation of vegetable fiber reinforced materials. Build Res Infor 1992;20(4):233-5.

[94] Savastano Jr H, Warden PG, Coutts RSP. Brazilian waste fibers as reinforcement for cement based composites. Cement Concr Compos 2000;22:379–84.

[95] Al-Oraimi S, Seibi A. Mechanical characterization and impact behavior of concrete reinforced with natural fibers. Compos Struct 1995;32:165–71.

[96] Ramakrishna G, Sundararajan T. Impact strength of a few natural fiber reinforced cement mortar slabs: a comparative study. Cem Concr Compos 2005;27:547–53.

[97] Razak A, Ferdiansyah T. Toughness characteristics of Arenga pinnata fibre concrete. J Nat Fibers 2005;2:89–103.

[98] Li Z, Wang L, Wang X. Compressive and flexural properties of hemp fiber reinforced concrete. Fibers Polym 2004;5:187–97.

[99] Reis J. Fracture and flexural characterization of natural fiber-reinforced polymer concrete. Constr Build Mater 2006;20:673–8.

[100] Li Z, Wang L, Wang X. Flexural characteristics of coir fiber reinforced cementitious composites. Fibers Polym 2004;7:286–94.

[101] Silva J, Rodrigues D, Dias. Compressive strength of low resistance concrete manufactured with sisal fiber. 51_ Brazilian congress of ceramics, Salvador, Brazil; 2007.

[102] Savastano H, Santos S, Radonjic M, Soboyejo W. Fracture and fatigue of natural fiber-reinforced cementitious composites. Cem Concr Compos 2009;31:232–43.

[103] Nelson PK, Li VC, Kamada T. Fracture toughness of microfiber reinforced cement composites. J Mater Civ Eng 2002;14(5):384–91.

[104] Khare L. Performance evaluation of bamboo reinforced concrete beams. Master of Science in Civil Engineering, University of Texas; 2005.

[105] Silva F A, Mobasher B, Filho R D. Cracking mechanisms in durable sisal fiber reinforced cement composites. Cement Concrete Composites 2009; 31(10):721-30.

[106] Silva F A, Filho R D, Filho J A, Fairbairn E M. Physical and mechanical properties of durable sisal fiber-cement composites. Construction and building Materials 2010; 24(5):777-85.

[107] Yao W, Li Z. Flexural behavior of bamboo‐fiber-reinforced mortar laminates. Cement Concrete Research 2003; 33(1):15-19.

[108] Li Z, Liu C P, Yu T. Laminate of Reformed Bamboo and Extruded Fiber-Reinforced Cementitious Plate. J. Mate. Civ. Eng., 2002; 14(5):359-365

[109] Tonoli G H D, Savastano Jr H, Fuente E, Negro C, Blanco A, Rocco Lahr F A. Eucalyptus pulp fibres as alternative reinforcement to engineered cement-based composites. Industrial Crops and Products 2010; 31(2):225-232.

[110] Bilba K, Arsene M A, Ouensanga A. Study of banana and coconut fibers: Botanical composition, thermal degradation and textural observations. Bioresources Technology 2007; 98(10):58-68.

[111] Asasutjarit C, Hirunlabh J, Khedari J, Zeghmati B, Cheul S U. Development of coconut coir-based lightweight cement board. Construction and Building Materials 2007; 21(2):277-88.

[112] Banthia N, Sappakittipakorn. Toughness enhancement in steel fiber reinforced concrete through fiber hybridization. Cement Concrete Research 2007; 18(2):1366-72.

[113] Bindiganavile V, Banthia N. Polymer and Steel Fiber-Reinforced Cementitious Composites under Impact Loading—Part 1: Bond-Slip Response. ACI Materials Journal 2001; 98(1):10-16.

[114] Naaman A E. Engineered steel Fibers with Optimal Properties for Reinforcement of Cement Composites. Journal of Advance Concrete Technology 2003; 1(3):241-252.

[115] Eissa A-B, Batson G. Model for predicting the fracture process zone and R-curve for high strength FRC. Cement Concrete Composites 1996; 18(2):125-33.

[116] Savastano Jr H, Warden PG, Cutts RSP. Microstructure and mechanical properties of waste fiber-cement composites. Cement Concrete Composites 2005; 27(5):583-92.

[117] Callister WD. Material Science and Engineering: An Introduction. 7th ed. John Wiley, New York; 2007. p. 414-459 [chapter 12].

[118] Ashbee KH. Fundamental Principles of Fiber Reinforced Composites, 2nd edition, Technomic Publishing Company, Lancaster, PA, 1993.

[119] Mallick PK. Fiber-Reinforced Composites, Materials, Manufacturing, and Design, 2nd edition, Marcel Dekker, New York, 1993.

[220] Soboyejo WO. Introduction to Composites. In: Mechanical properties of engineered materials. NY: Marcel Dekker Publisher; 2002. p. 269-87 [chapter 9].

[221] Soboyejo W O. Toughening mechanisms. Mechanical Properties of Engineered Materials. NY: Marcel Dekker Publishers; 2002. p. 414-55 [chapter 13].

[222] Li, M., Schaffer, H., and Soboyejo, W.O. (2000) J Mater Sci. vol. 35, pp 1339–1345.

[223] Budiansky B, Amazigo J C, Evans A G. Small-scale crack bridging and the fracture toughness of particulate-reinforced ceramics. J Mech Phys Solids 1988; 36(2): 167-87.

[224] Bloyer D R, Rao K T V, Ritchie R O. Fracture toughness and R-curve behavior of laminated brittle-matrix composites. Metal Meter Trans A 1998; 29A(10): 2483-96.

[225] Kung E, Mercer C, Allameh S, Popoola O, Soboyejo W O. An investigation of fracture and fatigue in a metal/polymer composite. Metall Mater Trans A 2001; 32A(8): 1997-2010.

[226] Savastano Jr H, Turner A, Mercer C, Soboyejo W O. Mechanical behavior of cement based materials reinforced with sisal fibers. J Mater Sci 2006; 41: 6938-48.

[227] Bloyer D R, Rao K T V, Ritchie R O. Fatigue-crack propagation behavior of ductile/brittle laminated composites. Metal Meter Trans A 1999; 30A(3): 633-42.

[228] Fett T, Munz D. Stress intensity factors and weight functions for one dimensional cracks. institut fur Materialforschung, Kernforschungszentrum Karlsruhe, Germany, 1994.

[229] Kelly A and Tyson WR. Tensile properties of fiber-reinforced metals. *J. Mech. Phys. Solids*, 13 (1965) 329-350.

[230] Becher PF, Hsueh CH, Angelini P and Tiegs TN. Toughening behavior in fiber-reinforced ceramic matrix composites. *J. Am. Ceram. Soc.*, 71 (12) (1988) 1050-1061.

[231] Broutman LJ. Modern Composite Materials ed Broutman LJ and Krock RH. New York: Addison-Wesley, 1967. Pp 391-394.

[232] Wells JK and Beaumont PWR. Debonding and pull-out processes in fibrous composites. *J. Mater. Sci.*, 1985, 20 (4) 1275-1284.

[233] Kerans, RJ and Triplicane AP. Theoretical analysis of the fiber pullout and pushout tests. *J. Am. Ceram. Soc.*, 1991, 74 (7) 1585-1596.

[234] Marshall DB and Oliver WC. Measurement of interfacial mechanical properties in fiber-reinforced ceramics composites. 1987, 70 (8) 524-548.

[235] Mandell JF, Kong KCC and Grande DH. Interfacial shear strength and sliding resistance in metal and glass-ceramic matrix composites. *Ceram. Eng. Sci. Proc.*, 1987, 8 (7-8) 937-940.

[236] Griffin CW, Limaye SY, Richardson DW and Shetty DK. Evaluation of Interfacial Properties in Borosilicate- SiC Composites using Pull-out Tests. *Ceram. Eng. Sci Proc.*, 1988, 72 (10) 671-678.

[237] Goettler RW and Faber KT. Interfacial shear stresses in SiC and Alumina Fiber Reinforced Glasses. *Ceram. Eng. Sci. Proc.*, 1988, 9 (7-8) 861-872.

[238] Greszczuk LB. theoretical studies of the mechanics of the fiber-matrix interface in composites. In: ASTM special technical publication, STP-452, Interfaces in Composites. American Society for Testing and Materials, Philadelphia, PA, 1969.

[239] Lawrence P. some theoretical considerations of fiber pull-out from an elastic matrix. *J. Mater. Sci.*, 1972 (7) 1-6.

[239] Takaku A and Arridge RGC. The effect of Interfacial radial and shear stress on fiber pull-out in composite materials. *J. Phys. D*, 1973 (6) 2038-2047.

[240] Hutchinson J W and Jenson H M. Models of fiber debonding and pullout in brittle composites with friction, Rep. MECH-157, Harvard University, Cambridge, MA, 1990.

CHAPTER THREE: STRENGTH AND FRACTURE TOUGHNESS OF EARTH-BASED NATURAL FIBER-REINFORCED COMPOSITES

3.1 Introduction

Although the choice of building materials is influenced by the cost and availability of robust materials [1], most developing countries have focused largely on the application of relatively expensive cementitious building materials that have been associated with ~5% of the global carbon dioxide emissions [2]. This has made it relatively difficult for poor people to afford durable homes in most developing countries. However, in most of these countries, there are large deposits of industrial, agricultural and human wastes that can be recycled into robust building materials that could make homes more affordable for a significant fraction of the world's rural and urban poor [3].

In the case of industrial wastes, such as blast furnace slag, Savastano et al. [4] have shown that wastes can be mixed with cements to produce robust materials that reduce the amount of cement that is needed to ensure adequate strength and fracture toughness in building materials. Similarly, natural fibers, such as sisal, eucalyptus fiber, bamboo fiber, coconut fiber and banana fiber have been incorporated into cementitious matrices to produce durable composites that are resistant to crack growth and fracture [5]. Such composites are now being used in eco-friendly housing that includes: roofing elements [6] and building blocks [7] that reduce the cost of building materials.

Recently, composite building materials have undergone various forms of optimization, with most attention being focused on the introduction of different types of reinforcements. A report reference [8] suggests that most developed countries have adopted wood fiber-reinforced cement products

for buildings. Hence, in an attempt to provide an alternative for low cost building materials, Agopyan and John [9] reported the use of natural fiber-reinforced cement based materials.

Savastano et al. [10] also studied the possibility of using Brazilian agricultural waste as fibers for reinforcement in cement-based composites. In their work, they used different types of Brazilian fibrous residues to reinforce cementitious matrices. These include: banana pseudo-stem fibers; waste Eucalyptus grandis pulp, and sisal field by-products. Using specimens with fiber mass percentages from 4% to 12%, they studied the dependence of strength and fracture toughness of these materials after 28 days of exposure to the laboratory air with a relative humidity of ~ 80%. Their results showed that composites reinforced with ~ 8% fiber had strengths that were ~ 65% greater than those of the unreinforced matrix materials. In a related study, Banthia and Sheng [11] predicted the effects of polymer fiber used as reinforcements in cement based matrix using resistance-curve approaches. At about 3% by volume of fibers, they were able to improve the matrix fracture toughness to levels of ~1.9 MPa$\sqrt{m}$.

Most recently, there was a study of the mechanical fracture and fatigue behavior of natural fiber-reinforced cement-based materials [12]. Their results showed that the reinforced composites had fracture toughness values between 1.6 and 1.9 MPa$\sqrt{m}$. This is significantly greater than values reported for unreinforced plain matrix (0.2 – 0.3 MPa$\sqrt{m}$). They also showed that the fracture toughness is enhanced in natural fiber-reinforced composites via crack-bridging that results from the crack growth process [12, 13]

There has been considerable progress in our understanding of ecomaterials for sustainable buildings; much of the effort has focused on the study of cement based composite materials [14-

16]. In contrast, earth-based materials of laterite and clay have not been modeled using the mechanistic models that have been applied to the study of cementitious matrix composites.

This chapter presents the results of a combined experimental and theoretical study of the strength and fracture toughness of earth-based composites reinforced with straw fibers. It explores the strength and fracture toughness of earth-based matrices produced from laterite and clay mixtures. The effects of straw reinforcement are also elucidated using composites rule-of-mixtures and crack-tip shielding fracture mechanics models. The measured strength and predicted strengths are compared with those of control samples obtained from fired clay bricks. The implications of the results are then discussed for the design of robust earth-based building materials.

3.2 Materials and Composite Processing

3.2.1 Materials

The earth-based materials used in this work were obtained directly from their deposition sites in Abeokuta, Ogun State, South-West Nigeria. One of which is laterite (lateritis) [17], a soil type that is rich in iron and aluminum. The name originate from the Latin word “Later (brick)” [18]. Laterites in the moist state can be cut without difficulty and reshaped but it gradually hardens when exposed to air [19].

Clay obtained from Abeokuta, Ogun State, Nigeria, was used as a stabilizer. The fine-grained, clay (consisting primarily of hydrated silicates of aluminum with traces of iron oxide) also serves as a binder in the predominantly lateritic matrix [20]. Straw (Andropogon virginicus) [21] was used as a reinforcing agent. Straw is a dry stalk of cereal plants. It is an agricultural by-product obtained

after the grain and chaff have been removed. Lastly, Type I Ordinary Portland cement (composed of high calcium silicate) was procured from Lafarge cement factory, Ewekoro, Ogun state, Nigeria. The Ordinary Portland cement compliments the fine-grained clay as a binder.

3.2.2 Processing

Chemical and physical characterizations of the raw materials used were carried out. The former was achieved via energy dispersive X-ray spectroscopy (EDS) analysis and the later via particle size distribution measurement. Laterite, clay and Ordinary Portland cement of maximum particle sizes of 250 microns, 150 microns and 74 microns respectively were used in this study. These particle sizes were obtained by measuring and converting mesh sizes of the sieves to microns. Straw of average diameter of 1.85 mm was cut into whiskers of average length 10 mm. This was used as reinforcement (randomly oriented) in the predominant earth-based matrix.

Bricks of different material compositions (matrices and reinforcements) were produced from the materials acquired. Macro-mechanical characterizations of the specimens were carried out to obtain compressive strength, flexural strength and fracture toughness. The cementitious materials were dry mixed manually with the aid of a hand trowel for about 2 minutes for homogenization. Samples were prepared in varying dimensions in a mold using a hydraulic press at a pressure of 2 MPa for 5 minutes. This pressure was chosen after optimization. The samples were cured for 28 days in air at average temperature of $23^{O}C$ with average relative humidity of 80%.

Fired clay (control samples) was also obtained by firing of molded clay at ~$800^{o}C$ for 6 hours in a kiln. Samples of dimensions $25 \times 12.5 \times 100$ mm^3 were used for compression and flexural strength test while $12.5 \times 25 \times 100$ mm^3 specimens were for Single-edged notched bending (SENB) to study their fracture toughness.

Different matrix compositions (Tables 3.1 and 3.2) were produced to serve as the control samples. The matrices were prepared by direct mixing of dry constituent material(s) followed by addition of water at approximate water-cement ration of 0.5. The mixtures were then molded to the required sample shapes. The material composition in the matrix preparation was based on percentage composition by volume of laterite, clay and cement. The matrix compositions were 100% laterite, fired clay and laterite-cement (combined in different proportions by volume).

Table 3.1: Percentage composition by volume of laterite and cement in the matrix samples.

Samples	Volume percentage of laterite used (%)	Volume percentage of cement used (%)
I	80	20
II	90	10
III	95	5

Table 3.2: Percentage composition by volume of laterite, clay and cement in the matrix samples.

Samples	Volume percentage of laterite used (%)	Volume percentage of clay used (%)	Volume percentage of cement used (%)
I	70	10	20
II	60	20	20
III	50	30	20

Natural fiber (straw)-reinforced composites were produced with volume percentages of fiber ranging from 5% to 20%. These volume fractions used was determined based on the volume ratios of the initial solid raw materials. Two matrix compositions were considered in this study. The first matrix contained 80% of laterite and 20% of cement, while the second contained 70% laterite, 10% of clay and 20% of cement. These proportions of the constituent materials were chosen based on the results obtained from preliminary tests. In both cases, the samples were prepared with composite (matrix and fiber) compositions as shown in Table 3.3.

Table 3.3: Percentage composition by volume of matrix and fiber in the composite samples.

Samples	Volume of matrix (%)	Volume of fiber (%)
I	95	5
II	90	10
III	80	20

3.3 Experimental Methods

An Instron 3360 series (Norwood, MA, USA) with a 50kN load cell was used for the determination of strengths and fracture toughness of earth-based composites. The samples were tested at room temperature with average relative humidity of 65%. In the determination of compressive strength, the compression specimens were deformed at a loading rate of 3.3 N/s until fracture occurred by separation of specimens into two or more pieces. A curve of compressive load (kN) versus compressive displacement (mm) was used to estimate the peak load, F_A. The compressive strength was then estimated using the following equation:

$$\sigma = F_A/A_o \tag{3.1}$$

where F_A is the peak load at the onset of fracture and A_o is the initial cross-sectional area. A total of five compression tests were conducted for each condition.

A three-point bend loading configuration was used to estimate the flexural/bend strengths and fracture toughness values of the samples. A loading span of 80 mm was used for the entire three-point bend test. The mechanical properties were measured 42 days after the fabrication of the specimens. The specimens were loaded monotonically at a loading rate of 3.3 N/s. For each matrix and composite formulation, five specimens were tested. The flexural/bend strength, σ_f, was obtained from:

$$\sigma_f = 3FL/2BH^2 \tag{3.2}$$

where F is the maximum load, L is the loading span, B and H are the specimen breadth and height, respectively. Fracture toughness, K_c, was estimated using a single edge notch bend (SENB) test approach. This was appropriate for earth samples, in the same way that it applies to other ceramic matrix composite materials (CMC). However, the specimen sizes were chosen to be sufficient to enable the crack-tip fields to sample the heterogeneous microstructures of earth-based materials. The fracture toughness was obtained from [22]:

$$K_c = F(a/w)\sigma_f\sqrt{\pi a} \tag{3.3}$$

where $F(a/w)$ is a compliance function, σ_f is the flexural stress at the peak load and a is the crack length. The compliance function for the single edge notched bend (SENB) specimen can be obtained in the ASTM E399-90 [23]:

$$f\left(\frac{a}{w}\right) = \frac{3(a/w)^{0.5}}{2(1+2a/w)(1-a/w)^{1.5}} \times [1.99 - (a/w)(1 - a/w)(2.15 - 3.93\, a/w + 2.7\, a^2/w^2)] \tag{3.4}$$

The morphology of the matrix and composite samples were observed using a Carl Zeiss MA-10 Scanning Electron Microscope (SEM) equipped with an Oxford Energy Dispersive Spectroscopy (EDS) system for elemental analysis.

3.4 Models

3.4.1 Rule of mixture (ROM)

For a two phase whisker/fiber-reinforced composite, the strength may be estimated from rule of mixture. The constant strain rule of mixture assumes that the applied load is parallel to the fiber direction. This gives [22]:

$$\sigma_c = V_m\sigma_m + V_f\sigma_f\eta_f\eta_o \tag{3.5}$$

where V_m and V_f are volume fractions of the matrix and fiber, respectively while σ_m and σ_f are matrix and fiber strengths, respectively. The parameters η_f corresponds to a fiber length efficiency while η_o corresponds to the fiber orientation efficiency that will be discussed in the next section.

3.4.2 Short fiber theory (SFT)

In the case of short fibers/whiskers, the average fiber stresses are less than those associated with long fibers. Under such condition, the average fiber stress is given by [22]:

$$\bar{\sigma}_f = (1/2)\sigma_f(l/l_c) \tag{3.6}$$

where the term $l/2l_c$ is known as the fiber efficiency factor (η_f) for short fibers, and l_c is the critical fiber length. The critical fiber length (l_c) is given by [22]:

$$l_c = \sigma_f d/2\tau \tag{3.7}$$

where σ_f is the fiber strength, d is fiber diameter and τ is the fiber-matrix bond strength. This expression for the average fiber strength can be substituted into the simple rule of mixture theory for very short fiber lengths. Hence, the average fiber strength for very short fibers is given by:

$$\bar{\sigma}_f = (l/2l_c)\sigma_f = \eta_f\sigma_f \tag{3.8}$$

An additional parameter known as the orientation efficiency factor (η_o), is needed to account for the decrease in composite strength due to random orientations of the fibers. When this is taken into consideration, the average fiber strength is now given by [25]:

$$\bar{\sigma}_f = \eta_o\eta_f\sigma_f \tag{3.9}$$

where η_o have values of 0.375 and 0.2 for random two-dimensional and three-dimensional orientation respectively [26]. The composite strengths are given by equation 3.5.

3.4.3 Toughening due to Crack Bridging

A toughening model proposed originally by Budiansky et al. was used to study the toughening due to crack bridging by the straw fibers. This small-scale bridging model gives [27]:

$$K_c = K_m + \Delta K_b = K_m + \alpha V_f \sqrt{2/\pi} \int_0^L \sigma_f \Big/ \sqrt{x}\, dx \tag{3.10}$$

where K_m is the matrix fracture toughness, K_c is the composite fracture toughness, x is the horizontal distance from the crack-tip, α is the constraint factor [27], V_f is the volume fraction of bridging phase and L is the bridge length. In this case, the fracture toughness is taken to correspond to the point of instability on the resistance-curve, which is approximated by the peak loads in the fracture toughness experiments.

3.5 Results and Discussion

3.5.1 Materials and Microstructure

The Scanning Electron Microscopy (SEM) images of the matrix and composite samples (Figures 3.1a and 3.1b) show the surface morphologies of the specimens. They also reveal the fiber morphologies in the composite structures. The images of the composite samples reveal that the straw fibers are all bonded to the matrix materials. Such good bonding is consistent with the relatively high strengths of the straw fiber composites with fiber volume percentages of 20%. The bright region observed in Figure 3.1b resulted from electron charging effect due to non-conducting nature of the samples.

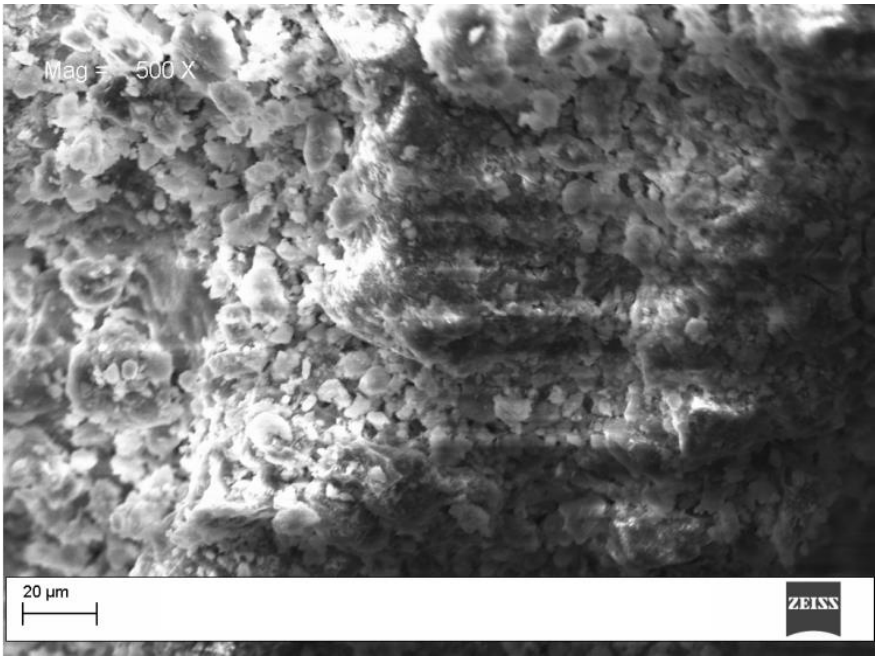

(a)

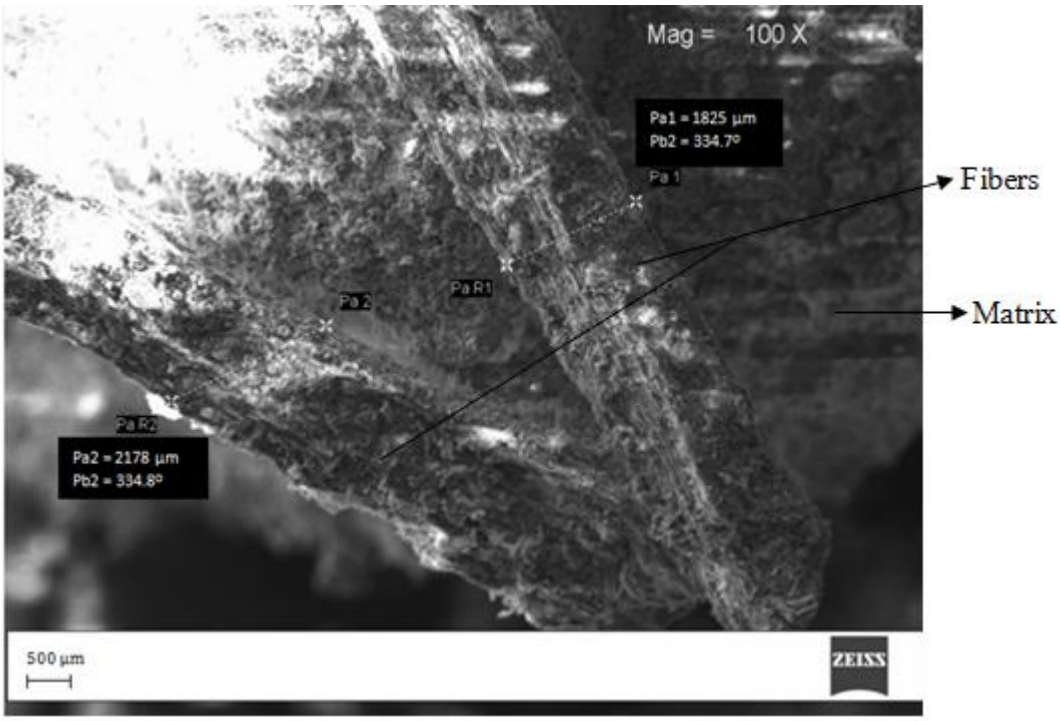

(b)

Figure 3.1: SEM micrograph of: (a) Laterite + Clay + Cement (Mag. 500x) and (b) Matrix (L-C) + Fiber (Mag. 100x)

The energy dispersive X-ray spectroscopy (EDS) analysis shows the elemental composition of the samples. For pure laterite samples (Figure 3.2a), the EDS analysis revealed the presence of structures consisting of Al, Si, O, Ti and Fe. Further analysis revealed additional Ca, Mg and K precipitated by the cement-laterite and cement–laterite-clay interactions (Figures 3.2b and 3.2c). These correspond to the by-products (calcium silicate hydrate and calcium hydroxide) of hydration reactions that result in the binding of laterite particles by hydrated cement ligaments [28]. Depending on the strengths (compared to those of laterite ligaments), such ligaments could affect the strength and fracture toughness levels of the cement-stabilized laterite matrices. This will be discussed in the next section.

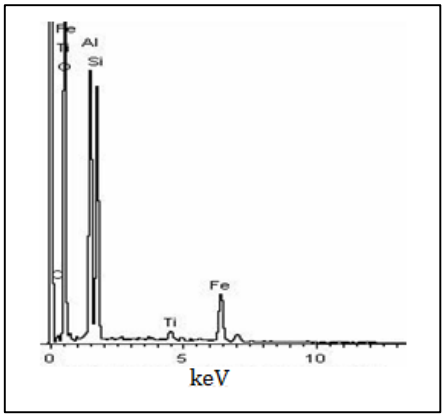

(a)

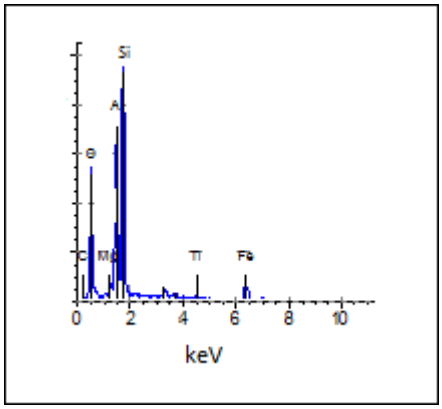

(b)

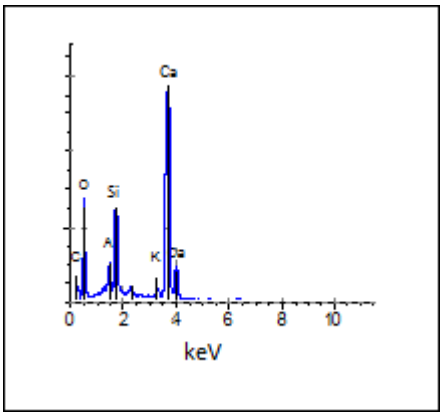

(c)

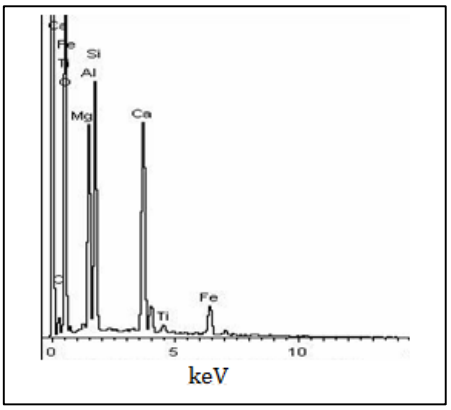

(d)

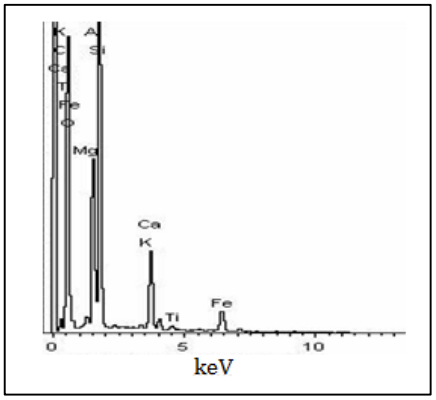

(e)

Figure 3.2: EDS analysis of matrix samples: (a) Laterite (b) Clay (c) Ordinary Portland Cement (d) Laterite + Cement and (e) Laterite + Clay + Cement.

3.5.2 Compressive/Flexural Strength

The introduction of cement into the matrix resulted in the presence of calcium to the composition (Figure 3.2d and 3.2e). The resulting hydration reactions and the increased bonding of laterite particles (by the cement) are expected to increase the matrix strength and fracture toughness of the laterite. However, this was not the case in the current work in which the laterite matrix was found to exhibit higher strengths than the cement–stabilized laterite materials (Figures 3.3 and 3.4).

The results show that the compressive strengths of composite samples are increased to a maximum at a fiber volume fraction of 20 vol. %. For such high fiber contents, the compressive strength was as high as 2.91±0.14 MPa. The results also show that clay in the matrices and the composites contributed to the enhancement of strengths. This suggests that clay ligaments bind the laterite particles together; just as hydrated cement ligaments bind sand particles together in cement mortar and blocks.

The compressive strength of 3.03±0.15 MPa obtained for the 100% laterite samples is fascinating. This is greater than the strength of the straw fiber-reinforced cement-stabilized matrix, but below that of the fired clay (compressive strength of 4.95±0.24 MPa). However, for composites reinforced with natural fibers, the compressive and flexural strengths increased with increasing fiber volume fraction, for fiber volume fractions between 5 and 20 vol. %. The observed effects of fiber volume fraction are comparable to the results from prior work by Savastano et al. [29] on natural fiber-reinforced cementitious composites.

The relatively high compressive strengths are due to the combined effects of the high strength of the laterite matrix and strengthening effects of the straw fibers. The high strength of the laterite matrix is illustrated clearly by the mechanical properties of the plain laterite sample. Furthermore,

the current results show that the strengthening effects of the straw fibers improve the composite strength with increasing fiber volume fractions up to 20 vol.%. However, the effects of defects and voids (introduced during composite processing) and fiber touching reduce the composite strengths for fiber volume fractions above 20 vol.%.

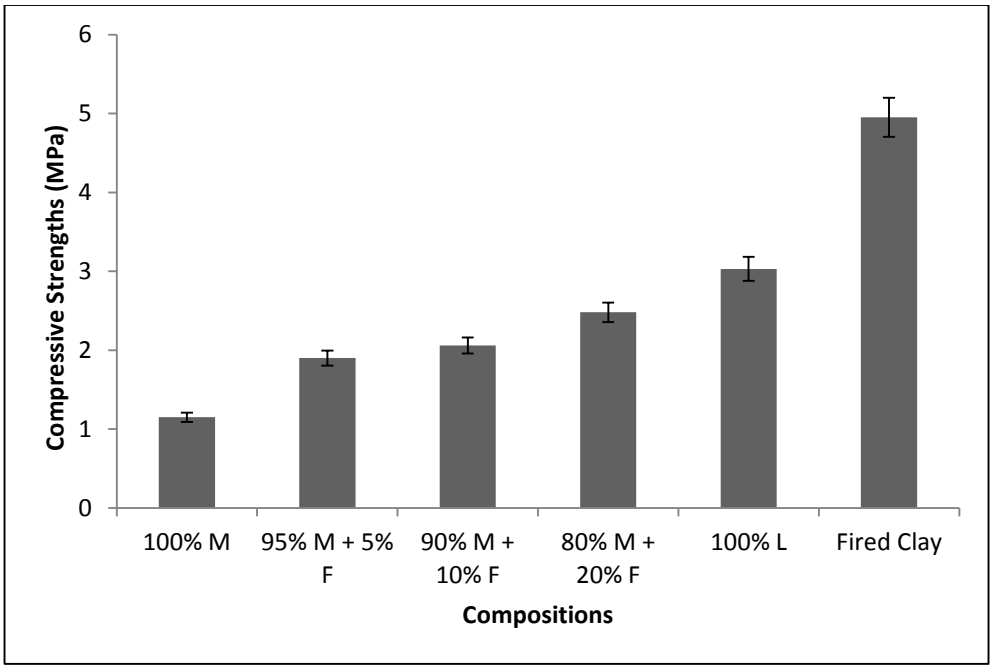

(a)

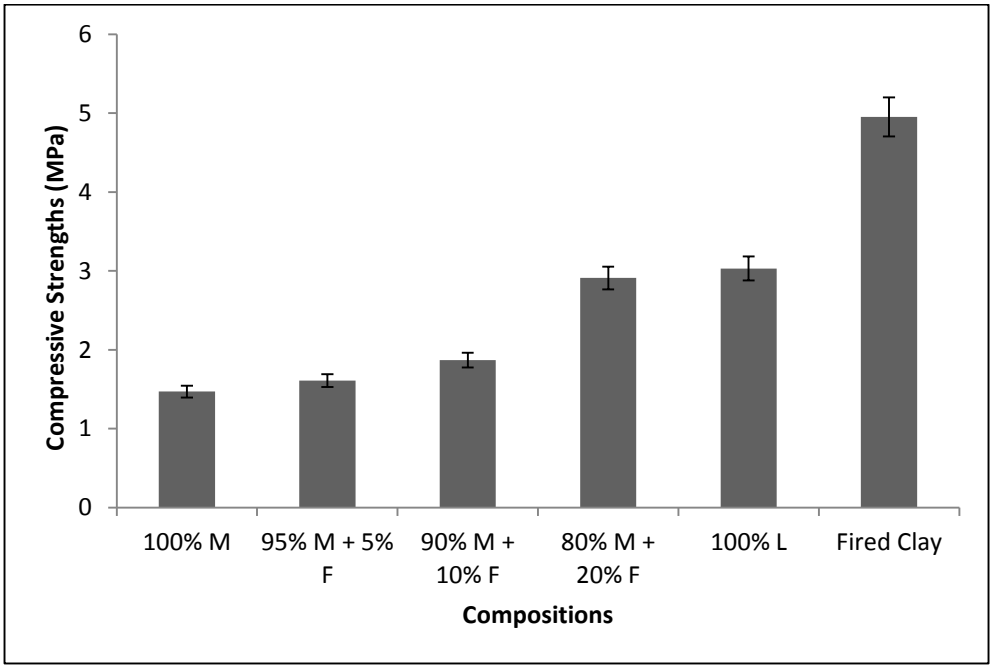

(b)

Figure 3.3: Compressive strengths obtained for: (a) stabilized laterite (Matrix = 80% Laterite + 20% Cement) composites and (b) stabilized laterite-clay (Matrix = 70% Laterite+ 10%Clay + 20% Cement) composites. [M = Matrix, F = Fiber and L = Laterite]

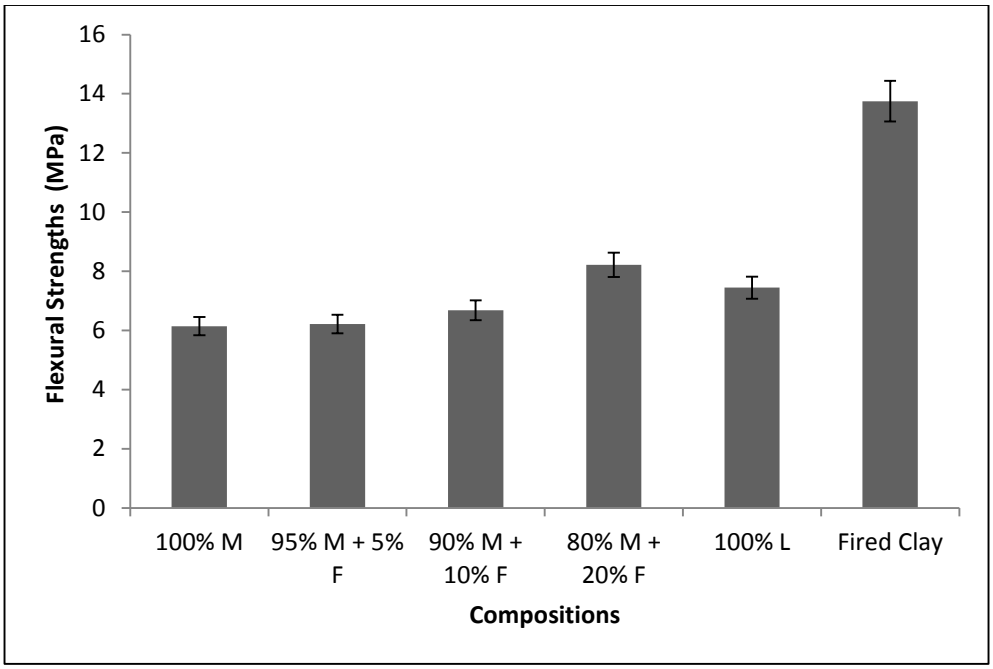

(a)

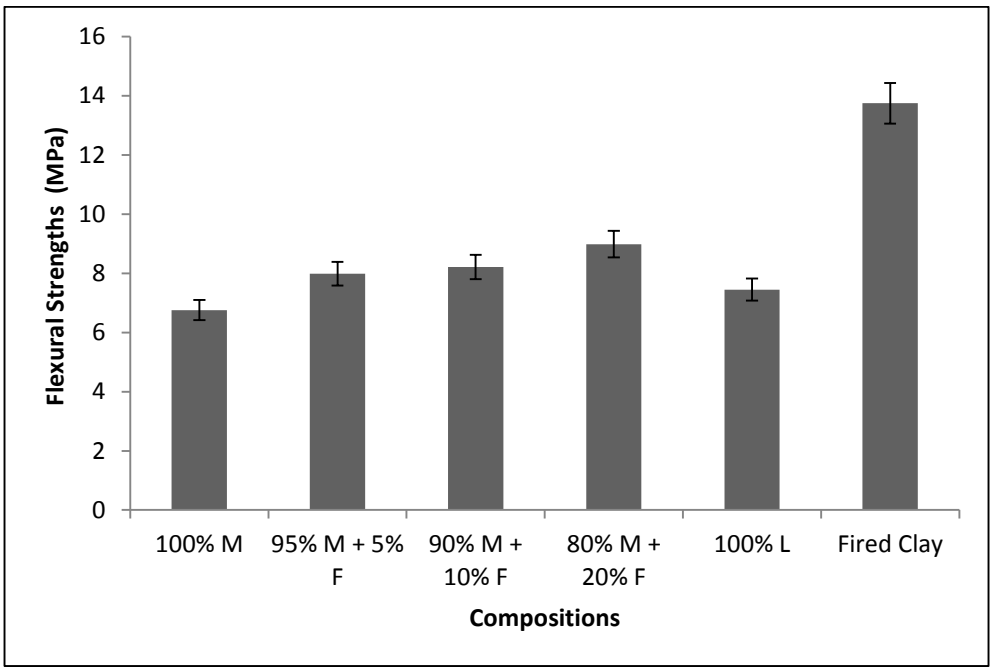

(b)

Figure 1Figure 3.4: Flexural strengths obtained for: (a) stabilized laterite (Matrix = 80% Laterite + 20% Cement) composites and (b) stabilized laterite-clay (Matrix = 70% Laterite+ 10%Clay + 20% Cement) composites. [M = Matrix, F = Fiber and L = Laterite]

3.5.3 Fracture Toughness

The results of the fracture toughness tests are presented in Figure 3.5, revealing that fiber volume fraction results in increased fracture toughness. Similar observations have also been reported in prior work by Savastano et al. [10, 29] and Agopyan [9], whose studies used vegetable fibers reinforced cementitious matrices that resulted in composite fracture toughness values between 0.5 MPa$\sqrt{m}$ and 1.0 MPa$\sqrt{m}$. In the current work, high fracture toughness values (between 1.0 and 1.4 MPa$\sqrt{m}$) were obtained for the natural fiber (straw) toughening of a matrix consisting of a mixture of clay, cement and laterite.

The increase in fracture toughness attained as a result of fiber-reinforcement can be attributed to shielding of the remote loads by bridging fibers [27] as seen in figure 3.6. This can be modeled using the crack bridging model presented in section 4.3. It is also interesting to note that debonding can result in frictional energy losses that can add to the fracture toughness [8].

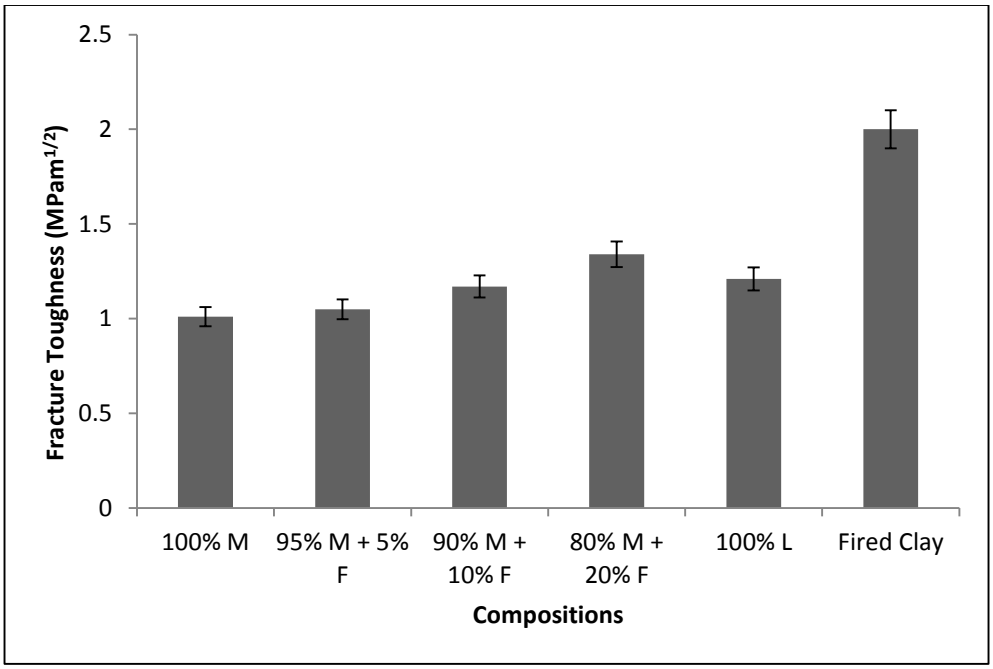

(a)

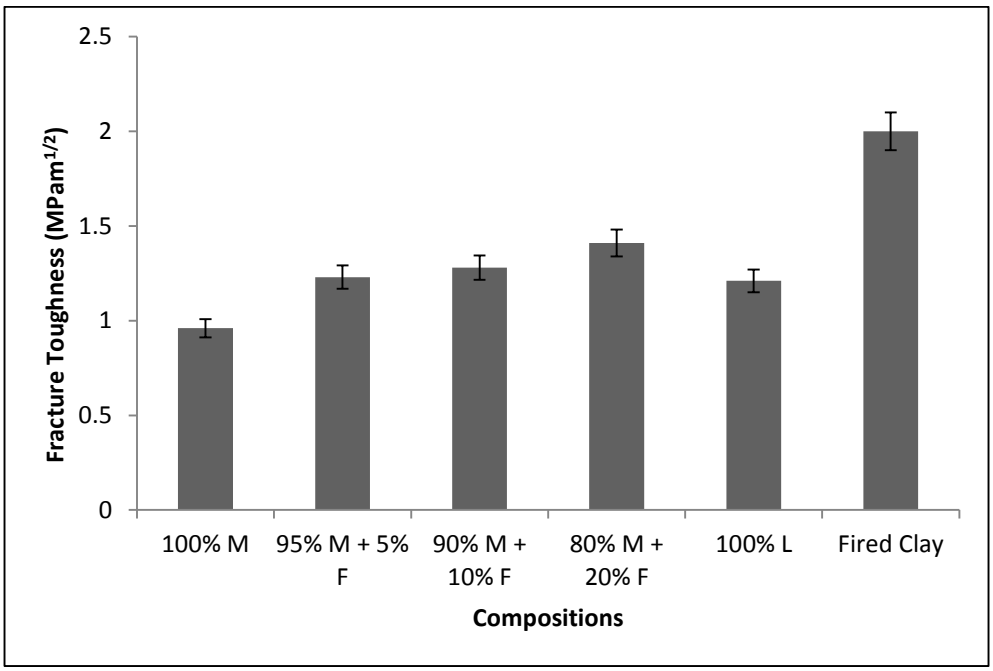

(b)

Figure 3.5: Fracture toughness obtained for: (a) stabilized laterite (Matrix = 80% Laterite + 20% Cement) composites and (b) stabilized laterite-clay (Matrix = 70% Laterite+ 10%Clay + 20% Cement) composites. [M = Matrix, F = Fiber and L = Laterite]

(a)

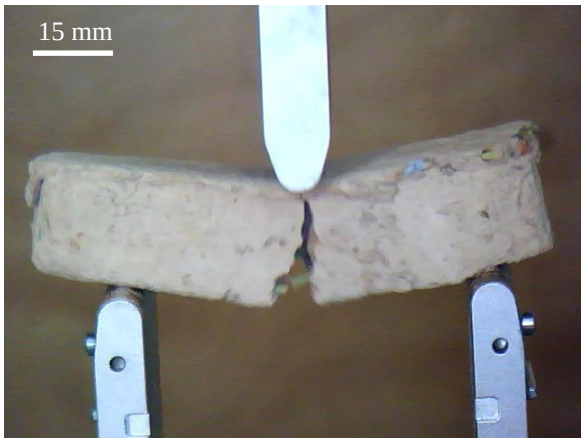

(b)

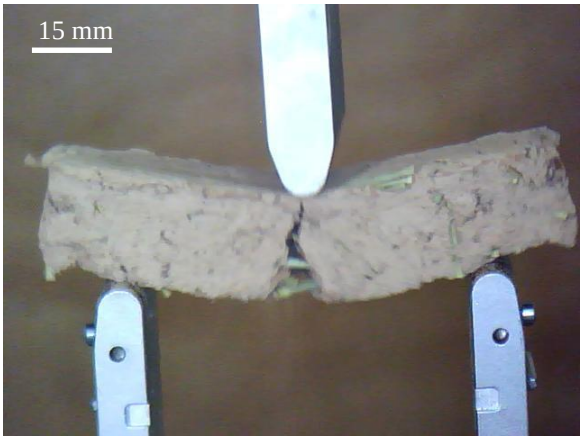

(c)

Figure 3.6: Optical microscopy images showing crack bridging by fibers for: (a) fiber volume fraction of 0.05, (b) fiber volume fraction of 0.1 and (c) fiber volume fraction of 0.2.

3.5.4 Comparison of Modeling and Experimental Results

The results obtained experimentally were compared with mechanistic model for flexural strength and fracture toughness. Figure 3.7 and 3.8 shows comparison between experimental results and mechanistic model (rule-of-mixtures and short fiber theory) of compressive and flexural strengths measured. Figure 3.7 shows that the results for compressive strength are not consistent because the rule-of-mixture theory failed. This may be attributed to the complex nature of composite failure under compressive loading (i.e. via shear and fiber buckling at an angle to the loading direction). However, the results are consistent for the flexural strength measurements, affirming the effects of fiber and orientation efficiency factors.

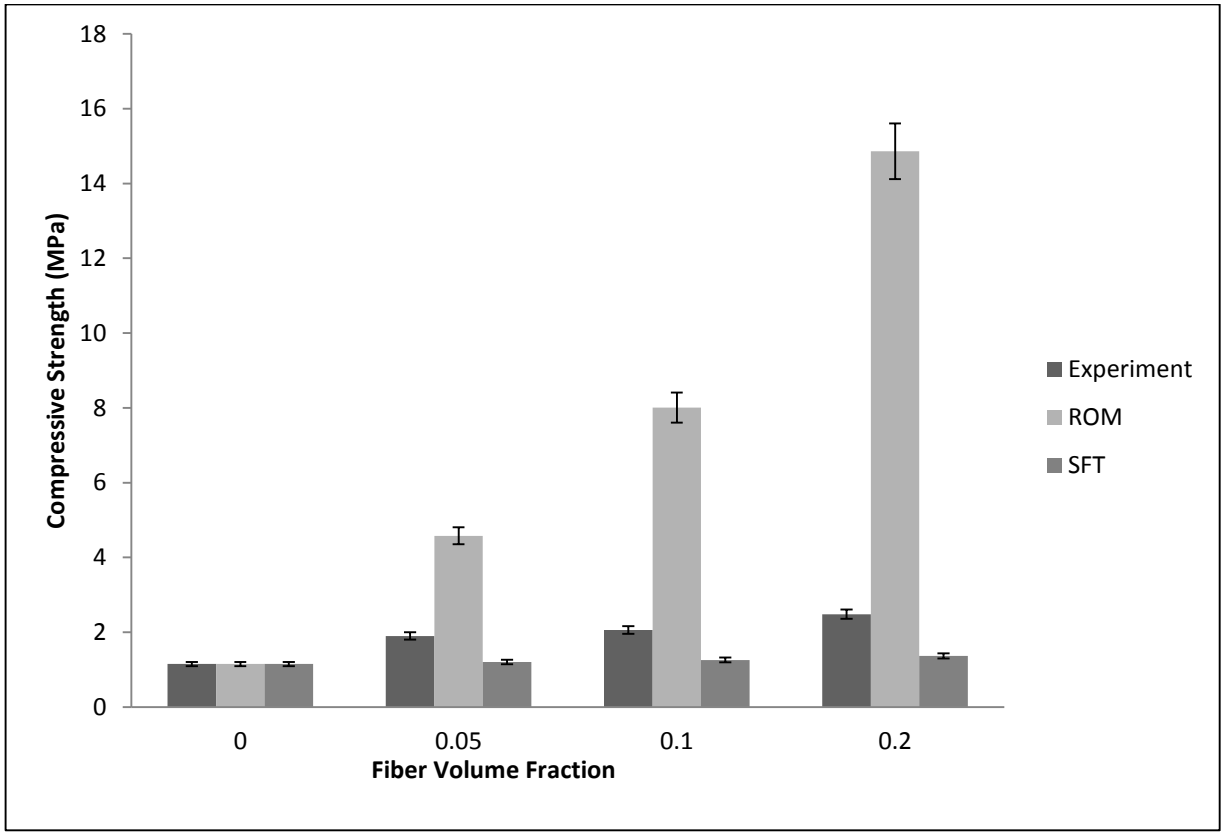

(a)

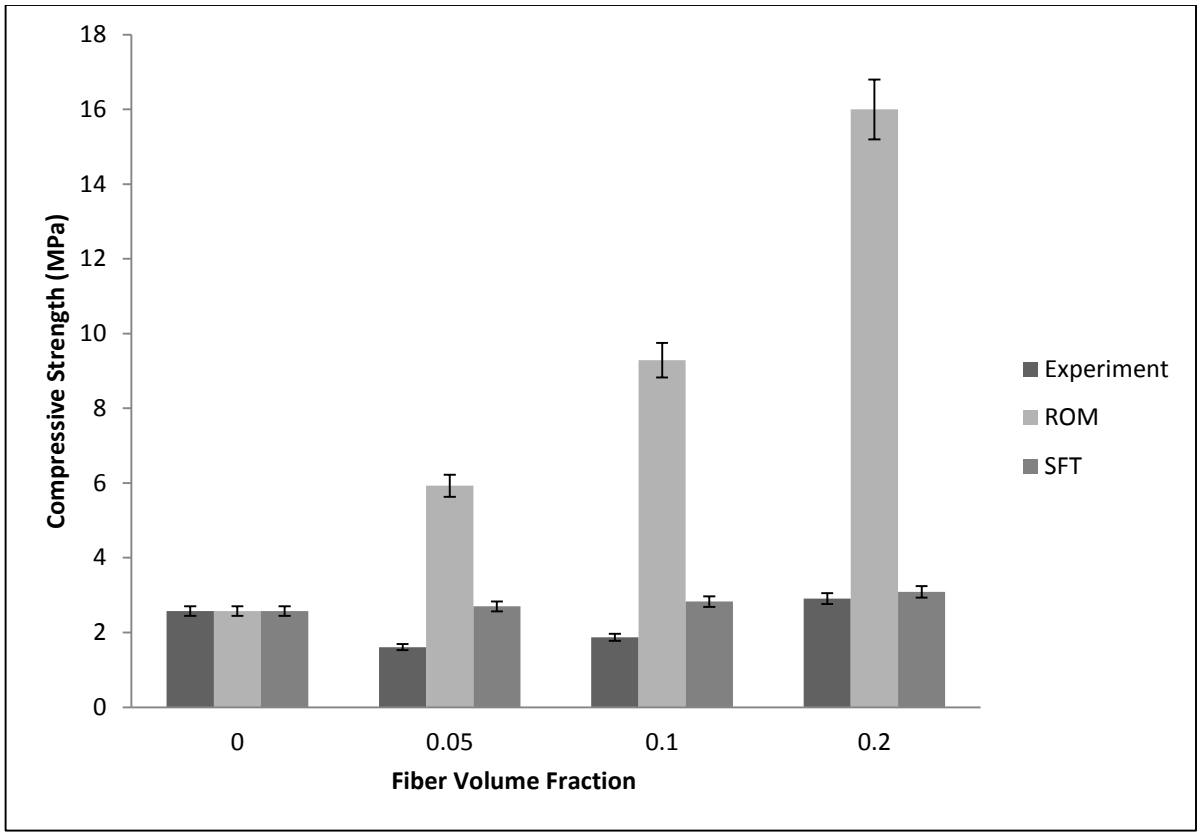

(b)

Figure 3.7: Plots showing comparisons of experimental results and predictions of Compressive strength from mechanistic models (rule-of-mixture and short fiber theory) for: (a) stabilized laterite composites and (b) stabilized laterite-clay composites.

Figure 3.9 shows comparison between experimental results and toughening model (crack bridging) of fracture toughness measured. The plots obtained from crack bridging models are consistent with those from experiments. From these observations, it is apparent that the source of improved toughness in the fiber reinforced specimens can be attributed primarily to the crack-tip shielding that result from crack bridging. The contribution to toughness can be obtained from equation 11 as explained in section 4.3.

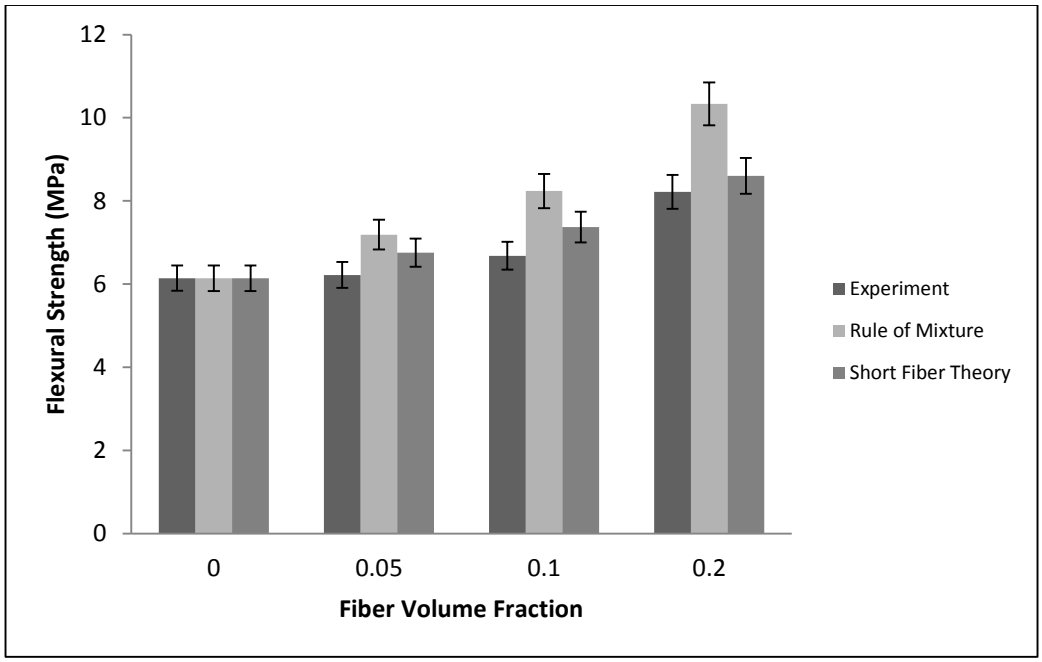

(a)

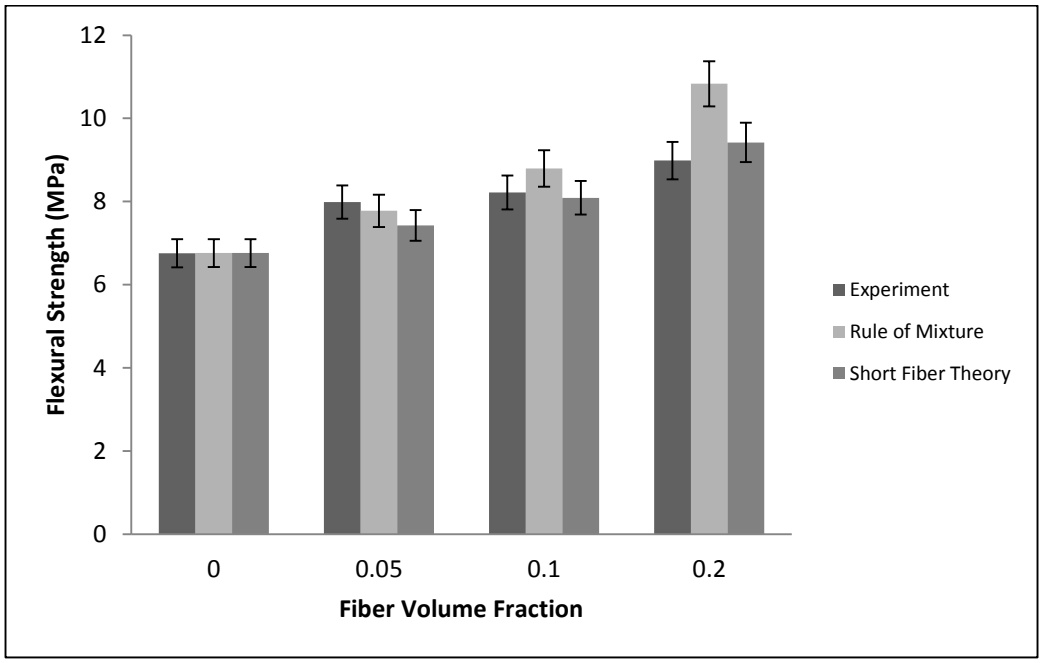

(b)

Figure 3.8: Plots showing comparisons of experimental results and predictions of flexural strength from mechanistic models (rule-of-mixture and short fiber theory) for: (a) stabilized laterite composites and (b) stabilized laterite-clay composites.

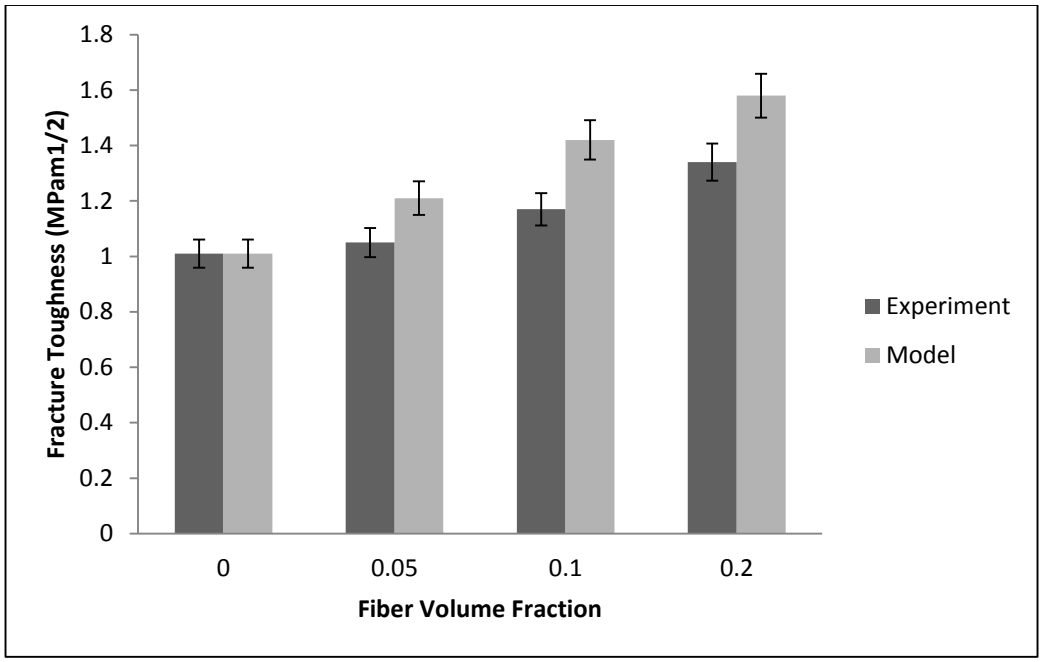

(a)

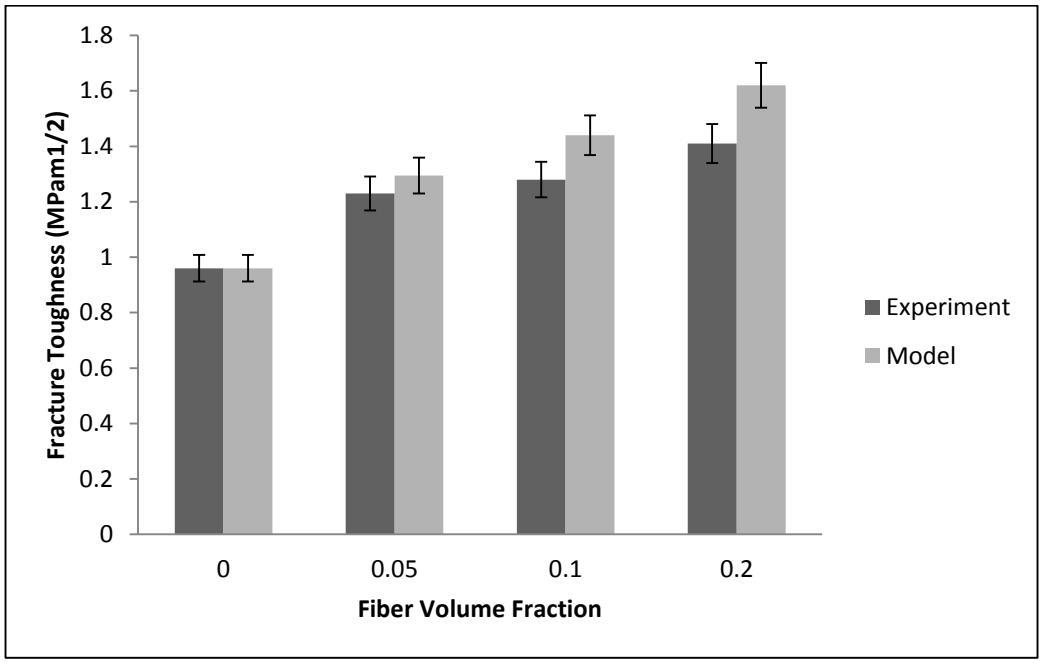

(b)

Figure 3.9: Plots showing comparisons of experimental results and predictions of fracture toughness from crack bridging models for: (a) stabilized laterite composites and (b) stabilized laterite-clay composites.

3.7 Summary and Concluding Remarks

Composites consisting of earth-based materials reinforced with natural fiber (straw), and plain matrices were prepared. The mechanical properties of the various compositions (in both matrices and composites) were determined. The results were compared to measure the effects of reinforcement.

Fiber-reinforcement resulted in an increase in compressive strength from 2.57±0.12 MPa to 2.91±0.14 MPa at maximum compressive strength. Interestingly, pure laterite had a compressive strength of 3.03±0.15 MPa. This value was the closest to that of fired clay (4.95±0.24 MPa). Samples reinforced with straw fibers had increased flexural strengths and fracture toughness. Composites with fiber volume percentage of 20% had the highest flexural strengths and fracture toughness values of up to 8.99±0.45 MPa and 1.41±0.07 MPa$\sqrt{m}$, respectively. These values exceed the respective values obtained for the matrix material (6.76±0.34 MPa and 1.08±0.05 MPa$\sqrt{m}$).

The measured strengths and fracture toughness levels are consistent with predictions from mechanistic models studied. The rule-of-mixture and short fiber theory strength predictions account for the effects of whiskers and random orientation to provide reasonable estimate of flexural strength. Furthermore, the modelling of crack shielding by crack bridging provides adequate estimates of toughening in the straw-reinforced earth-based composites that were examined in this study.

References

[1] Coutts RSP. A review of Australian research into natural fiber cements composites. Cement & Concrete Composites 2005; 27(5): 518-526.

[2] Ernst W, Lynn P, Nathan M, Chris H and Leticia OM. Carbon dioxide emissions from the global cement industry, Annual Review of Energy and the Environment, Environment and Resources, 2001. vol. 26: 303-329.

[3] John VM, Zordan SE. Research and development methodology for recycling residues as building materials –a proposal. Waste Mgmt 2001; 21:213-9

[4] Savastano Jr H, Warden PG, Coutts RSP. Blast furnace Slag cement reinforced with cellulose fibers. In: Proc. 8th National Meeting on Technology of the Built Environment: Modernity and Sustainability, Salvador, Brazil, April 25-28, 2000. V II. p 948-55.

[5] Savastano Jr H, Warden PG, Coutts RSP. Potential of alternative fiber cements as building materials for developing areas. Cement & Concrete Composites 2003; 27(5):585-92.

[6] Lola CR. Fiber Reinforced Concrete Roofing Sheets: Technology Appraisal Report, AT International, Washington, D.C. 1985.

[7] Heinricks H, Berkenkamp R, Lempfer K, Ferchland HJ. Global review of technologies and markets for building materials. In: ganic-Bonded Wood and Fiber Composite Materials Conference. Moscow: University of Idaho; 2000.

[8] Coutts RSP. Sticks and stone. Forest Product Newsletter, CSIRO Div Chem Wood Technol 1988; 2(1):1-4.

[9] Agopyan V, John VM. Durability evaluation of vegetable fiber reinforced materials. Build Res Infor, 1992; 20(4):233-5.

[10] Savastano Jr H, Warden PG, Coutts RSP. Brazilian waste fibers as reinforcement for cement based composites. Cement & Concrete Composites 2000; 22(5):379-84.

[11] Banthia N, Sheng J. Fracture toughness of micro-fiber reinforced cement composites. Cement & Concrete Composites 1996; 18(4):251-69.

[12] Savastano Jr H, Santos SF, Radonjic M, Soboyejo WO. Fracture and fatigue of natural fiber-reinforced cementitious composites. Cement & Concrete Composites 2009; 31(5):232-43.

[13] Nelson PK, Li VC, Kamada T. fracture toughness of microfiber reinforced cement composites. J Mater Civ Eng 2002; 14(5):384-91.

[14] Swamy RN. Fiber-reinforced cement and concrete. In: Proceedings of the forth International symposium held by RILEM, Sheffield, July 1992 (Spon, London, 1992).

[15] Coutts RSP. Wood fiber-reinforced cement composites. In: Coutts Swamy RN, editor. Natural fiber-reinforced cement and concrete. Glasgow: Blackie; 1988. p. 1-62.

[16] Benture A. Fiber-reinforced cementitious materials. In: Skalny JP, editor. Material Science of concrete. Waterville: The American Ceramics Society; 1989. p. 223-84.

[17] Aleva GJJ. (Ed.) (1994): Laterites. Concepts, Geology, Morphology and Chemistry. 153 p. ISRIC, Wageningen, ISBN 90-6672-053-0.

[18] Sivarajasingham S, Alexander LT, Cady JG et al. “Laterite”. Advances in Agronomy 1962; 14, 1-60.

[19] Tardy Y. Petrology of laterites and tropical soils. 1997. ISBN 90-5410-678-6.

[20] Hillier S. “Clay Mineralogy. In: Encyclopedia of sediments and sedimentary rocks”. Kluwer Academic Publishers, Dordrecht. 2003. pp 139-142. John

[21] Robert HM. USDA-NRCS PLANTS Database / USDA SCS. 1991. Southern wetland flora: Field office guide to plant species. South National Technical Center, Fort Worth.

[22] Callister WD. Material Science and Engineering: An Introduction. 7th ed. John Wiley, New York; 2007. p. 414-459 [chapter 12].

[23] American Society for Testing and Materials. Standard test method for plane-strain fracture toughness of metallic materials, E399-90. West Conshohocken: ASTM; 1997. P. 31 [Book of Standards v. 03.01].

[24] Ashbee KH. Fundamental Principles of Fiber Reinforced Composites, 2nd edition, Technomic Publishing Company, Lancaster, PA, 1993.

[25] Mallick PK. Fiber-Reinforced Composites, Materials, Manufacturing, and Design, 2nd edition, Marcel Dekker, New York, 1993.

[26] Soboyejo WO. Introduction to Composites. In: Mechanical properties of engineered materials. NY: Marcel Dekker Publisher; 2002. p. 269-87 [chapter 9].

[27] Budiansky B, Amazigo JC, Evans AG. Small scale crack bridging and the fracture toughness of particulate-reinforced ceramics. J Mesh Phys Solids 1988; 36(2):167-87.

[28] Andrzej MB. Structure of cement composites. In: Cement-Based Composites: Materials, mechanical properties and performance. Second Edition, Taylor & Francis Publishers; 2009. p. 137-83 [chapter 6].

[29] Savastano Jr H, Agopyan V. Transition zone studies of vegetable fiber-cement paste composites. Cem Concr Compos 1999; 21(1):49-57.

CHAPTER FOUR: RESISTANCE-CURVE BEHAVIOR OF NATURAL FIBER-REINFORCED EARTH-BASED COMPOSITES

4.1 Introduction

Fracture resistance is a non-unique process which depends on the crack-growth history. The history dependence of the fracture resistance can be characterized by a Resistance curve (Figure 4.1), which relates the resistance, K, to the extent of crack growth, Δa [1].

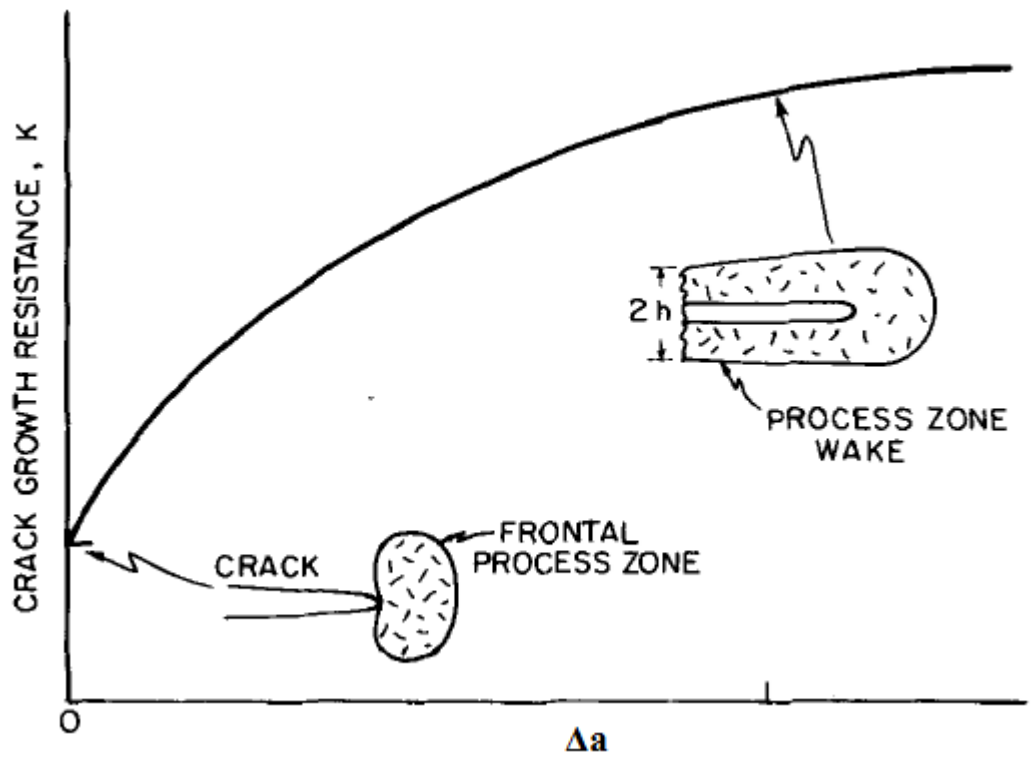

Figure 4.1: Schematic diagram of a crack growth resistance curve

Recent studies have shown that substantial efforts have been made to develop natural fiber-reinforced cementitious composites for affordable and sustainable infrastructure including housing [2]. To improve the low intrinsic toughnesses of brittle matrices, extrinsic toughening techniques

that invoke crack-tip shielding mechanisms are often used in composite design and development. Such mechanisms, which include crack bridging via ductile or brittle reinforcements, primarily act behind the crack tip and locally shield the crack from the applied driving force [3, 4]. This additional energy to fracture the bridging ligaments is typically exhibited in the form of resistance-curve (*R*-curve) behavior, where the toughness increases with crack extension, commensurate with the development of a bridging zone in the crack wake [5]. The toughening can also be described in terms of stress intensities, where the steady-state toughness, K_{ss}, can be modeled by superposing the reinforcement toughening contribution with the intrinsic fracture toughness of the composite, K_o (*i.e.*, the matrix or crack-initiation toughness) [6, 7].

Savastano et al. [8] also studied the possibility of using Brazilian agricultural waste as fibers for reinforcement in cement-based composites. In their work, they used different types of Brazilian fibrous residues to reinforce cementitious matrices. These include: banana pseudo-stem fibers; waste Eucalyptus grandis pulp, and sisal field by-products. Using specimens with fiber mass percentages from 4% to 12%, they studied the dependence of strength and fracture toughness of these materials after 28 days of exposure to the laboratory air with a relative humidity of ~ 80%. Their results showed that composites reinforced with ~ 8% fiber had strengths that were ~ 65% greater than those of the unreinforced matrix materials. In a related study, Banthia and Sheng [9] predicted the effects of polymer fiber used as reinforcements in cement based matrix using resistance-curve approaches. At about 3% by volume of fibers, they were able to improve the matrix fracture toughness to levels of ~1.9 MPa$\sqrt{m}$.

Most recently, there was a study of the mechanical fracture and fatigue behavior of natural fiber-reinforced cement-based materials [10]. Their results showed that the reinforced composites had

fracture toughness values between 1.6 and 1.9 MPa$\sqrt{m}$. This is significantly greater than values reported for unreinforced plain matrix (0.2 – 0.3 MPa$\sqrt{m}$). They also showed that the fracture toughness is enhanced in natural fiber-reinforced composites via crack-bridging that results from the crack growth process [10, 11].

Eissa and Batson [12] have studied the resistance-curve behavior of steel fiber-reinforced concrete with hooked-end and crumped fibers with fiber volume percentages between 1.0 and 1.5%. Their studies showed that the crimped fibers result in higher toughening than equivalent volume percentages of hooked-end fibers. Similar studies of resistance-curve behavior have been carried out by Savastano and co-workers [10] on cementitious composites with natural fibers [13]. These studies, which were carried out on composites with matrices produced from recycled blast furnace slag and Ordinary Portland cement, have been used to explore the role of small- and large-scale bridging on the toughening of natural fiber-reinforced composites reinforced with pulped fibers of sisal, banana fibers and bleached eucalyptus pulp.

This chapter presents the results of a combined experimental and theoretical study of the resistance-curve behavior of affordable earth-based composites with a cement-stabilized laterite matrix and straw fibers. It explores the effects of fiber reinforcement in composite. The single-edge notched bend specimens (SENB) were used in the present work. The toughening and resistance curve behavior of the matrix and composite materials are studied using resistance-curve experiments and small-/large-scale bridging models. The measured resistance-curves are compared with predictions from theoretical fracture mechanics models. The implications of the results are then discussed for the design of robust, affordable and sustainable building materials from natural fiber-reinforced earth-based composites.

4.2 Materials and Composite Processing

4.2.1 Materials

The earth-based materials used in this work were obtained directly from their deposition sites in Abeokuta, Ogun State, South-West Nigeria. One of which is laterite (lateritis) [14], a soil type that is rich in iron and aluminum. The name originate from the Latin word "Later (brick)" [15]. Laterites in moist state can be cut without difficulty and reshaped but it gradually hardens when exposed to air [16] Clay obtained from Abeokuta, Ogun State, Nigeria, was used as a stabilizer.

The fine-grained, clay (consisting primarily of hydrated silicates of aluminum with traces of iron oxide) also serves as a binder in the predominantly lateritic matrix [17] Straw (Andropogon virginicus) [18] was used as a reinforcing agent. Straw is a dry stalk of cereal plants. It is an agricultural by-product obtained after the grain and chaff have been removed. Lastly, Type I Ordinary Portland cement (composed of high calcium silicate) was procured from Lafarge cement factory, Ewekoro, Ogun state, Nigeria. The Ordinary Portland cement compliments the fine-grained clay as a binder.

4.2.2 Processing

Chemical and physical characterizations of the raw materials used were carried out as explained in chapter three. Bricks of different material compositions (matrices and reinforcements) were produced from the materials acquired. A macro-mechanical characterization of the specimens was carried out to obtain resistance-curve measurements. The cementitious materials were dry mixed manually with the aid of a hand trowel for about 2 minutes for homogenization. Samples were

prepared in varying dimensions in a mold using a hydraulic press at a pressure of 2 MPa for 5 minutes. This pressure was chosen after optimization. The samples were cured for 28 days in air at average temperature of $23^{O}C$ with average relative humidity of 80%. Samples of dimensions $25 \times 25 \times 100$ mm^3 specimens were prepared for Single-Edged Notched Bending (SENB) to study their resistance curve behavior.

Matrix composition of 70% laterite, 10% of clay and 20% of cement was considered in this study. The matrices were prepared by direct mixing of dry constituent material(s) followed by addition of water at approximate water-cement ration of 0.5. The material composition in the matrix preparation was based on percentage composition by volume of laterite, clay and cement. Natural fiber (straw)-reinforced composites were then produced with volume percentages of fiber ranging from 5% to 20%. These volume fractions used was determined based on the volume ratios of the initial solid raw materials. These proportions of the constituent materials were chosen based on the results obtained from preliminary tests. The mixtures were then molded to the required sample shapes.

4.3 Resistance-curve Experiments

Samples with dimensions of $25 \times 25 \times 100$ mm^3 were molded by pressing mixtures of laterite, clay, cement and straw fibers to produce composites with compositions as explained in section 4.2. This was achieved by the use a hydraulic press at a pressure of 2 MPa for 5 minutes. Single edge notched bend (SENB) specimens were produced by creating notch (with notch length to width ratios of 0.40-0.45) into the samples. After molding, the SENB specimens were air dried at room temperature (~ $25^{O}C$) with average relative humidity of 80% for 28 days. The samples were

then tested in a dual column universal testing system (Instron 3360 series 50 kN, Norwood, MA, USA) that was operated under load control at a loading rate of 2 N/s.

The resistance-curve measurements were obtained by loading in incremental steps until stable crack growth was initiated. The crack extensions were then measured using an in-situ optical microscope (model AY11336, manufactured by BARSKA, United States). The underlying crack/microstructure interactions were also elucidated via optical microscopy. The resistance-curve experiments were continued until steady-state conditions were achieved. The stress intensity factors in the resistance-curve were obtained from equation 3.3. Under three-point bend loading, the remote stress σ_f was taking as the flexural strength and obtained from equation 3.2.

4.4 Toughening Due to Crack Bridging

The toughening due to crack bridging by the straw fibers was modeled and added to the initiation fracture toughness to predict the composite fracture toughness and resistance-curve behavior [19]. This was done for small-scale bridging (SSB) [20] and large-scale bridging (LSB) [21]. A small scale bridging model proposed by Budiansky et al. [20] was used for modeling the initial stages of stable crack growth (bridge length < 0.5 mm).

Under SSB conditions, the shielding due to crack bridging ΔK_{SSB} is given by:

$$\Delta K_{SSB} = \alpha V_f \sqrt{\frac{2}{\pi}} \int_0^L \frac{\sigma_y}{\sqrt{x}} dx \tag{4.1}$$

where α is the constraint/triaxiality factor (theorectically between 1 and 3 and taken as ~ 3 in this study) [22], V_f is the volume fraction of the reinforcement phase, L is the bridging length (the distance from the crack-tip to the last unfractured reinforcement), σ_y is the uniaxial yield stress, and x is the distance from the crack face behind the crack-tip as described by Savastano et al. [23]. For large-scale crack bridging (LSB) conditions, the contribution to composite toughness due to crack bridging [21, 24] can be modeled. The model uses a weighting function by Fett and Munz [25] to estimate the weighted distributions of bridging traction across the reinforcements as shown schematically in Figure 4.2.

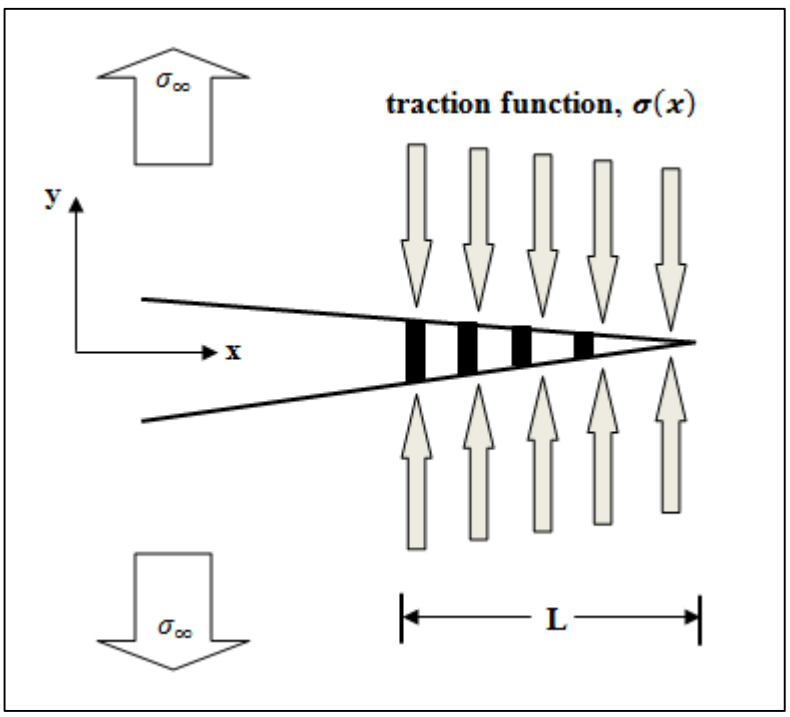

Figure 4.2: Schematic representation of a large scale bridging model [21]

The shielding from large scale bridging, ΔK_{lsb}, is given by [21]:

$$\Delta K_{lsb} = V_f \int_L \alpha \sigma_y h(a,x) dx \tag{4.2}$$

where α is the constraint/triaxiality factor (theorectically between 1 and 3 and taken as ~3 in this study) [22], V_f is the volume fraction of the reinforcement phase, L is the bridging length, σ_y is the uniaxial yield stress and x is the distance from the last unfractured fiber to the crack-tip. Also, $h(a,x)$ is the weighting function given by Fett and Munz as [25]:

$$h(a,x) = \sqrt{\frac{2}{\pi a}} \frac{1}{\sqrt{1-\frac{x}{a}}} \left[1 + \sum_{(\nu,\mu)} \frac{A_{\nu,\mu}\left(\frac{a}{W}\right)}{\left(1-\frac{a}{W}\right)} \left(1-\frac{x}{a}\right)^{\nu+1} \right] \tag{4.3}$$

where 'a' is the crack length and 'w' is the specimen width. The coefficients $(A_{\nu,\mu})$ are given in Table 4.1 for the SENB specimen.

Table 4.1: Summary of Fett and Munz [24] parameters for SENB specimen

ν	μ				
	0	1	2	3	4
0	0.4980	2.4463	0.0700	1.3187	-3.067
1	0.5416	-5.0806	24.3447	-32.7208	18.1214
2	-0.19277	2.55863	-12.6415	19.7630	-10.986

Hence, the expression for the estimation of the composite fracture toughness/resistance-curve behavior is given by equation 4.4:

$$K_R = K_i + \Delta K_B \tag{4.4}$$

where K_R is the composite fracture toughness characterized by the resistance-curve and ΔK_B is the shielding due to crack bridging. Note that $\Delta K_B = \Delta K_{SSB}$ for small-scale bridging and $\Delta K_B = \Delta K_{LSB}$ for large scale bridging. The R-curves can therefore be predicted from the measured bridging parameters and material properties in Table 4.2.

Table 4.2: Bridging toughness and parameters used in the toughening model

Volume percentages of reinforcement	V_b	$L\ (mm)$	α	$\Delta K_b(MPa\sqrt{m})$ Models	$\Delta K_b(MPa\sqrt{m})$ Experiments
5 vol% Fiber	0.050	4.5	3	0.25±0.01	0.24±0.01
10 vol% Fiber	0.075	4.5	3	0.38±0.02	0.30±0.02
20 vol% Fiber	0.100	4.5	3	0.50±0.03	0.42±0.02

V_b = Fiber volume fraction in the bridge zone, L = Length of the bridge zone, α = Triaxiality factor, ΔK_b = Bridging toughness.

4.5 Results and Discussion

The resistance-curve obtained for natural fiber (straw) reinforced earth-based cementitious composites is presented in Figure 4.4. This was done for fiber volume fractions of 5%, 10% and 20%. Stable crack initiation occurred in the composites at matrix toughness of ~ 1.0 MPa$\sqrt{\text{m}}$. The initial resistance curve was steep during the early stages of crack growth($\Delta x \leq \sim 0.5$ mm). A gradual transition to nearly-steady-state condition was observed during the final stages of crack growth. The measured resistance-curve can be attributed to the interactions of the crack with straw that bridged the crack faces (Figure 4.3). This suggested that the measured resistance-curve was largely due to shielding effects of crack bridging.

The toughening was also modeled using resistance-curve behavior involving the small-scale and large scale bridging models (equations 4.1 and 4.2 respectively). The predicted resistance-curve is shown alongside the experimental measurement in Figure 4.4. The bridging toughness and parameters used in the predictions are presented in Table 4.2. Note that the predictions and the measured resistance-curve curves showed that the trend of improved toughness was retained.

Figure 4.3: Crack/Fiber interaction in stabilized laterite matrix.

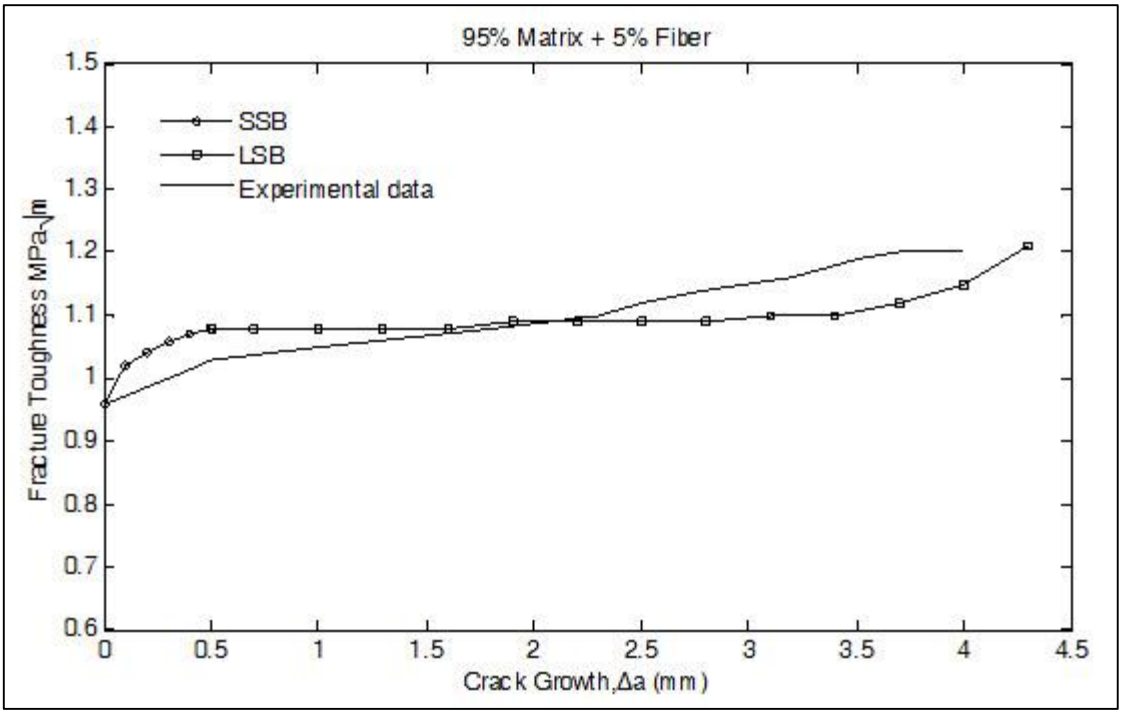
95% Matrix + 5% Fiber
SSB
LSB
Experimental data
Fracture Toughness MPa√m
Crack Growth,Δa (mm)
1.5
1.4
1.3
1.2
1.1
1
0.9
0.8
0.7
0.6
0
0.5
1
1.5
2
2.5
3
3.5
4
4.5

(a)

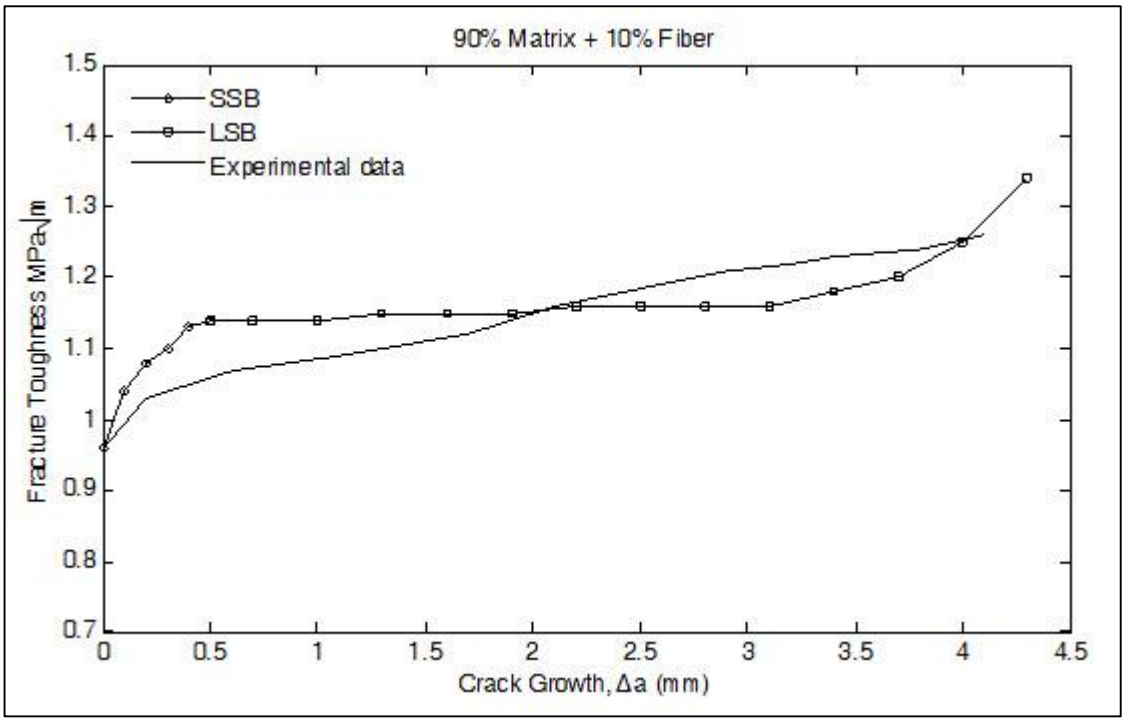
90% Matrix + 10% Fiber
SSB
LSB
Experimental data
Fracture Toughness MPa√m
Crack Growth, Δa (mm)
1.5
1.4
1.3
1.2
1.1
1
0.9
0.8
0.7
0
0.5
1
1.5
2
2.5
3
3.5
4
4.5

(b)

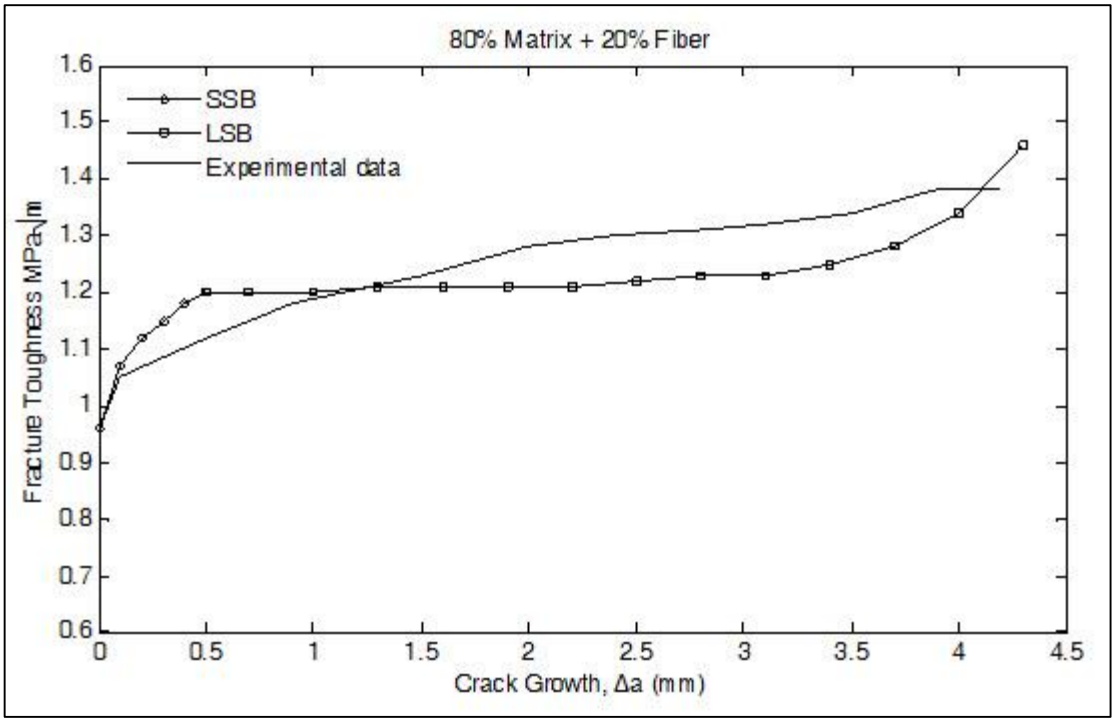

(c)

Figure 4.4: Resistance-curve measurement of stabilized laterite-clay reinforced with (a) 5%, (b) 10% and (c) 20% volume fractions of straw with calculated curves from small and large-scale bridging models (SSB and LSB respectively).

4.6 Summary and Concluding Remarks

The resistance-curve behavior of natural fiber-reinforced earth-based composites has been studied within a combined experimental and theoretical framework. The following conclusions have been reached:

i. Toughening occurs via small- and large-scale bridging mechanisms. These give rise to strong resistance-curve behavior during the early stages of crack growth, and a gradual transition towards a near steady-state in the large-scale bridging region.

ii. Evidence of crack-bridging and fiber pull-out was observed on the fracture surfaces of the resistance-curve specimens. The strong interaction between the cementitious matrix and the straw can be inferred from mineralization by cementitious hydration products.

iii. The measured resistance-curve behavior was compared with the predicted based on the micromechanical model presented. Small-scale bridging (SSB) was presumed to occur for crack growth, Δa, less than 0.5 mm, and large-scale bridging (LSB) was assumed for Δa greater than or equal to 0.5 mm.

iv. The modeling of crack shielding by crack bridging provides adequate estimates of toughening in the straw-reinforced earth-based composites that were examined in this study. This is evident in the trends of resistance-curve behavior obtained from small- and large-scale bridging models.

v. The trends in the predictions of resistance-curve behavior obtained from the bridging models are in agreement with the corresponding experimental measurements. Specifically, the resistance-curve curves showed that the trend of improved toughness in the predicted and the measured values were retained.

References

[1] McMeeking R. M. and Evans A. G., "Mechanics of Transformation Toughening in Brittle Materials," *J. Am. Ceram.* Soc., 65 [5] 242-45 (1982).

[2] Swamy RN, editor. Natural fibre reinforced cement and concrete. Concrete technology and design, 5. Glasgow: Blackie; 1988.

[3] A.G. Evans: *J. Am. Ceram. Soc.*, 1990, vol. 72 (2), pp. 187-206.

[4] R.O. Ritchie: *Mater. Sci. Eng. A*, 1988, vol. A103, pp. 15-28.

[5] M.F. Ashby, F.J. Blunt, and M. Bannister: *Acta Metall.*, 1989, vol. 37 (7), pp. 1847-57.

[6] A.G. Evans and R.M. McMeeking: *Acta Metall.*, 1986, vol. 34 (12), pp. 2435-41.

[7] B. Budiansky, J.C. Amazigo, and A.G. Evans: *J. Mech. Phys. Solids*, 1988, vol. 36 (2), pp. 167-87.

[8] Savastano Jr H, Warden PG and Coutts RSP. Brazilian waste fibers as reinforcement for cement based composites. Cem. Concr. Compos. 2000; 22(5): 379-84.

[9] Banthia N and Sheng J. Fracture toughness of micro-fiber reinforced cement composites. Cem. Concr. Compos. 1996; 18(4): 251-69.

[10] Savastano Jr H, Santos SF, Radonjic M et al. Fracture and fatigue of natural fiber-reinforced cementitious composites. Cem. Concr. Compos. 2009; 31(5): 232-43.

[11] Nelson PK, Li VC and Kamada T. Fracture toughness of microfiber reinforced cement composites. J Mater Civ Eng 2002; 14(5): 384-91.

[12] Eissa A-B and Batson G. Model for predicting the fracture process zone and R-curve for high strength FRC. Cem. Concr. Compos. 1996; 18(2): 125-33.

[13] Savastano Jr H, Warden PG and Cutts RSP. Microstructure and mechanical properties of waste fiber-cement composites. Cem. Concr. Compos. 2005; 27(5): 583-92.

[14] Aleva, GJJ. Laterites: concepts, geology, morphology and chemistry. International Soil Reference and Information Centre (ISRIC), 1994.

[15] Sivarajasingham S, Alexander LT, Cady JG et al. "Laterite". Advances in Agronomy 1962; 14, 1-60.

[16] Tardy Y. Petrology of laterites and tropical soils. AA Balkema, 1997.

[17] Hillier S. "Clay Mineralogy. In: Encyclopedia of sediments and sedimentary rocks". Kluwer Academic Publishers, Dordrecht. 2003. pp 139-142.

[18] Robert HM. USDA-NRCS PLANTS Database / USDA SCS. 1991. Southern wetland flora: Field office guide to plant species. South National Technical Center, Fort Worth.

[19] Soboyejo W O. Toughening mechanisms. Mechanical Properties of Engineered Materials. NY: Marcel Dekker Publishers; 2002. p. 414-55 [chapter 13].

[20] Budiansky B, Amazigo JC, Evans AG. Small scale crack bridging and the fracture toughness of particulate-reinforced ceramics. J Mesh Phys Solids 1988; 36(2):167-87.

[21] Bloyer D R, Rao K T V, Ritchie R O. Fracture toughness and R-curve behavior of laminated brittle-matrix composites. Metal Meter Trans A 1998; 29A(10): 2483-96.

[22] Kung E, Mercer C, Allameh S, Popoola O and Soboyejo W O. An investigation of fracture and fatigue in a metal/polymer composite. Metall Mater Trans A 2001; 32A(8): 1997-2010.

[23] Savastano Jr H, Turner A, Mercer C and Soboyejo W O. Mechanical behavior of cement based materials reinforced with sisal fibers. J Mater Sci 2006; 41: 6938-48.

[24] Bloyer D R, Rao K T V and Ritchie R O. Fatigue-crack propagation behavior of ductile/brittle laminated composites. Metal Meter Trans A 1999; 30A (3): 633-42.

[25] Fett T and Munz D. Stress intensity factors and weight functions for one dimensional cracks. institut fur Materialforschung, Kernforschungszentrum Karlsruhe, Germany, 1994.

CHAPTER FIVE: PULLOUT BEHAVIOR OF NATURAL FIBER FROM EARTH-BASED MATRICES

5.1 Introduction

The toughening provided by fibers in fiber-reinforced composites via crack bridging depends significantly on the mechanical properties of the matrix, the fibers, and the fiber-matrix interface [1]. The interfacial strength between the matrix and the fibers is often the key to composite toughening and fracture properties [2]. Prior work has also shown that the best overall toughening of ceramic matrix composite may require debonding and frictional sliding to occur at the interfaces between the fibers and matrix [1].

The mechanics of interfacial de-bonding have been studied by number of authors [3-5]. These studies have shown that the initial elastic deformation is truncated by load drops, corresponding to the onset of interfacial debonding. This is followed by fiber pull-out, during which frictional stresses and residual clamping stresses resist the pull-out of the fibers from the matrix materials [6]. In brittle-matrix composites, the interfacial strengths are often characterized by the debond stress or the frictional pull-out stess [7]. The interfacial strengths also have a strong influence on composite strength and composite fracture toughness [8]. This has motivated several researchers to study the fiber/matrix interface properties in such composites. An investigation by Marshall et al. and other authors was focused at determination of the force required to slip a fiber through a matrix [9, 10]. Other efforts centered on measuring interfacial strength via fiber pull-out tests [11, 12]. For cement matrix composites, there have also been considerations of load-deflection behavior in fiber pull-out process [13-15].

During the fiber pull-out process, Kelly and Tyson [2] showed that the force required to pull out a stiff fiber from a softer metal matrix is a linear function of the embedded length of the fiber in the matrix. In a related study, Greszczuk [16] developed a relationship between interface strength as a function of the embedded length of the fiber.

In modeling fiber pullout, characterization of fractional stress of fiber embedded in a matrix has been an open issue for a long time [17]. Most studies focus directly on measuring frictional stresses using theoretical models that are guided by experimental observations and measurement. Hence, depending on experimental results, most authors assume either a constant friction stress or coulomb friction [18]. A review of prior work on the modeling of fiber pull-out behavior, can be found in Ref. [19].

However, there have been no prior studies of the interfacial strengths of earth-based natural fiber composites that are being developed for structural applications in affordable housing. This will be explored in this study, using a combination of experiments and analytic models. These will be used to study the fiber pull out behavior of earth-based composites. The toughening due to fiber pull-out will also be modeled using crack-tip shielding concepts. The implications of the models will then be discussed for the design of robust/sustainable housing.

5.2 Materials Used

Natural fiber-reinforced earth-based composites were produced from locally sourced materials obtained directly from their deposition sites in Abeokuta, Ogun State, South-West Nigeria. These included: laterite (lateritis) [20], clay (which was used as a stabilizer) and straw fibers (Andropogon virginicus) [21]. The clay was obtained from Abeokuta, Ogun State, Nigeria. The

fine-grained, clay (consisting primarily of hydrated silicates of aluminum with traces of iron oxide) also serves as a binder in the predominantly lateritic matrix [22]. Type I Ordinary Portland cement (composed of calcium silicate) was procured from Lafarge cement factory, Ewekoro, Ogun State, Nigeria. The cement was also used as a binder.

5.3 Sample Preparation

The fiber pull-out specimens had a prismatic shape of 25 mm x 25 mm x 100 mm. Matrix materials were dry mixed manually with the aid of a hand trowel. This was done for about 2 minutes (for homogenization), followed by the addition of water at water-cement ratio of 0.5. The mixtures were then molded to the stipulated shapes. The surfaces of the fibers were cleaned and embedded at the center of the specimen. The natural fibers were then aligned with a fixture, without any significant pre-tension, prior to molding. The samples were then prepared in a mold using a hydraulic press at a pressure of 2 MPa for 5 minutes. This pressure was chosen after optimization. The samples were cured for 28 days in air at average temperature of $23^{O}C$ and an average relative humidity of 80%.

4. Experimental Procedures

The stages of the experiments are presented schematically in Figure 5.1. This shows a schematic diagram required for the study of the interfacial strengths of natural fiber-reinforced earth-based composites. The effects of fiber embedment length and fiber volume fraction (on the fiber pull-out characteristics) were considered. Three different fiber embedment lengths: 15 mm, 20 mm and 25

mm were tested. Three different fiber volume fractions (5%, 10% and 20%) were used within the matrix.

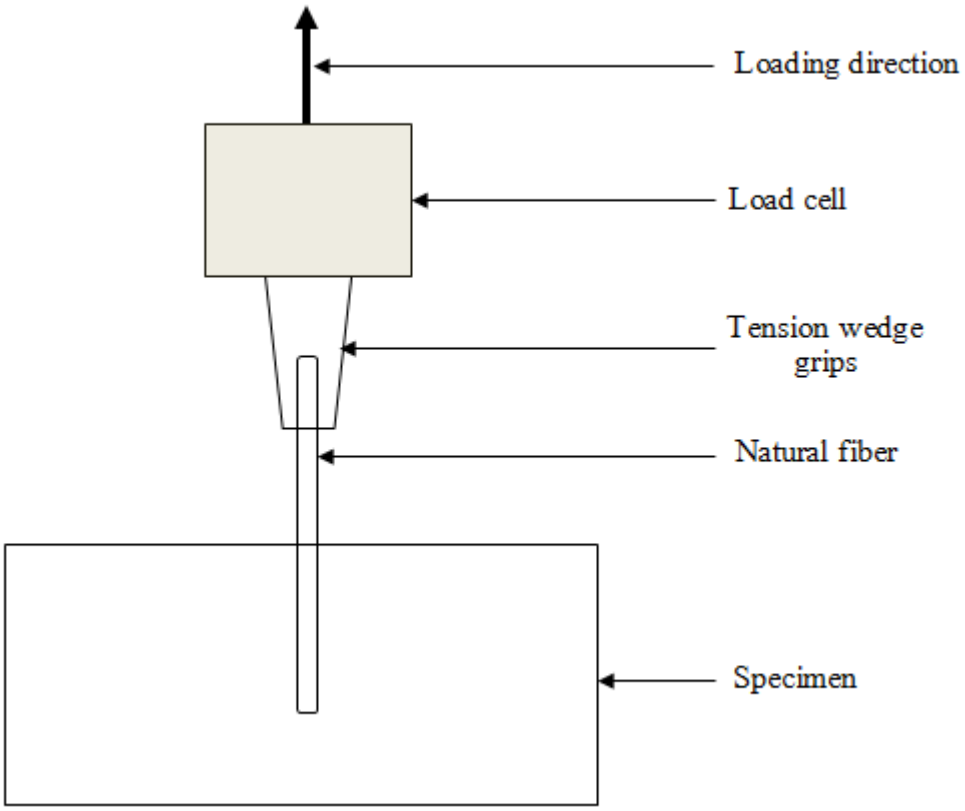

Figure 5.1: Schematic diagram of the pullout specimen.

An Instron 3360 series (Norwood, MA, USA) electro-mechanical testing machine was used to obtain plots of load versus displacement of the embedded fiber. This was done at a loading rate of 3.3 N/s. The samples were tested at room temperature with average relative humidity of 65%. The other ends of the embedded fibers were held firmly by tension wedge grips attached to a 2 kN load cell, while the specimen was fixed securely to the Instron with the aid of G-clamps, as shown in Figure 5.2. The fiber displacement was monitored using an in-situ optical microscope.

Figure 5.2: Experimental setup for pullout of natural fiber from earth-based cementitious matrix

5.5 Modeling of Fiber Pull-out (Debonding with Constant Friction)

The choice of the model for this study is motivated by the experimental observation of the frictional bond stress obtained relative to fiber embedment lengths. The results (Figure 5.7) show a constant friction stress, τ, between the fiber and the matrix and the radial component of stress at the interface is greater than zero ($\sigma_r > 0$).

A model proposed originally by Hutchinson and Jensen [23] was used in this study. This model, which assumes a constant friction stress between fiber and matrix, was adopted to model the effects of fiber pull-out on the toughening of earth-based composite. In the model, the fiber-matrix system was modeled by a cylindrical composite (Figure 5.3 and 5.4), comprising a fiber (radius r_f) surrounded by matrix with a circular cylindrical outer boundary of radius r. The area fraction of the fiber is taken as $\rho = (r_f/r)^2$.

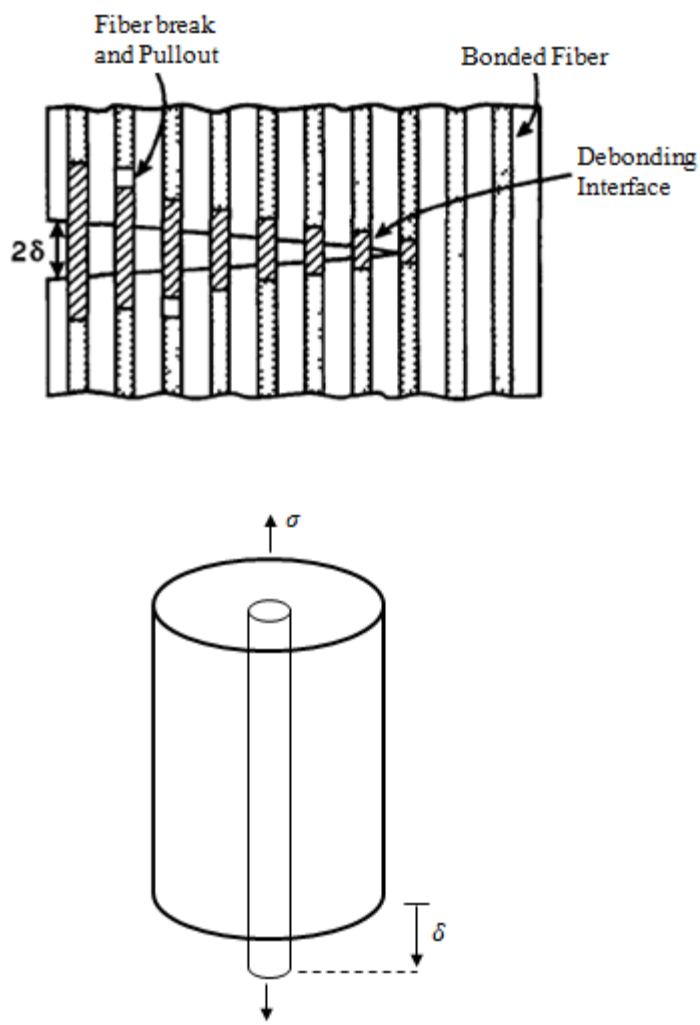

Figure 5.3: Schematic of fiber debonding and pullout in a cylindrical cell model [20, 21]

In the model adopted, the average stress in the fiber (below the debond crack tip) varies according to:

$$d\sigma_f/dz = (2/r_f)\tau \tag{5.1}$$

where σ_f is the average axial stress in the fiber, r_f is the radius of the fiber and τ is friction stress between the matrix and the fiber.

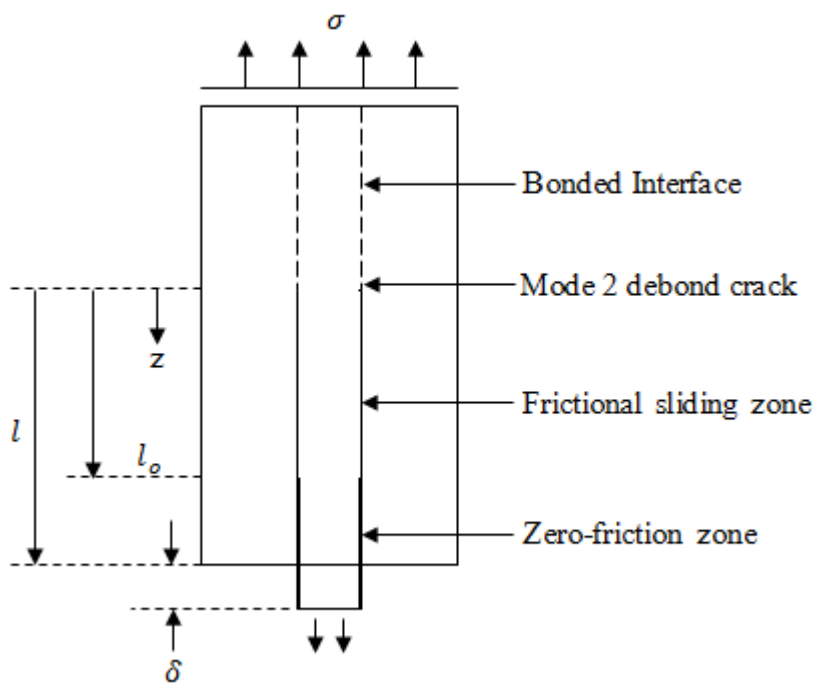

Figure 5.4: Conventions and definitions of fiber debonding and pullout in a cylindrical cell model [23]

The Equation is a valid approximation, provided that τ is small compared to σ_f. Also, another essential approximation that was made in the analysis of the model, is that the axial and radial stresses in any section transverse to the z-axis are characterized by a Lame problem.

For $0 < z < l_o$,

$$\sigma_f = \sigma_f{}^* + 2\tau\left(z/r_f\right) \tag{5.2}$$

while

$$\sigma_m = \sigma_m{}^* - 2\rho(1-\rho)^{-1}\tau\left(z/r_f\right) \tag{5.3}$$

where $\sigma_f{}^*$ and $\sigma_m{}^*$ are the respectively fiber and matrix strengths, just below the debond crack tip. If the zero-friction zone shown in Figure 5.4 exists, then:

$\sigma_f = \overline{\sigma}/\rho$ and $\sigma_m = 0$ for $l_o < z < l$.

When $\overline{\sigma} < \overline{\sigma_o}$,

then $\sigma_f = \overline{\sigma}/\rho$ and $\sigma_m = 0$ at $z = l_o$.

In either case,

$$l_o/r_f = \left(\overline{\sigma}/\rho - \sigma_f{}^*\right)/(2\tau) \tag{5.4}$$

where $\overline{\sigma}$ is the average axial stress and$\overline{\sigma_o}$ is the maximum value of $\overline{\sigma}$. To determine $\sigma_f{}^*$ and $\sigma_m{}^*$, the fracture condition $G = G_c$ (where G and G_c are energy release rate of debond crack and mode II toughness respectively) at the debond crack tip is imposed. This is done using result from a model of the steady-state energy release rate. This is given by:

$$G = \left(r_f/E_m\right)\left[\rho(1-\rho)^{-1}c_1c_3\left(\sigma_f{}^- - \sigma_f{}^+\right)\right]^2 \tag{5.5a}$$

$$G = \left(r_f/E_m\right)[c_1(\overline{\sigma} - c_3\sigma_m{}^*)c_2E_m\epsilon^T]^2 \tag{5.5b}$$

where

$$c_1 = (2\rho)^{-1}(1-\rho a_1)(b_2+b_3)^{1/2}$$

$$c_2 = \frac{1}{2}a_2(b_2+b_3)^{1/3}$$

$$c_3 = (1-\rho)/(1-\rho a_1)$$

and a_i, b_i and c_i are non-dimensional coefficients [23].

For an isotropic fiber, the relationship between the mode 2 stress intensity factor, K_2, and the energy release rate is given by [22]:

$$G = \frac{1}{2}\left(\frac{1-\nu_f{}^2}{E_f} + \frac{1-\nu_m{}^2}{E_m}\right)K_2{}^2 \tag{5.6}$$

When the fiber and matrix surfaces are loaded by a constant frictional stress τ and the fiber slides but does not lose contact with the matrix, the variation of K_2 is approximated by [23]:

$$K_2/\left(\tau r_f{}^{1/2}\right) = (1-\rho)^{-1/2}\left(l/r_f\right) \tag{5.7}$$

5.6 Results and Discussion

5.6.1 Single Fiber Pull-out

The results of the single fiber pull-out tests are presented in Figures 5.6, 5.7 and 5.8. The pullout curves obtained in this study can be divided into three stages, as obtained in prior work on other ceramic matrix composites in the literature [32-34]. These include: (i) a linear elastic deformation stage; (ii) a partial fiber debonding stage, and (iii) a frictional pull-out stage [34]. This is shown schematically presented in Figure 5.5. Frictional bond strength values were also calculated by

dividing the maximum pullout load by embedded fiber surface area. The value obtained will be used to predict the maximum contribution of the fiber pull-out load to the composite fracture toughness in section 5.6.2.

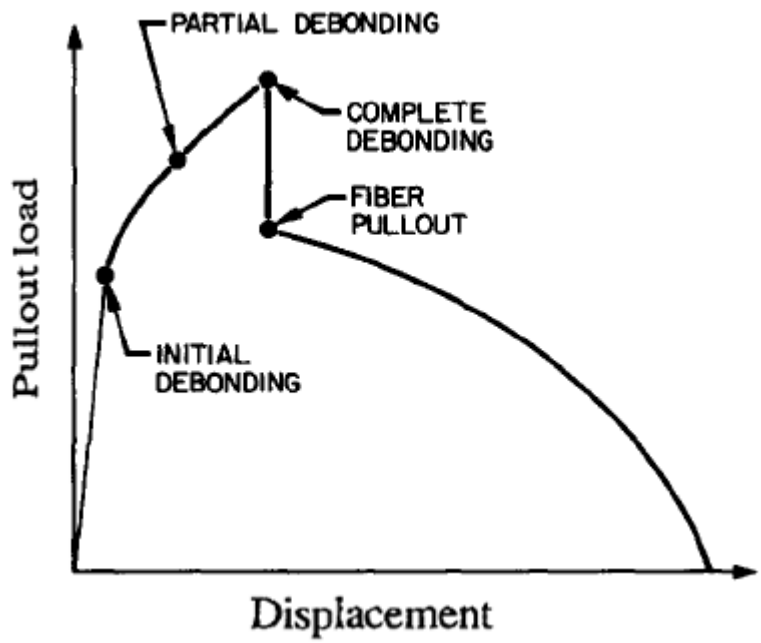

Figure 5.5: Schematic diagram showing load-displacement relationship for embedded fiber during fiber pullout test [24].

All specimens tested failed by fiber debonding and pullout. Figure 5.6 shows the effect of embedment length on peak pullout load. A significant increase was observed in the peak fiber pull-out load (while keeping other parameters constant) with increasing fiber embedment length (from 15 mm to 25 mm). This is attributed to the increase in the fiber/matrix contact area that occurs with increasing fiber embedment length.

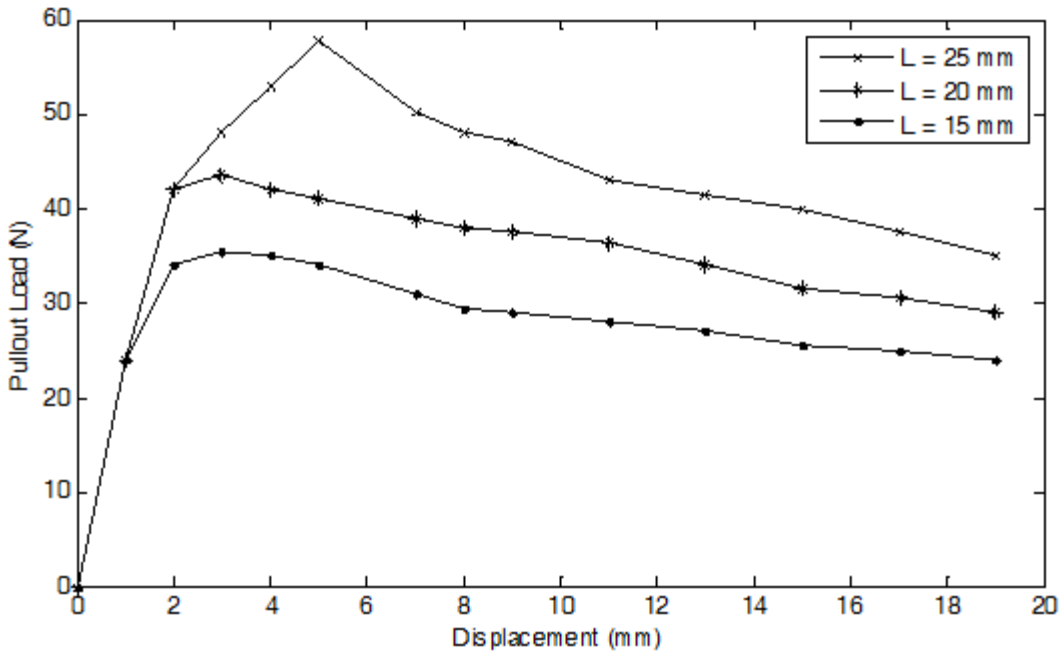

(a)

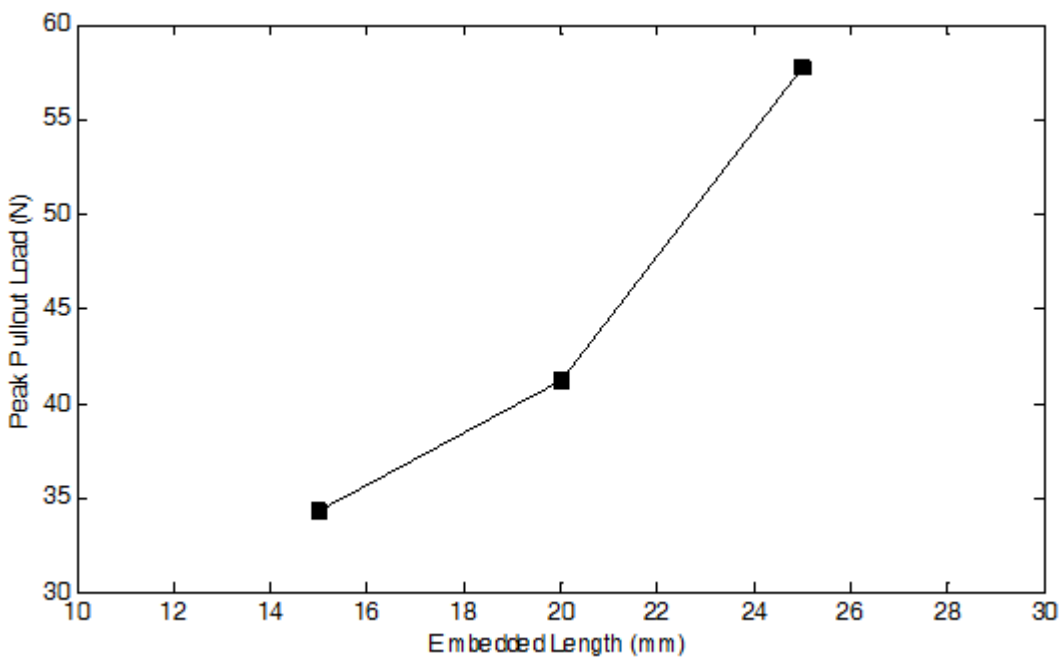

(b)

Figure 6: (a) Effect of embedment length on the pullout behavior of natural fiber from earth-based cementitious matrices and (b) Effect of fiber embedment length on peak pullout load.

Meanwhile, Figure 5.6b shows that the peak fiber pull-out load does not appear to be directly proportional to the fiber embedment length. This is because the onset of fiber debonding corresponds to the condition at which the interfacial crack driving force is equal to the interfacial fracture toughness at the local mode mixity. Since this will depend non-linearly on the internal crack lenths and elastic properties of the materials, the fiber pull-out loads are unlikely to exhibit a linear dependence of the fiber embedment length.

The results (Figure 5.7) obtained show that fiber pull-out occurred with a constant frictional bond stress at the interface between the fiber and earth-based cementitious matrices. An average frictional bond strength of about 0.34±0.02 MPa was obtained for earth-based cementitious matrix. Other results obtained for composites (with vary fiber fractions) will be used in the next section to predict the toughening due to debonding and fiber pull-out.

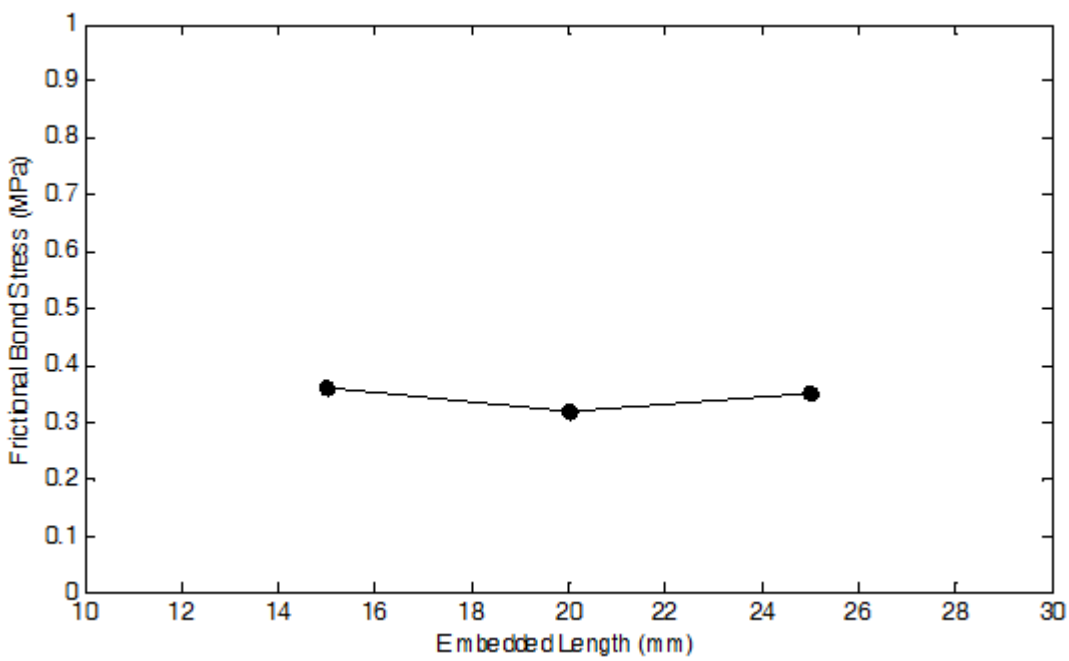

Figure 5.7: Effect of fiber embedment length on frictional bond strength for earth-based cementitious matrices.

Figure 5.8 shows the fiber pull-out strengths obtained for fiber volume fractions between 0 to 20 %. While keeping other parameters constant, the result shows that increasing the fiber volume fraction resulted in increasing peak pullout load. This increase in the pull-out load can be attributed to the increase in fiber bundle/composite ligament strength that occurs with increasing fiber volume fraction. Hence, the increase in the volume fraction of fibers provides increased shielding due to crack bridging and fiber pull-out.

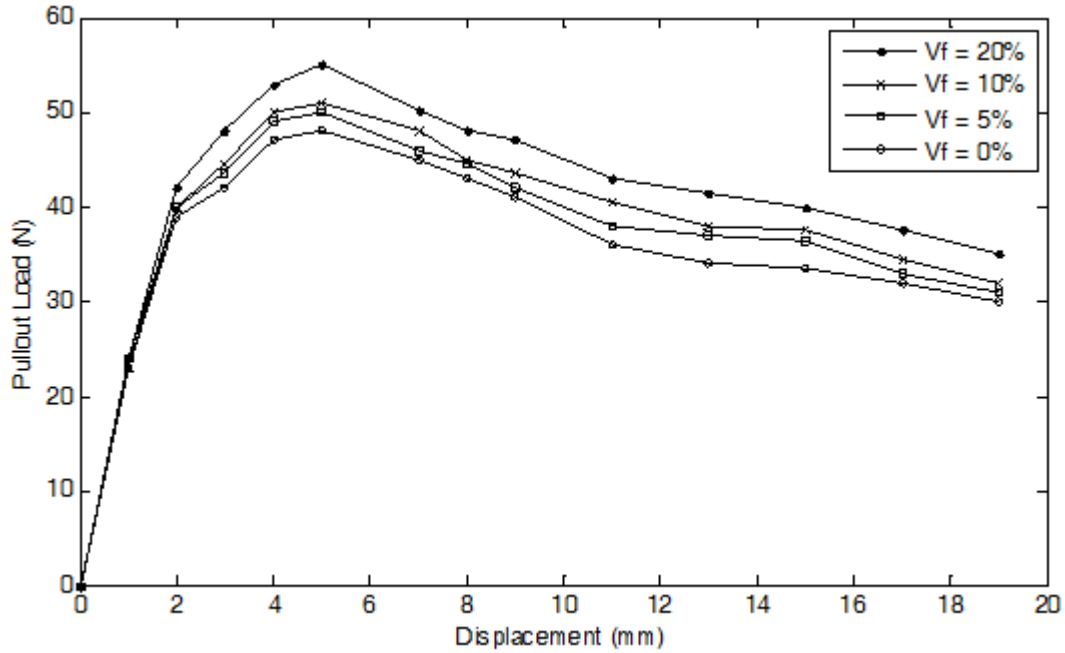

Figure 5.8: Effect of fiber volume fraction on the pullout of natural fiber from earth-based cementitious matrices.

5.6.2 Composite Toughening due to debonding and pull-out

Using data summarized in Table 5.1, the shielding contribution from fiber pull-out model described in section 5.5 are presented. The results primarily show that increasing fiber volume fraction results in increased toughening. This increase in fracture toughness attained as a result of

fiber-reinforcement can be attributed to shielding of the remote loads by interfacial strength and bridging fibers.

The results also revealed that a positive mode II exists along the matrix fiber interface. This implies that debonding, sliding and pull-out contributes to toughness. The sliding resistance that exist in this study is governed by the frictional characteristic of the debond interface provided by the rough morphology of the fiber [17]. Also, for fibers that debonded without fiction, they primarily contribute to toughness via crack bridging. Lastly, the toughness resulting from the combined mechanisms will be discussed in the next chapter.

Table 5.1: Parameters used in the toughening due to fiber pull-out model

Volume percentages of reinforcement	τ (MPa)	r_f (m)	r (m)	ρ	$\Delta K\ (MPa\sqrt{m})$
5 vol% Fiber	0.39±0.02	0.001	0.002	0.25	0.13±0.01
10 vol% Fiber	0.40±0.02	0.001	0.002	0.25	0.17±0.01
20 vol% Fiber	0.44±0.02	0.001	0.002	0.25	0.29±0.01

τ = friction stress between the matrix and the fiber, r_f = radius of the fiber, r = radius of cylindrical outer boundary of matrix, ρ = area fraction of the fiber, ΔK = Pull-out toughness.

5.7 Summary and Concluding Remarks

The interfacial strengths and fiber pull-out characteristics have been studied in earth-based composites reinforced with straw fibers. Salient conclusions arising from the combined experimental and theoretical study are as follows:

I. The fiber pull-out strengths increase with increasing fiber embedment length and fiber volume fractions up to 0.2. The measured improvements are consistent with predictions from composites and interfacial fracture models.

II. Following the onset of debonding, a regime of constant frictional pull-out stress was observed. This suggests that the friction stress was not significantly affected by the degree of pull-out.

III. The predicted toughening obtained from the fracture mechanics analyses is consistent with the experimental resistance curves. These predictions are also consistent with the ranges in the toughening/resistance-curve behavior obtained for the earth-based composites with different volume fractions of fibers between 0 and 20 vol. %.

REFERENCES

[1] Becher, P. F., HSUEH, C. H., Angelini, P., & Tiegs, T. N. Toughening Behavior in Whisker-Reinforced Ceramic Matrix Composites. *Journal of the American Ceramic Society* 1988, *71*(12), 1050-1061.

[2] Kelly A and Tyson WR. Tensile properties of fiber-reinforced metals. *J. Mech. Phys. Solids,* 13 (1965) 329-350.

[3] Broutman LJ. Modern Composite Materials ed. Broutman LJ and Krock RH. New York: Addison-Wesley, 1967, 391-394.

[4] Wells JK and Beaumont PWR. Debonding and pull-out processes in fibrous composites. *J. Mater. Sci.,* 1985, 20 (4) 1275-1284.

[5] Kerans, RJ and Triplicane AP. Theoretical analysis of the fiber pullout and push-out tests. *J. Am. Ceram. Soc.,* 1991, 74 (7) 1585-1596.

[6] Kim, J. K., Baillie, C., & Mai, Y. W. Interfacial debonding and fiber pull-out stresses. *Journal of materials science*, 1992, 27(12), 3143-3154.

[7] Hsueh, C. H. Interfacial debonding and fiber pull-out stresses of fiber-reinforced composites. *Materials Science and Engineering: A*, 1990, *123*(1), 1-11.

[8] Kim, J. K., & Mai, Y. W. High strength, high fracture toughness fibre composites with interface control - a review. *Composites Science and Technology*, 1991, *41*(4), 333-378.

[9] Marshall DB and Oliver WC. Measurement of interfacial mechanical properties in fiber-reinforced ceramics composites. 1987, 70 (8) 524-548.

[10] Mandell JF, Kong KCC and Grande DH. Interfacial shear strength and sliding resistance in metal and glass-ceramic matrix composites. *Ceram. Eng. Sci. Proc.,* 1987, 8 (7-8) 937-940.

[11] Griffin CW, Limaye SY, Richardson DW and Shetty DK. Evaluation of Interfacial Properties in Borosilicate- SiC Composites using Pull-out Tests. *Ceram. Eng. Sci Proc.*, 1988, 72 (10) 671-678.

[12] Goettler RW and Faber KT. Interfacial shear stresses in SiC and Alumina Fiber Reinforced Glasses. *Ceram. Eng. Sci. Proc.*, 1988, 9 (7-8) 861-872.

[13] Greszczuk LB. theoretical studies of the mechanics of the fiber-matrix interface in composites. In: ASTM special technical publication, STP-452, Interfaces in Composites. American Society for Testing and Materials, Philadelphia, PA, 1969.

[14] Lawrence P. some theoretical considerations of fiber pull-out from an elastic matrix. *J. Mater. Sci.*, 1972 (7) 1-6.

[15] Takaku A and Arridge RGC. The effect of Interfacial radial and shear stress on fiber pull-out in composite materials. *J. Phys. D*, 1973 (6) 2038-2047.

[16] Greszczuk LB. interface in Composites (ASTM STP 452) (Philadelphia: American Society for Testing and Materials) p 49.

[17] Marshall, D B and Evans A G. Failure mechanisms in Ceramic-Fiber/Ceramic-Matrix Composites, *J Am Ceram Soc*, 1985, 68[5], 225-31

[18] Bright, J B, D K Shetty, C W Griffin and S Y Limaye, Interfacial bonding and friction m silicon carbide (filament)-reinforced ceramic- and glass-matrix composites, J *Am Ceram Soc*, 1989, *72*, 1891-1898

[19] Gao Y C, Mai Y W and Cotterell B. Fracture of fiber-reinforced materials. *J. Appl. Math. Phys.*, 1988, 39, 550 – 572.

[20] Aleva GJJ. (Ed.) (1994): Laterites. Concepts, Geology, Morphology and Chemistry. 153 p. ISRIC, Wageningen, ISBN 90-6672-053-0.

[21] Robert HM. USDA-NRCS PLANTS Database / USDA SCS. 1991. Southern wetland flora: Field office guide to plant species. South National Technical Center, Fort Worth.

[22] Hillier S. "Clay Mineralogy. In: Encyclopedia of sediments and sedimentary rocks". Kluwer Academic Publishers, Dordrecht. 2003. p 139-142.

[23] Hutchinson J W and Jenson H M. Models of fiber debonding and pullout in brittle composites with friction, Rep. MECH-157, Harvard University, Cambridge, MA, 1990.

[24] Soboyejo W O. Toughening mechanisms. Mechanical Properties of Engineered Materials. NY: Marcel Dekker Publishers; 2002. p. 414-55 [chapter 13].

CHAPTER SIX: TOUGHENING BEHAVIOR IN NATURAL FIBER-REINFORCED EARTH-BASED COMPOSITES

6.1 Introduction

Recent studies of whisker-reinforced ceramics reveal that substantial improvements in fracture toughness and resistance to slow crack growth are achieved via the incorporation of strong, small-diameter whiskers into ceramic matrices [1, 2]. The toughening behavior of fiber-reinforced earth-based cementitious composite was analyzed in terms of a bridging zone immediately behind the crack tip and fiber pullout. These approaches are consistent with microscopy observations which reveal that intact bridging whiskers exist behind the crack tip in addition to debonding of the whisker-matrix interface. The experimental and theoretical results based on both the stress intensity and the energy change introduced by bridging whiskers reveal the dependence of toughening upon the composition and matrix, interface, and whisker properties. The analytical models of whisker bridging accompanied by limited pullout will accurately describe experimental observations of the toughening behavior in the natural fiber-reinforced earth-based composites. Such analytical descriptions as described in previous chapters indicate that fiber, matrix and interface properties will result in further increases in toughness by whisker reinforcement.

In this study, the mechanisms responsible for such whisker toughening include both whisker bridging and whisker pullout within a zone immediately behind the crack tip. Compared to some continuous-fiber-reinforced ceramics in which extensive fiber pullout occurs, whisker pullout is more limited. This is, in part, a result of the short whisker lengths, and hence small pullout lengths as compared to those that can be obtained in continuous-fiber-reinforced composites [3]. Increases in toughness by extensive fiber or whisker pullout require minimization of the shear strength of

the fiber-matrix interface [4]. Fiber bridging requires at least modest interfacial strength to transfer load to the fiber and high fiber tensile strength to sustain the applied stress within the wake of the crack tip [5]. Activation of these processes during fracture of fiber-reinforced composites is indicated by the observed increase in toughness with increase in the whisker volume content and when the crack plane is oriented normal versus parallel to the plane containing the longitudinal axes of the whiskers [1]. Evidence of whisker bridging (Figure 3.6) and pull-out (Figure 6.2) are noted in fracture surface observations using optical and scanning electron microscopy (SEM) respectively.

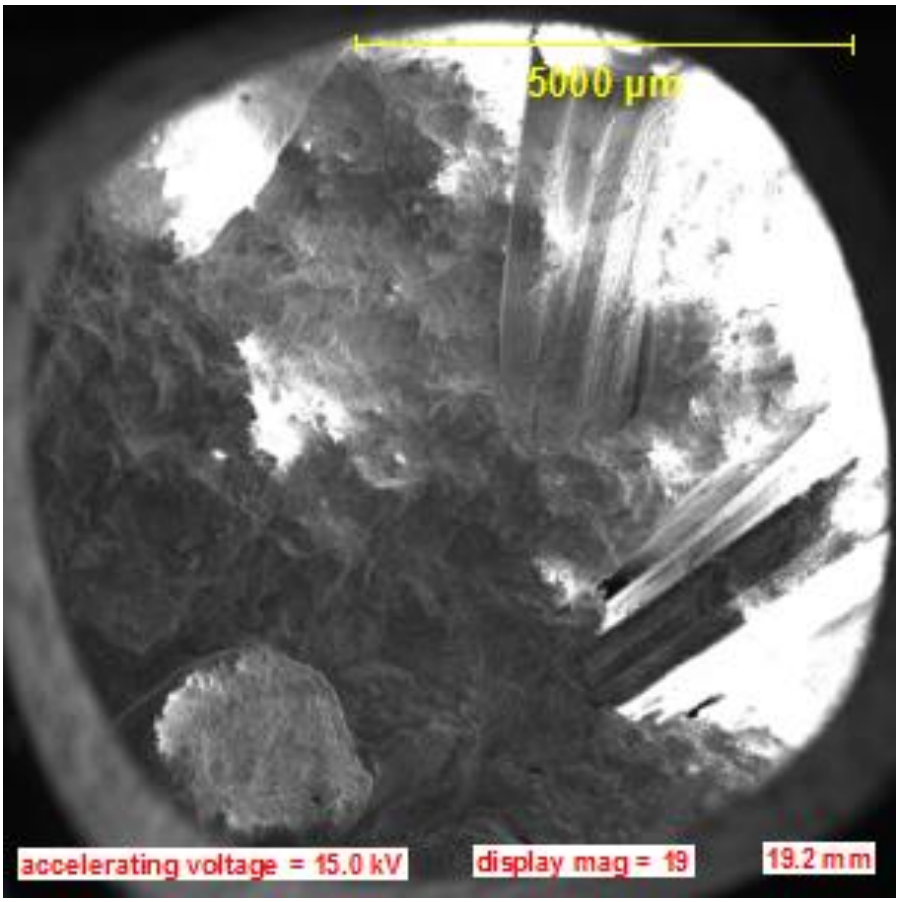

(a)

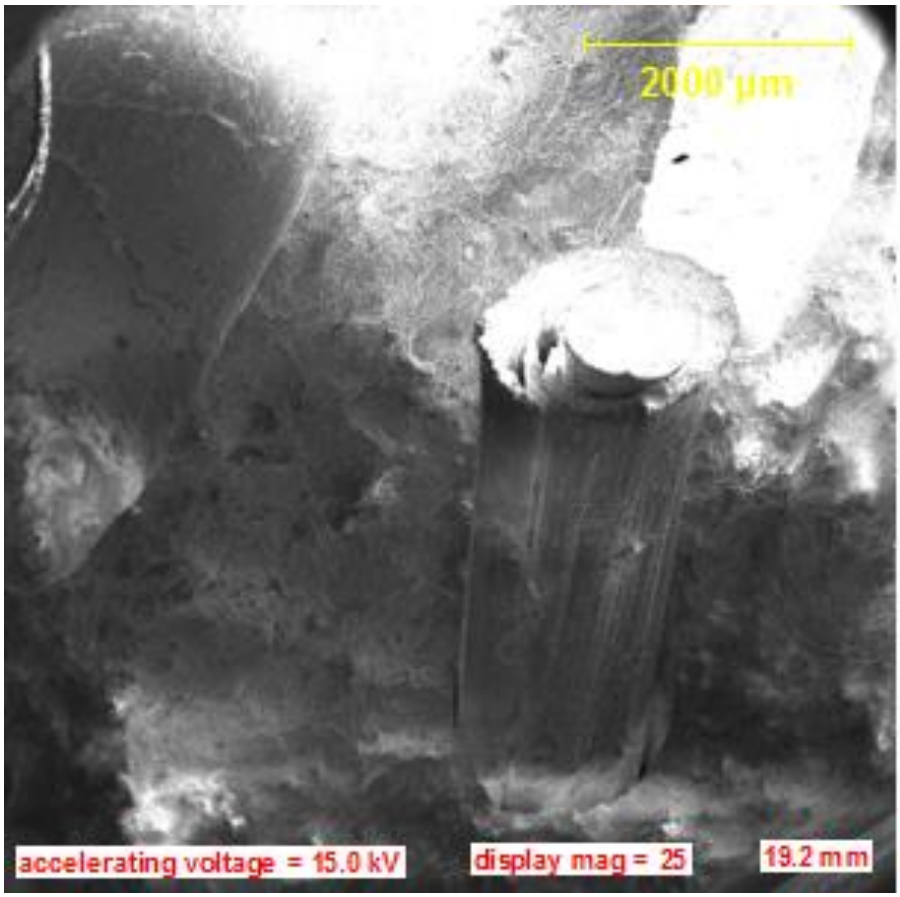

(b)

Figure 6.1: SEM images of fracture surfaces showing evidence of debonding and fiber pullout.

This chapter examines the failure of natural fiber-reinforced earth-based composites using single edge notch bend test. Mechanical test carried out indicated that failure occurs in several stages (similar to other brittle matrix composites): multiple matrix cracking, followed by fiber fracture and pullout. The application of conventional fracture mechanics to describe failure has been elucidated individually in previous chapters. The in situ observations provide direct indication of the importance of bridging and frictional bonding between the matrix and fibers. Some novel methods for measuring the frictional forces and residual stresses are investigated.

6.2 Toughening Due to Crack Bridging

The natural fiber-reinforced earth-based composite considered in this study belong to the family of ceramic composite systems toughened by whiskers which involve matrix and reinforcing phases with modest toughness. The whisker reinforcement alters the conditions required for crack extension in the matrix, and this can occur by formation of a zone of bridging whiskers behind the crack tip. In order to establish a zone behind the crack tip in which the whiskers remain intact, we then address how the crack tip propagates through the matrix without fracturing the whiskers.

Bridging of the crack surfaces behind the crack tip by a strong discontinuous reinforcing phase imposes a closure force on the crack and is, at times, accompanied by pull-out of the reinforcement. This section concentrates on the toughening due to crack bridging by the reinforcing phases, where the reinforcement simply bridges the crack surfaces and effectively reduces the crack driving force. This increases the resistance to crack extension. The bridging contribution to the toughness is given by equation 4.1 and 4.2.

6.3 Toughening Due to Fiber Pull-out

Prior studies have shown that the mechanical behavior of fiber-reinforced composites is also influenced by interfacial properties of the fiber-matrix system [6]. The toughening of a ceramic composite is primarily due to bridging of the crack surfaces by intact fibers when the composite is subjected to some loading condition. While the bridging stresses in the fibers contribute to the toughening, the relative displacements in the loading direction between the fibers and the matrix at the crack surface are required to accommodate the crack-opening displacement. Subsequently,

optimal conditions for toughening of ceramic composites also require debonding at the fiber-matrix interfaces via fiber pull-out, and frictional sliding between the fibers and the matrix [7, 8].

The fiber pull-out test was adopted to study the interfacial properties of natural fiber-reinforced earth based composite (Chapter 5). During fiber pull-out, interfacial debonding initiates at the surface, where the fiber enters the matrix and where the interfacial shear stress is a maximum. At initial debonding, the applied stress on the fiber overcomes the bonding between the fiber and the matrix. Residual clamping stresses often exist at the interface and result in interfacial friction for the debonded interface during fiber pull-out. Hence, after initial debonding, further debonding requires the applied stress to overcome the Interfacial strength of the debonded interface, and the bond strength at the bonded interface. The toughening contribution due to debonding and fiber pull-out can be obtained from equation 5.7.

6.4 Model for the estimation of shielding due to crack bridging and fiber pull-out.

The expression for the estimation of the composite fracture toughness based on the toughening mechanisms observed in the failure of natural fiber-reinforced earth-based composite is given by [9, 10]:

$$\mathrm{K_R} = \mathrm{K_i} + \Delta\mathrm{K} \qquad [11]$$

where $\mathrm{K_R}$ is the composite fracture toughness and $\Delta\mathrm{K}$ is the shielding due to crack bridging and fiber pull-out. For toughening due to fiber pull-out at constant frictional stress, $\Delta K = \Delta K_F$ and for bridging toughening, $\Delta\mathrm{K} = \Delta\mathrm{K_B}$ (for a combined small- and large- scale bridging).

In this study, multiple toughening mechanisms operate; therefore, the total toughening has to be estimated from the sum of the contributions due to each mechanism. A linear superposition models which neglect the possible interactions between individual mechanisms is used. These synergistic interactions between the toughening mechanisms provide a more realistic estimation of toughening than the individual toughening components [11]. For toughening by crack bridging and fiber pullout with constant fractional stress, the overall toughening is given by [12]:

$$\Delta K = \lambda \Delta K_B + (1 - \lambda)\Delta K_F \qquad [12]$$

where ΔK is the total toughening, λ is the toughening ratio due to crack bridging, ΔK_B and ΔK_F are the shielding due to crack bridging and fiber pull-out respectively.

6.5 Results and discussion

This study revealed that when a composite (natural fiber-reinforced earth-based) is subjected to residual stress at the interface, a mode II fracture exist along the debond and shielding of crack-tip via bridging. Debonding and sliding resistance as well as bridging contributed to toughness of the composite. Using data summarized in Table 6.1 and 6.2, the shielding contribution from fiber pull-out and crack bridging models described in chapter 5 and 4 respectively are presented. The predictions for toughening due to fiber pull-out only, crack bridging only and the shielding due to both crack bridging and fiber pull-out are presented in Table 6.3.

Table 6.1: Parameters used in the toughening due to fiber pull-out model.

Volume percentages of reinforcement	τ (MPa)	r_f (m)	r (m)	ρ	$\Delta K_F\left(MPa\sqrt{m}\right)$
5 vol% Fiber	0.39±0.02	0.001	0.002	0.25	0.13±0.007
10 vol% Fiber	0.40±0.02	0.001	0.002	0.25	0.17±0.009
20 vol% Fiber	0.44±0.02	0.001	0.002	0.25	0.29±0.010

τ = friction stress between the matrix and the fiber, r_f = radius of the fiber, r = radius of cylindrical outer boundary of matrix, ρ = area fraction of the fiber, ΔK_b = Bridging toughness.

Table 6.2: Parameters used in the toughening due to crack bridging model.

Volume percentages of reinforcement	V_b	$L\ (mm)$	α	$\Delta K_B\left(MPa\sqrt{m}\right)$
5 vol% Fiber	0.050	4.5	3	0.21±0.010
10 vol% Fiber	0.075	4.5	3	0.29±0.010
20 vol% Fiber	0.100	4.5	3	0.43±0.020

V_b = Fiber volume fraction in the bridge zone, L = Length of the bridge zone, α = Triaxiality factor, ΔK_B = Bridging toughness.

Table 6.3: Toughening due to combined effect of fiber pull-out and crack bridging.

Volume percentages of reinforcement	$\Delta K_F\ (MPa\sqrt{m})$	$\Delta K_B\ (MPa\sqrt{m})$	$\Delta K\ (MPa\sqrt{m})$
5 vol% Fiber	0.13±0.007	0.21±0.010	0.17±0.009
10 vol% Fiber	0.17±0.009	0.29±0.010	0.23±0.010
20 vol% Fiber	0.29±0.010	0.43±0.020	0.36±0.020

$\Delta K = \lambda \Delta K_B + (1-\lambda)\Delta K_F,\ \lambda = 0.5$

The results primarily show that increasing fiber volume fraction results in increased toughening. Similar observations have also been reported in prior work by Savastano et al. [9, 10] and Agopyan [13], whose studies used vegetable fiber-reinforced cementitious matrices. This increase in fracture toughness attained as a result of fiber-reinforcement can be attributed to shielding of the remote loads by interfacial strength and bridging fibers.

The measured toughness of natural fiber-reinforced earth-based composites is presented in Figure 6.2. This shows comparison between results obtained experimentally and those from analytical models. The effect of fiber reinforcement is evident as fiber volume fraction is increased. The results also confirm that multiple toughening mechanisms operate and the total toughening can be estimated from the sum of the contributions due to each mechanism. The synergistic interactions between individual toughening mechanisms represent a better estimate of toughening than the simple individual toughening components.

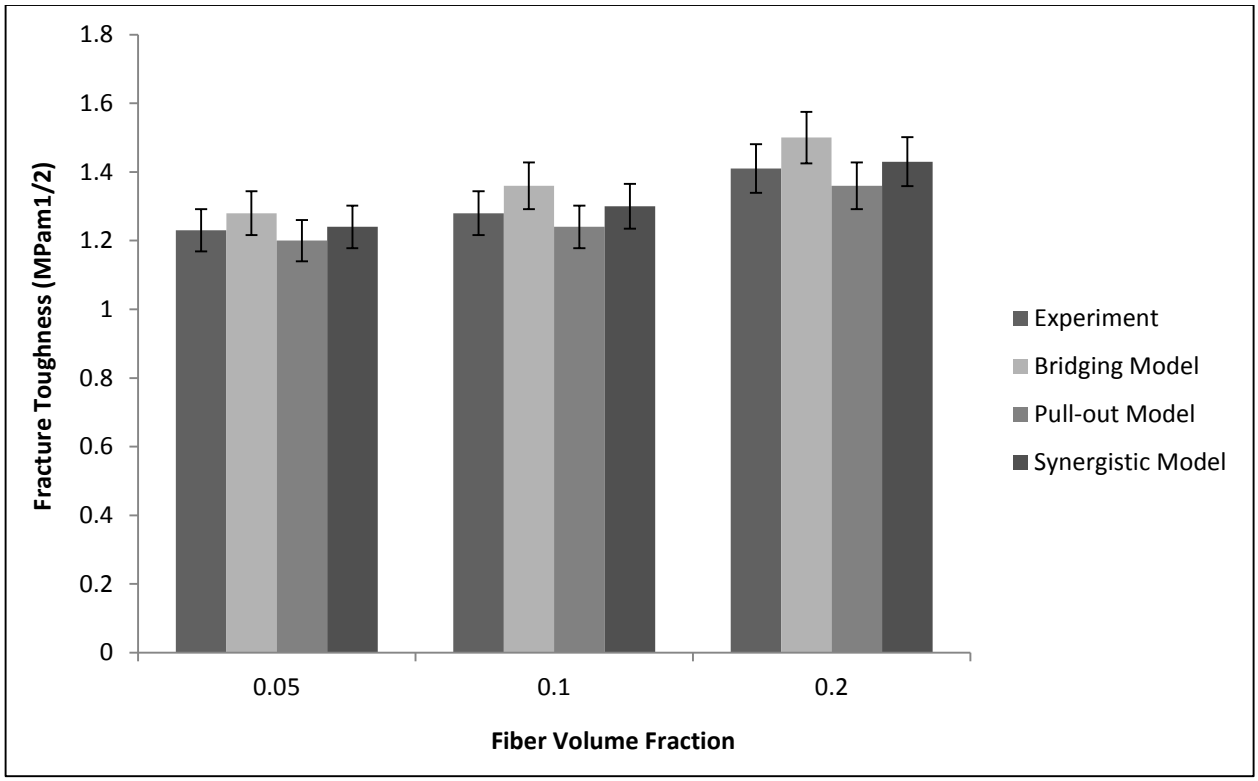

Figure 6.2: Comparison between experimental results and toughening models.

References

[1] P F. Becher, T. N. Tiegs, I. C. Ogle, and W. H Warwick, "Toughening of Ceramics by Whisker Reinforcement": pp. 61-73 in Fracture Mechanics of Ceramic, Vol. 7. Edited by R. C. Bradt, A. CT 'Evans, D. P. H. Hasselinan, and F. F. Lange. Plenum Publishing COT., New York, 1986.

[2] T. N. Tiees and P. F. Becher. "Whisker Reinforced Ceramics Composites": pp. 639-47 in Tailoring of Multiphase and Composite Ceramics. Edited by R. Tresrler. G. Messing, C. Pantano, and R. Newnham. Plenum Publishing Corp., New York, 1986.

[3] Kerans, RJ and Triplicane AP. Theoretical analysis of the fiber pullout and pushout tests. *J. Am. Ceram. Soc.,* 1991, 74 (7) 1585-1596.

[4] Wells JK and Beaumont PWR. Debonding and pull-out processes in fibrous composites. *J. Mater. Sci.,* 1985, 20 (4) 1275-1284.

[5] Evans A*G* and McMeeking RM, "On the Toughening of Ceramic by Strong Reinforcements," *Acta Metall.,* 34 [12] 2435-41 (1986).

[6] A. Kelly and W. R. Tyson, Tensile properties of fiber-reinforced metals, J, Mech. Phys. Solids, 13 (1965) 329-350.

[7] A. G. Evans and R. M. McMeeking, On the toughening of ceramics by strong reinforcements, Acta Metall., 34 (12)(1986) 2435-2441.

[8] P. F. Becher, C. H. Hsueh, P. Angelini and T. N. Tiegs, Toughening behavior in fiber-reinforced ceramic matrix composites, J. Am. Ceram. Soc., 71 (12) (1988) 1050-1061.

[9] Savastano Jr H, Warden PG and Coutts RSP. Brazilian waste fibers as reinforcement for cement based composites. Cem. Concr. Compos. 2000; 22(5): 379-84.

[10] Savastano Jr H, Agopyan V. Transition zone studies of vegetable fiber-cement paste composites. Cem. Concr. Compos. 1999; 21(1):49-57.

[11] Budiansky, B., Amazigo, J., and Evans, A.G. (1988) J Mech Phys Solids. vol. 36, p 167.

[12] Shum, D.K.M. and Hutchinson, J.W. (1989) On Toughening by Microcracks. Rep no. Harvard University, Cambridge, MA, MECH-151.

[13] Agopyan V and John VM. Durability evaluation of vegetable fiber reinforced materials. Build Res Infor, 1992; 20(4): 233-5.

CHAPTER SEVEN: IMPLICATION, CONCLUSION AND FUTURE WORK

7.1 Implications

The implications of the current research are very significant for the design of composite materials for sustainable and affordable housing. Most of the research carried out recently has focused on the development of natural fiber-reinforced cement-based composites for affordable housing [1-3]. This work has shown an improvement in the mechanical properties of earth-based matrices when they are reinforced with straw. The mechanistic models revealed that the contribution of fibers to the improvement of composite mechanical properties is very important. This is evident in the increased composite mechanical properties as volume fractions of fiber are increased considerably.

Specifically, toughening of the composites was enhanced via crack bridging and fiber pull-out [4-8] precipitated by fiber (straw) reinforcement. The application of fracture toughness testing to the materials used in this study is based on the ceramic (brittle) matrix composite resulting from the cementitious matrix formed. The fracture toughness test measures material resistance to crack propagation and is directly applicable to fracture control in describing the material property for crack growth resistance. The results from the test procedures in this study can serve as a basis in micro-mechanical characterization, performance evaluation and quality assurance for sustainable and affordable construction (building) products.

Hence, sustainable and low cost housing can be achieved using locally sourced materials expounded in this work. Finally, CO_2 emissions associated with conventional building materials can be reduced using earth-based materials.

7.2 Conclusions

The Strength and toughening (crack bridging and fiber pull-out) characteristics have been studied in earth-based composites reinforced with straw fibers. Salient conclusions arising from the combined experimental and theoretical study are as follows:

i. Composites consisting of earth-based materials reinforced with natural fiber (straw), and plain matrices were prepared. The mechanical properties of the various compositions (in both matrices and composites) were determined. The results were compared to measure the effects of reinforcement.

ii. Microscopy studies reveal that cracks in whisker-reinforced ceramics can propagate in the matrix and leave intact whiskers which bridge the crack immediately behind the crack tip. Whisker bridging occurs as the whisker-matrix interface debonds when the crack tip approaches the interface. Further behind the crack tip, the whiskers are pulled out of the matrix as the crack-opening displacement increases.

iii. Fiber-reinforcement resulted in an increase in compressive strength from 2.57±0.13 MPa to 2.91±0.15 MPa at maximum compressive strength. Interestingly, pure laterite had a compressive strength of 3.03±0.15 MPa. This value was the closest to that of fired clay (4.95±0.25 MPa). Samples reinforced with straw fibers had increased flexural strengths and fracture toughness. Composites with fiber volume percentage of 20% had the highest flexural strengths and fracture toughness values of up to 8.99±0.45 MPa and 1.41±0.07 MPa$\sqrt{m}$, respectively. These values exceed the respective values obtained for the matrix material (6.76±0.34 MPa and 1.08±0.05 MPa$\sqrt{m}$).

iv. The measured strengths and fracture toughness levels are consistent with predictions from mechanistic models studied. The rule-of-mixture and short fiber theory strength predictions account for the effects of whiskers and random orientation to provide reasonable estimate of flexural strength.

v. The modeling of crack shielding by crack bridging and fiber pull-out provide adequate estimates of toughening in the straw-reinforced earth-based composites that were examined in this study. This is evident in the trends of resistance-curve and single fiber pull-out test.

vi. The toughness of a brittle material has been shown to increase in the presence of a process zone of micro cracks. The influence of the wake is manifest in R-curve behavior, wherein the fracture resistance increases continuously with crack growth.

vii. The results of the bridging models are in agreement with the corresponding experimental measurements. Specifically, the resistance-curve curves showed that the trend of improved toughness in the predicted and the measured values were retained.

viii. Fiber pull-out strengths increase with increasing fiber embedment length and fiber volume fractions up to 0.2. The measured improvements are consistent with predictions from composites and interfacial fracture models.

ix. Following the onset of debonding, a regime of constant frictional pull-out stress was observed. This suggests that the friction stress was not significantly affected by the degree of pull-out.

x. The predicted toughening obtained from the fracture mechanics analyses is consistent with the experimental resistance curves. These predictions are also consistent with the ranges in the toughening/resistance-curve behavior obtained for the earth-based composites with different volume fractions of fibers between 0 and 20 vol. %.

7.3 Future work

This study presents motivation for further studies of mechanical properties of earth-based composites. The stability and degradation of earth-based composites was not considered in the present study, future research is needed to test the durability of earth-based composites under a range of weathering conditions. There is also need to explore actual performance of earth-based composites in sustainable building.

References

[1] John VM and Zordan SE. Research and development methodology for recycling residues as building materials - a proposal. Waste Mgmt 2001; 21: 213-9.

[2] Savastano Jr H, Warden PG and Coutts RSP. Potential of alternative fiber cements as building materials for developing areas. Cem. Concr. Compos. 2003; 27(5): 585-92.

[3] Heinricks H, Berkenkamp R, Lempfer K et al. Global review of technologies and markets for building materials. In: ganic-Bonded Wood and Fiber Composite Materials Conference. Moscow: University of Idaho; 2000.

[4] Savastano Jr H, Santos SF, Radonjic M et al. Fracture and fatigue of natural fiber-reinforced cementitious composites. Cem. Concr. Compos. 2009; 31(5): 232-43.

[5] Nelson PK, Li VC and Kamada T. Fracture toughness of microfiber reinforced cement composites. J Mater Civ Eng 2002; 14(5): 384-91.

[6] Becher, P. F., HSUEH, C. H., Angelini, P., & Tiegs, T. N. Toughening Behavior in Whisker-Reinforced Ceramic Matrix Composites. *Journal of the American Ceramic Society* 1988, *71*(12), 1050-1061.

[7] Kelly A and Tyson WR. Tensile properties of fiber-reinforced metals. *J. Mech. Phys. Solids*, 13 (1965) 329-350.

[8] Broutman LJ. Modern Composite Materials ed Broutman LJ and Krock RH. New York: Addison-Wesley, 1967, 391-394.